

**The N-terminus of Sec61p plays key roles in ER protein
import and ERAD**

Dissertation

zur Erlangung des Grades

des Doktors der Naturwissenschaften

der Naturwissenschaftlich-Technischen Fakultät

der **Universität des Saarlandes**

von

Francesco Elia M.Sc.

Saarbrücken, 2017

Tag des Kolloquiums: 05.09.2017

Dekan: Prof. Dr. Guido Kickelbick

Berichterstatter: Prof. Dr. Karin Römisch
Prof. Dr. Richard Zimmermann i.V. für Prof. Dr. Manfred J.
Schmitt

Vorsitz: Prof. Dr. Volkhard Helms

Akad. Mitarbeiter: Dr. Jens Neunzig

Index

List of figures	6
List of tables.....	8
List of abbreviations	9
Abstract.....	15
Zusammenfassung	16
1. Introduction	17
1.1. The secretory pathway	17
1.2. Protein translocation into the ER	22
1.3. ER quality control and ERAD	26
1.4. The Unfolded Protein Response	31
1.5. The Sec61 complex	34
1.6. The Sec61p N-terminus	38
1.7. The Sec complex	39
1.8. Protein N-terminal acetylation	40
1.9. Aim of this study	42
2. Materials and Methods	44
2.1. Materials	44
2.1.1. Laboratory equipment.....	44
2.1.2. Reagents, chemicals and consumables	45
2.1.3. <i>E. coli</i> and <i>S. cerevisiae</i> strains	48
2.1.4. Plasmids	49
2.1.5. Primers	50
2.1.6. Antibodies	50

2.1.7. Growth media	51
2.2. Methods.....	52
2.2.1. Sterilization.....	52
2.2.2. Growth of <i>E. coli</i>	52
2.2.3. Growth of <i>S. cerevisiae</i>	52
2.2.4. Polymerase chain reaction	52
2.2.5. Agarose gel electrophoresis	54
2.2.6. Preparation of chemically competent <i>E. coli</i> cells.....	55
2.2.7. Transformation of chemically competent <i>E. coli</i> cells.....	55
2.2.8. Transformation of <i>S. cerevisiae</i>	56
2.2.9. Drop test.....	57
2.2.10. β -galactosidase assay	57
2.2.11. Preparation of yeast cell extracts and cycloheximide chase.....	58
2.2.12. Protein gel electrophoresis	58
2.2.13. Western blot analysis	58
2.2.14. Pulse-labeling and immunoprecipitation	59
2.2.15. Lyticase preparation	60
2.2.16. Preparation of rough yeast microsomes	61
2.2.17. <i>In vitro</i> transcription.....	62
2.2.18. <i>In vitro</i> post-translational translocation	63
2.2.19. Fractionation of Sec complex	64
2.2.20. Sucrose gradient centrifugation.....	65
3. Results	66
3.1. Generation of <i>sec61</i> N-terminal mutants	66
3.2. Growth analysis of <i>sec61</i> N-terminal mutants	68

3.3. Stability and expression levels of <i>sec61</i> N-terminal variants	69
3.4. UPR induction in <i>sec61</i> N-terminal mutants	72
3.5. ERAD of CPY* in <i>sec61</i> N-terminal mutants	73
3.6. Co-translational import in <i>sec61</i> N-terminal mutants	78
3.7. Post-translational import in <i>sec61</i> N-terminal mutants	79
3.8. Post-translational protein import into <i>sec61S2Y</i> , <i>sec61ΔH1</i> and <i>sec61ΔN21</i> microsomes	82
3.9. Stability of heptameric Sec complexes in <i>sec61</i> N-terminal mutants	88
3.10. Stability of trimeric Sec61 complexes in <i>sec61</i> N-terminal mutants	91
3.11. Growth of <i>sec61</i> N-terminal mutants upon Sbh1p overexpression.....	94
3.12. Clogging of the Sec61 translocon in <i>sec61</i> N-terminal and <i>Δsbh1Δsbh2</i> mutants	95
4. Discussion	98
4.1. Role of Sec61p N-acetylation.....	99
4.2. Role of the Sec61p N-terminal amphipathic helix	103
4.3. Concluding remarks	106
5. References	108
Publications	137
Acknowledgements	138

List of figures

Figure 1.1.	The secretory pathway	21
Figure 1.2	Co-translational protein translocation into the ER	24
Figure 1.3	Post-translational protein translocation into the yeast ER	26
Figure 1.4	N-linked glycan processing in the yeast ER	28
Figure 1.5	ERAD pathways in yeast	31
Figure 1.6	The UPR in yeast	33
Figure 1.7	The Sec61p subunit	37
Figure 1.8	N-terminal acetylation of proteins by NATs	41
Figure 2.1	Schematic representation of the PCR-mediated plasmid DNA deletion method	54
Figure 3.1	Topology of Sec61p	66
Figure 3.2	Expression of Sec61 Δ H1p and Sec61 Δ N21p	68
Figure 3.3	Temperature- and tunicamycin-sensitivity of the <i>sec61ΔH1</i> and <i>sec61ΔN21</i> strains	69
Figure 3.4	Stability of Sec61 Δ H1p and Sec61 Δ N21p	70
Figure 3.5	Stability of Sec61S2Yp	71
Figure 3.6	Liquid β -galactosidase assay with <i>sec61</i> N-terminal mutants	73
Figure 3.7	ERAD of CPY* in <i>sec61ΔH1</i> and <i>sec61ΔN21</i> cells	75
Figure 3.8	ERAD of CPY* in <i>sec61ΔH1</i> and <i>sec61ΔN21</i> cells (90 min)	76
Figure 3.9	ERAD of CPY* in <i>sec61S2Y</i> cells	77
Figure 3.10	Co-translational ER import of newly synthesized DPAPB in <i>sec61ΔH1</i> and <i>sec61ΔN21</i> cells	78
Figure 3.11	Co-translational ER import of newly synthesized DPAPB in <i>sec61S2Y</i> cells	79

Figure 3.12	Post-translational ER import of pp α F in <i>sec61ΔH1</i> and <i>sec61ΔN21</i> cells	80
Figure 3.13	Post-translational ER import of newly synthesized ppCPY* in <i>sec61ΔH1</i> and <i>sec61ΔN21</i> cells	81
Figure 3.14	<i>In vitro</i> post-translational import of pp α F into <i>sec61S2Y</i> microsomes	83
Figure 3.15	<i>In vitro</i> post-translational import of pp α F into increasing amounts (0-0.5 eq) of wildtype microsomes	84
Figure 3.16	<i>In vitro</i> post-translational import of pp α F into limiting amounts of <i>sec61S2Y</i> microsomes	85
Figure 3.17	<i>In vitro</i> post-translational import of pp α F into <i>sec61ΔH1</i> and <i>sec61ΔN21</i> microsomes	86
Figure 3.18	<i>In vitro</i> post-translational import of pp α F into <i>sec61ΔH1</i> and <i>sec61ΔN21</i> microsomes (2 h)	87
Figure 3.19	Stability of heptameric Sec complexes in <i>sec61ΔH1</i> and <i>sec61ΔN21</i> membranes	88
Figure 3.20	Stability of heptameric Sec complexes in <i>sec61S2Y</i> membranes	90
Figure 3.21	Stability of Sec61 complexes in <i>sec61ΔH1</i> and <i>sec61ΔN21</i> membranes	92
Figure 3.22	Stability of Sec61 complexes in <i>sec61S2Y</i> membranes	93
Figure 3.23	Temperature sensitivity of <i>sec61ΔH1</i> and <i>sec61ΔN21</i> cells overexpressing <i>SBH1</i>	94
Figure 3.24	Measuring translocon clogging	96
Figure 3.25	Translocon unclogging in the Δ <i>sbh1</i> Δ <i>sbh2</i> strain	97
Figure 4.1	The acetylated Sec61p and Sec61S2Yp N-termini	101

List of tables

Table 2.1	Laboratory equipment used in this study	44
Table 2.2	Reagents, chemicals and consumables used in this study	45
Table 2.3	<i>E. coli</i> strains used in this study	48
Table 2.4	<i>S. cerevisiae</i> strains used in this study	49
Table 2.5	Plasmids used in this study	49
Table 2.6	Primers used in this study	50
Table 2.7	Antibodies used in this study and their working dilutions	51
Table 2.8	Concentrations of Ade, His, Leu, Lys, Trp and Ura in minimal medium	52

List of abbreviations

3gp α F	Triply glycosylated pro alpha factor
A	Alanine
AAA-ATPase	ATPase associated with diverse cellular activities
Ade	Adenine
Arl3p	ADP-ribosylation factor-like 3
Asn	Asparagine
ATF6	Activating transcription factor 6
ATP	Adenosine triphosphate
BiP	Immunoglobulin binding protein
C	Cysteine
C-terminal	Carboxy terminal
C-terminus	Carboxy terminus
CaCl ₂	Calcium chloride
Cdc48p	Cell division control protein 48
Cne1p	Calnexin and calreticulin homolog
CoA	Coenzyme A
Con A	Concanavalin A
COPI/II	Coat protein complex I/II
CPY	Carboxypeptidase Y
D	Aspartic acid
DEPC	Diethyl pyrocarbonate
Der1/3p	Degradation in the ER protein 1/3
dH ₂ O	Distilled water
DMSO	Dimethyl sulfoxide

DNA	Deoxyribonucleic acid
Doa10p	Degradation of alpha 2 protein 10
DPAPB	Diaminopeptidase B
DTT	Dithiothreitol
E	Glutamic acid
<i>E. coli</i>	<i>Escherichia coli</i>
E3	Ubiquitin-protein ligase
EDTA	Ethylene diamine tetraacetic acid
eIF2 α	Eukaryotic translation initiation factor 2 subunit alpha
Eq	Equivalent
ER	Endoplasmic reticulum
ERAD	ER-associated degradation
ERGIC	ER-Golgi intermediate compartment
ERp57	ER-resident protein 57
ERQC	ER quality control
F	Phenylalanine
G	Glycine
GlcNAc ₂ -Man ₉ -Glc ₃	N-acetylglucosamine ₂ Mannose ₉ Glucose ₃
GTP	Guanosine triphosphate
h	Hour(s)
H	Histidine
H6/7/8	Transmembrane helix 6/7/8
HA	Hemagglutinin A
Hac1p	Homolog to Atf/Creb1
HCl	Hydrochloric acid

HECT	Homologous with E6-associated protein C-terminus
HEPES	4-(2-hydroxyethyl)-1-piperazineethanesulfonic acid
His	Histidine
HO	Homothallic switching endonuclease
Hrd1/3p	HMG-CoA reductase degradation protein 1/3
Hsp70	70 kilodalton heat shock protein
Htm1p	Homolog to ER mannosidase 1
I	Isoleucine
IP	Immunoprecipitation
IPTG	Isopropyl- β -D-thio-galactopyranoside
IQ motif	Isoleucine-glutamine motif
Ire1p	Inositol-requiring protein 1
K	Lysine
KAc	Potassium acetate
Kar2p	Karyogamy protein 2
KCl	Potassium chloride
kDa	Kilodalton
KOAc	Potassium acetate
L	Leucine
LB	Lysogeny broth
Leu	Leucine
LiAc	Lithium acetate
Lys	Lysine
M	Methionine
MES	2-(N-morpholino)ethanesulfonic acid

Mg(OAc) ₂	Magnesium acetate
MgSO ₄	Magnesium sulphate
min	Minute(s)
MnCl ₂	Manganese chloride
MOPS	3-(N-morpholino)propanesulfonic acid
mRNA	Messenger RNA
N	Asparagine
N-terminal	Amino terminal
N-terminus	Amino terminus
Na ₂ CO ₃	Sodium carbonate
Na ₂ HPO ₄	Disodium phosphate
NaAc	Sodium acetate
NaCl	Sodium chloride
NaH ₂ PO ₄	Monosodium phosphate
NAT	N-terminal acetyltransferase
Npl4p	Nuclear protein localization protein 4
OD	Optical density
ON	Overnight
ONPG	Ortho-nitrophenyl-β-D-galactopyranoside
OST	Oligosaccharyl transferase
PCR	Polymerase chain reaction
Pdi1p	Protein disulfide isomerase
PEG	Polyethylene glycol
PERK	Protein kinase RNA-like ER kinase
PI	Protease inhibitor

PMSF	Phenylmethylsulfonyl fluoride
ppαF	Prepro alpha factor
Q	Glutamine
QC	Quality control
RAMP	Ribosome-associated membrane protein
RING	Really interesting new gene
RNC	Ribosome-nascent chain complex
RP	Regulatory particle
Rpn12p	Regulatory particle non-ATPase 12
RT	Room temperature
S	Serine
<i>S. cerevisiae</i>	<i>Saccharomyces cerevisiae</i>
Sbh1p	Sec61 beta homolog 1
SDS	Sodium dodecyl sulfate
SDS-PAGE	SDS-polyacrylamide gel electrophoresis
Sec61/62/63/71/72p	Protein transport protein Sec61/62/63/71/72
sec	Second(s)
Ser	Serine
Snd1/2/3 protein	SRP-independent targeting protein 1/2/3
SP	Signal peptidase
SR	SRP receptor
SRP	Signal recognition particle
Ssh1p	Sec sixty-one homolog 1
Sss1p	Sec sixty-one suppressor 1
Ste24p	Sterile protein 24

T	Threonine
TAE	Tris, acetate, EDTA
TBS	Tris-buffered saline
TBS-T	0.1% Tween 20 TBS
TCA	Trichloroacetic acid
TE	Tris-EDTA
TGN	Trans-Golgi network
Thr	Threonine
TM	Transmembrane
tRNA	Transfer RNA
Trp	Tryptophan
Ubx2p	Ubiquitin regulatory X domain-containing protein 2
Ufd1p	Ubiquitin fusion degradation protein 1
UPR	Unfolded Protein Response
UPRE	UPR element
Ura	Uracyl
Usa1p	U1 Snp1-associating protein
V	Valine
XBP1	X-box binding protein 1
Y	Tyrosine
Yos9p	Yeast OS-9 homolog
YP	Yeast peptone
YPD	Yeast peptone dextrose
YPD	Yeast peptone galactose

Abstract

Sec61p is the channel-forming subunit of the heterotrimeric Sec61 complex that mediates co-translational protein import into the endoplasmic reticulum (ER). In yeast, proteins can also be post-translationally translocated by the hetero-heptameric Sec complex, composed of the Sec61 and Sec63 complexes. Sec61 is also a candidate for the dislocation channel for misfolded proteins from the ER to the cytosol during ER-associated degradation (ERAD). The structure of Sec61p is highly conserved, but the roles of its N-terminal acetylation and N-terminal amphipathic helix were unknown so far. To investigate the function of the Sec61p N-terminus, I deleted its amphipathic helix, or both the helix and N-acetylation site, and characterized these two mutants together with a *sec61* mutant carrying a mutation of the N-terminal acetylation site previously shown to result in temperature-sensitivity and an ERAD defect. Mutation of the N-acetylation site on its own had no effect on protein import into the ER in intact cells. Yeast expressing *sec61* without the N-terminal helix displayed severe growth and post-translational ER import defects. Nevertheless, the formation of Sec complexes was not affected. Instead, removal of the N-terminal helix compromised the integrity of heterotrimeric Sec61 complexes. My data show that the Sec61p N-terminal helix is required for post-translational protein import into the ER and Sec61 complex stability, whereas Sec61p N-terminal acetylation plays a role in ERAD.

Zusammenfassung

Der heterotrimerer Sec61-Proteinkomplex vermittelt die Translokation sekretorischer Proteine ins Endoplasmatische Reticulum (ER) und ist ein putativer Transportkanal fehlgefalteter Proteine aus dem ER ins Cytosol während der ER-assoziierten Proteindegradation (ERAD). Die Untereinheit Sec61p bildet den Kanal und vermittelt den cotranslationalen Proteinimport in das ER. Proteine können in Hefen auch posttranslational durch den heteroheptameren Sec-Komplex, bestehend aus dem Sec61- und dem Sec63-Komplex, transloziert werden. Die Sec61p-Struktur ist hochkonserviert, aber die Funktion der N-Acetylierung und der N-terminalen amphipatischen Helix waren bisher nicht bekannt. Daher deletierte ich die Helix mit und ohne die Acetylierungsstelle und charakterisierte beide Mutanten zusammen mit einer kürzlich entdeckten *sec61* Mutante, die in der N-terminalen Acetylierungsstelle mutiert ist, temperatursensitiv ist und ERAD-Defekte aufweist. Die Mutation der Acetylierungsstelle hatte keinen Effekt auf den Proteinimport ins ER intakter Zellen. Hefen, die *sec61* ohne die N-terminale Helix exprimieren, zeigen einen starken Wachstums- und posttranslationalen ER-Importdefekt. Die Ausbildung des Sec-Komplexes war nicht betroffen, obwohl die Integrität des heterotrimeren Sec61-Komplexes beeinflusst war. Meine Daten belegen, dass die N-terminale Helix für den posttranslationalen Import ins ER und die Sec61-Komplexstabilität notwendig ist, wohingegen die N-Acetylierung eine Rolle in der ERAD spielt.

1. Introduction

1.1. The secretory pathway

Eukaryotic cells have an elaborate network of organelles that allow multiple biochemical environments to coexist in the cell and to be adapted independently (Diekmann and Pereira-Leal, 2013). Transport of newly synthesized proteins to specific cellular destinations is fundamental for generating and maintaining distinct environments that are crucial for different cellular functions (Cross et al., 2009).

While bacterial secreted proteins have either functions in the cell wall, the periplasm, the plasma membrane, or the outer membrane, between 20% and 30% of the eukaryotic cell proteome is destined for the extracellular environment or intracellular compartments (Delic et al., 2013; Gomez-Navarro and Miller, 2016). The pathway of eukaryotic protein secretion is the endoplasmic reticulum (ER) - Golgi pathway, which is initiated by translocation of a secretory protein through the ER membrane (Fig. 1.1) (Delic et al., 2013). In the ER, proteins undergo folding and assembly, and are ferried between compartments via transport vesicles that bud off from one donor compartment to fuse with a downstream acceptor compartment (Barlowe and Miller, 2013). After being translocated into the ER, newly synthesized secretory and transmembrane (TM) proteins are directed to the Golgi, where they are sorted between those transported to the plasma membrane or the exterior of the cell and those targeted to vacuoles (or lysosomes) (Feyder et al., 2015). Membrane proteins, such as those in the plasma membrane, also enter the secretory pathway, and are integrated into the lipid bilayer by TM segments of hydrophobic amino acids (Park and Rapoport, 2012). These folding and trafficking pathways dictate the fate of nearly one-third of proteins encoded by the eukaryotic genome (Wiseman et al., 2007).

Proteins are directed to the secretory pathway by their signal sequences (Kapp et al., 2009). Signal sequences are N-terminal extensions of nascent polypeptides approximately 15-50 amino acids in length that mediate protein targeting to the ER membrane (Blobel, 1980; von Heijne, 1983). They are characterized by a tripartite structure: (i) a hydrophilic, net positively charged n-region, (ii) a central hydrophobic h-region of 6-15 residues, (iii) a c-region with the cleavage site for signal peptidase (SP) (von Heijne, 1985). The consensus cleavage site consists of amino acids with short side chains at the -1 and no charged amino acids at the -3 position and no proline in the middle (von Heijne, 1986). When a signal sequence emerges from the ribosome, it is recognized by the signal recognition particle (SRP), which retards elongation of the nascent chain until the ribosome-nascent chain complex (RNC) has docked onto the SRP receptor (SR) at the ER membrane and the nascent chain is inserted into the ER translocon, the Sec61 channel (Walter and Blobel, 1981; Gilmore et al., 1982; Rapoport, 2007). Signal sequences are cleaved off as soon as the cleavage site is exposed in the ER lumen, but not all are cleaved co-translationally or immediately after translocation by SP (Chen et al., 2001; Paetzel et al., 2002). ER-resident proteins generally require specific signals for retention in order to be diverted from the bulk flow of secretory proteins and remain in the ER (Pagny et al., 1999). ER retention in yeast is mediated by a consensus HDEL sequence located at the C-terminal end of soluble proteins that reside in the ER lumen, while, both in yeast and mammals, the K(X)KXX (where X is any amino acid) structural motif at the extreme C-terminal position serves as an ER retention signal for type I TM ER-resident proteins (Pelham et al., 1988)

All proteins entering the secretory pathway have to be translocated into the ER (Fig. 1.1). After this event, secretory proteins do not have to cross any further membrane to reach other destinations along the pathway (Vitale and Denecke, 1999). The ER plays a central role in

protein biosynthesis and maturation, as it takes care of the folding and assembly not only of its own residents, but also of proteins destined to other locations (Vitale and Denecke, 1999). ER luminal enzymes catalyze the covalent addition of N-linked glycans, promote the formation of native disulfides, and assist folding/oligomerization of newly imported proteins (Araki and Nagata, 2011). Major players include Kar2p (BiP in mammals), which supports folding of imported proteins and keeps them soluble, and Pdi1p, which enables the *de novo* formation of disulphide linkages and the isomerization of non-native disulphide bonds (Simons et al., 1995; Tu and Weissman, 2004). Stringent quality control (QC) mechanisms ensure that only correctly folded proteins leave the ER and are sent to their final destinations (Sitia and Braakman, 2003). Proteins that fail to fold in the ER are retrotranslocated to the cytosol in order to be degraded by proteasomes, a process known as ER-associated degradation (ERAD) (Xie and Ng, 2010; Zattas and Hochstrasser, 2015). Despite this environment optimized for folding, aberrant misfolded proteins can accumulate in the ER, resulting in ER stress (Travers et al., 2000). ER stress activates a signaling pathway called the Unfolded Protein Response (UPR) to alleviate this stress and restore ER homeostasis, promoting cell survival and adaptation (Oslowski and Urano, 2011). The UPR is multifaceted and regulates proteins involved in QC, ERAD, and the secretory pathway (below) (Higashio and Kohno, 2002).

Once folded, proteins leave the rough ER and enter so-called ER “exit sites”, where the components of the COPII coat bud off vesicles for export to the Golgi complex (Fig. 1.1) (Lee and Miller, 2007). ER exit sites participate in ER QC (ERQC) by excluding misfolded proteins (Mezzacasa and Helenius, 2002). Cargo then moves from the ER to the ER-Golgi intermediate compartment (ERGIC) (Fig. 1.1) (Lord et al., 2013). From the ERGIC, cargo traffics toward the Golgi in an event mediated by COPII vesicles (Fig. 1.1) (Lord et al.,

2013). COPI vesicles mediate the formation of return vesicles to recycle membrane and nonresident ERGIC components back to the ER (Spang, 2013). Uptake into these retrograde vesicles is also selective, and therefore the ERGIC might serve as an additional QC site (Ellgaard et al., 1999).

Yeast cells seem to lack a distinct ERGIC compartment, and, instead, the first post-ER compartment where sorting occurs is the early Golgi (Cao et al., 1998). COPI-mediated retrograde traffic in yeast is also from the early Golgi (Fig. 1.1) (Letourneur et al., 1994). In mammals, after reaching the Golgi, the secretory cargo moves through the complex from the cis to intermediate to trans stacks, acquiring various modifications as it goes (Sanderfoot and Raikhel, 1999). At the same time, COPI vesicles mediate transport of material in the opposite direction so that missorted secretory cargo can be retained in specific Golgi stacks or returned to the ER (Sanderfoot and Raikhel, 1999). Anterograde transport through the Golgi apparatus in yeast seems to occur by maturation of the earlier cisternae into later cisternae while incoming ER-derived vesicles reform the cis-Golgi, although this may not be the case in all eukaryotic cells (Orci et al., 1997; Pelham et al., 1988). Finally, the trans-Golgi network, from which cargo moves to the plasma membrane and through endosomes to the vacuole (or lysosomes), serves as an additional QC checkpoint for the rerouting of misfolded proteins that are to be degraded (Fig. 1.1) (Ellgaard et al., 1999).

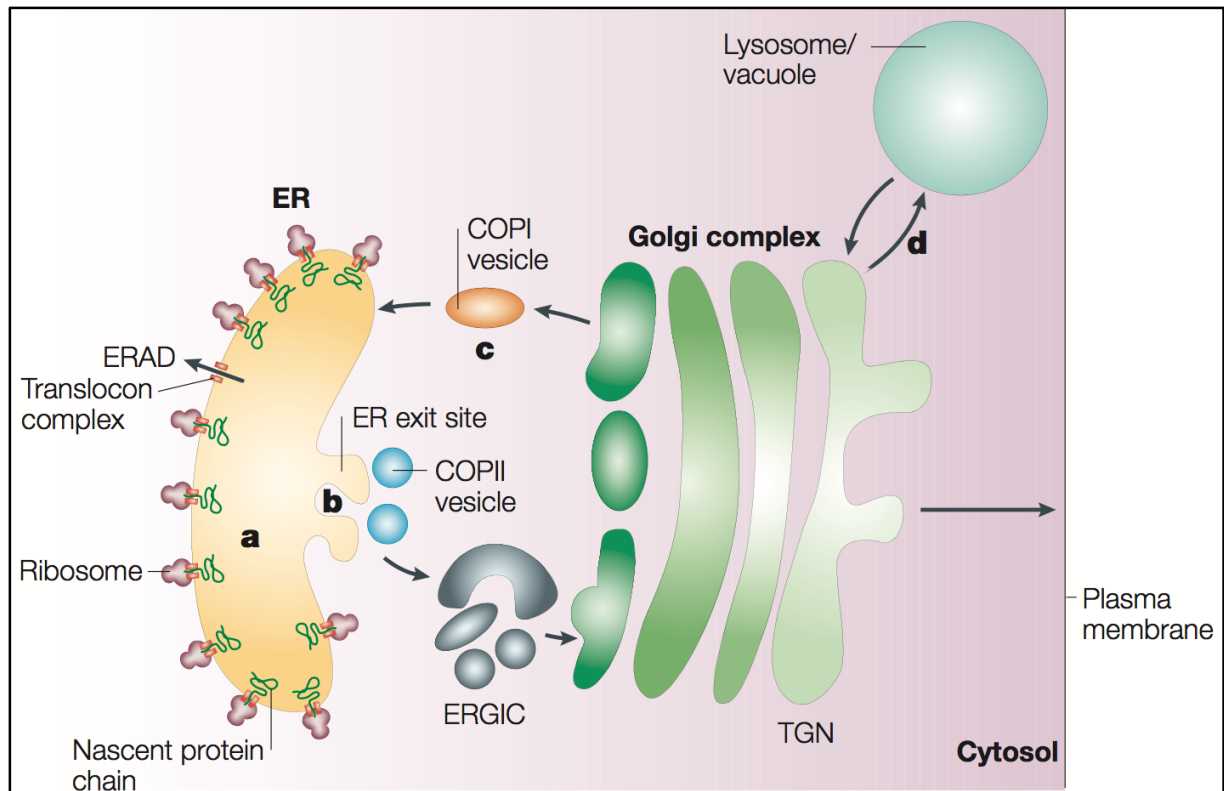


Figure 1.1. The secretory pathway. The ER is the site of synthesis and maturation of proteins entering the secretory pathway (a). In the ER, molecular chaperones and folding factors assist protein folding and retain non-native conformers. Terminally misfolded proteins and unassembled oligomers are retrotranslocated to the cytosol and degraded by the proteasome (ERAD). Once correctly folded, native conformers enter the ER exit sites (b) and are packaged into COPII vesicles to be transported through the ERGIC to the cis-face of the Golgi complex. Misfolded proteins are retrieved from the Golgi by COPI vesicles (c). Once they have passed through the cis-Golgi, proteins proceed through the trans-Golgi network (TGN) to the plasma membrane or beyond. Non-native proteins can be diverted from the TGN to the lysosome/vacuole for degradation (d) (Ellgaard and Helenius, 2003).

1.2. Protein translocation into the ER

Protein translocation into the ER is the first and decisive step in the biogenesis of secretory and organelle proteins of the secretory pathway (Zimmermann et al., 2011). Transport of newly synthesized proteins across the ER membrane through the Sec61 channel can occur either co- or post-translationally (Zimmermann et al., 2011). In yeast, post-translational import generally occurs for soluble proteins that carry only mildly hydrophobic signal sequences, whereas membrane proteins use the SRP-mediated co-translational pathway (Ast et al., 2013).

The Sec61 channel is a passive pore and must associate with partners that provide a driving force for translocation (Park and Rapoport, 2012). In co-translational translocation, the main partner is the ribosome (Park and Rapoport, 2012). The SRP pathway is essential in all organisms examined to date except the yeast *S. cerevisiae*, but even yeast cells are severely growth compromised in the absence of functional SRP (Mutka and Walter, 2001). Co-translational translocation begins with the signal or TM sequence of a growing polypeptide chain being recognized by SRP (Fig. 1.2) (Park and Rapoport, 2012). SRP delivers the nascent secretory protein together with the associated ribosome to the ER translocon (the Sec61 channel) via interaction with SR, a heterodimeric ER-resident membrane protein complex consisting of SR α and SR β both in yeast and mammals (Fig. 1.2) (Ogg et al., 1998; Nyathi et al., 2013). When the RNC engages the Sec61 complex, protein synthesis continues, enabling the elongating polypeptide to enter the membrane channel (Fig. 1.2) (Park and Rapoport, 2012; Nyathi et al., 2013). Soluble proteins cross the membrane completely and enter the ER lumen, where they can acquire their native conformation, while TM proteins move laterally to integrate into the membrane bilayer (Rapoport, 2007; Trueman et al., 2012).

SRP and SR belong to a class of GTPases regulated by GTP-dependent dimerization (Gasper et al., 2009). In the absence of biological cues, formation of a stable SRP-SR complex is extremely slow (Bradshaw et al., 2009). When SRP is loaded with the RNC, however, stable SRP-SR complex assembly is accelerated (Zhang et al., 2010). This ensures rapid delivery of cargo to the membrane and prevents futile SRP-SR interactions (Saraogi and Shan, 2011). At this point, rearrangements occur in both SRP and SR α to allow the formation of extensive contacts and direct interactions between the two GTP molecules across the dimer interface, thus giving a GTP-stabilized and activated closed complex (Shan et al., 2004; Saraogi and Shan, 2011). The closed state activates GTP hydrolysis, which drives the irreversible assembly of the SRP-SR complex (Nyathi et al., 2013). The RNC stabilizes the SRP-SR complex in the open conformation and delays its rearrangements to the closed state, thus providing the targeting complex with a time window to localize the translocon and preventing an abortive targeting reaction (Shan et al., 2007; Zhang et al., 2009). How the cargo delays GTP hydrolysis and how activation of the GTPase complex is coupled to cargo unloading, however, remain poorly understood.

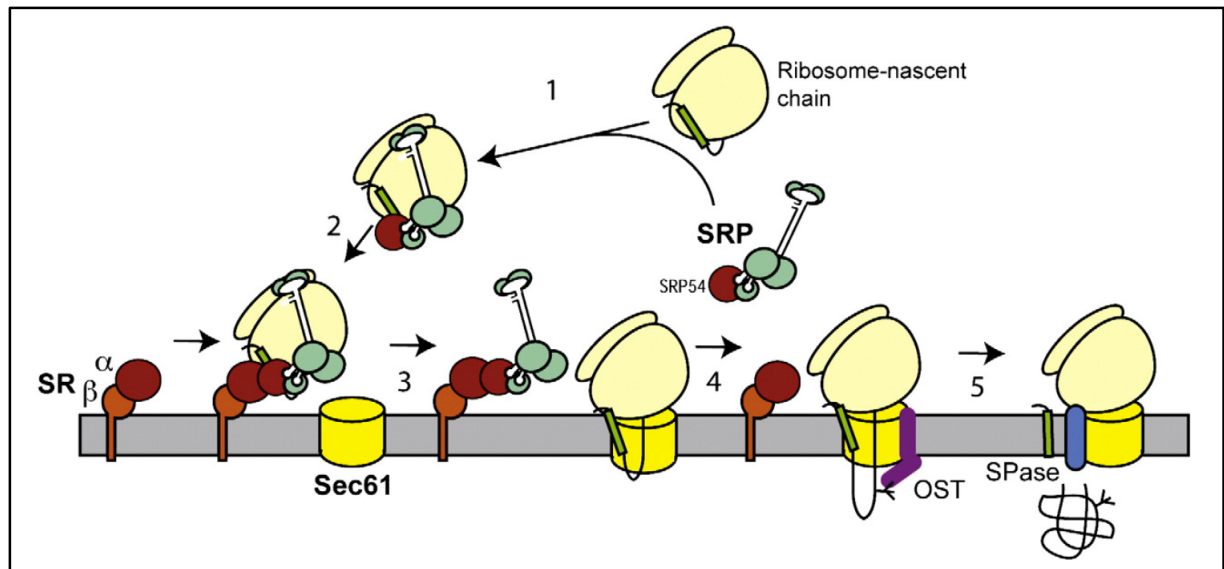


Figure 1.2. Co-translational protein translocation into the ER. SRP binds the signal sequence (green) as it emerges from the RNC-SRP complex. The SRP54 (54 kDa) subunit of SRP harbors GTPase activity, interacts with the signal sequence of secretory proteins and with SR (1). The RNC-SRP complex docks with the ER membrane by binding to SR (2). The RNC is then transferred from SRP-SR to the Sec61 channel, resulting in the intercalation of the signal sequence into the translocon pore and its opening (3). Translocation of the nascent chain proceeds through the pore and SRP disengages from SR (4). Concomitant with translocation, signal peptidase (SPase) and oligosaccharyl transferase (OST, described in 1.3) are recruited to the translocon to cleave the signal peptide and to add N-linked glycans to the nascent chain, respectively (5). Termination of protein synthesis releases the nascent chain from the ribosome (Nyathi et al., 2013).

Post-translational translocation of precursor polypeptides has most extensively been characterized in yeast. Post-translational translocation of secretory substrates requires ATP and cytosolic 70 kilodalton heat shock proteins (Hsp70s) (Hansen et al., 1986; Chirico et al., 1988). These chaperones likely prevent aggregation and keep polypeptides in a translocation competent state until their delivery to the ER translocon (Fig. 1.3) (Ngosuwan et al., 2003). The detailed mechanisms for recognition and targeting of post-translational import substrates, however, have not been fully elucidated. Three previously uncharacterized proteins, Snd1, Snd2, and Snd3, have been recently found to work together and have a prominent role in targeting a broad range of substrates to the ER independently of SRP (Aviram et al., 2016).

The three proteins could also synthetically compensate for loss of the SRP pathway, acting as a backup targeting system (Aviram et al., 2016). For post-translational import, the Sec61 complex associates with the heterotetrameric Sec63 complex (Sec62p, Sec63p, Sec71p, Sec72p) (Fig. 1.3) (Johnson and van Waes, 1999). Roles for Sec63p have also been identified in the SRP-dependent co-translational translocation reaction (Young et al., 2001). In the absence of ongoing translation, the driving force for translocation is provided by the luminal chaperone Kar2p that acts as a “molecular ratchet” to facilitate the transport of the polypeptide chain across the ER and probably also by folding of the translocated part of the protein (Fig. 1.3) (Matlack et al., 1999). As for co-translationally imported substrates, the signal sequences of post-translationally imported precursors are cleaved by SP and further degraded by SP, an enzyme that cleaves the hydrophobic segment within the membrane (Rapoport, 2007).

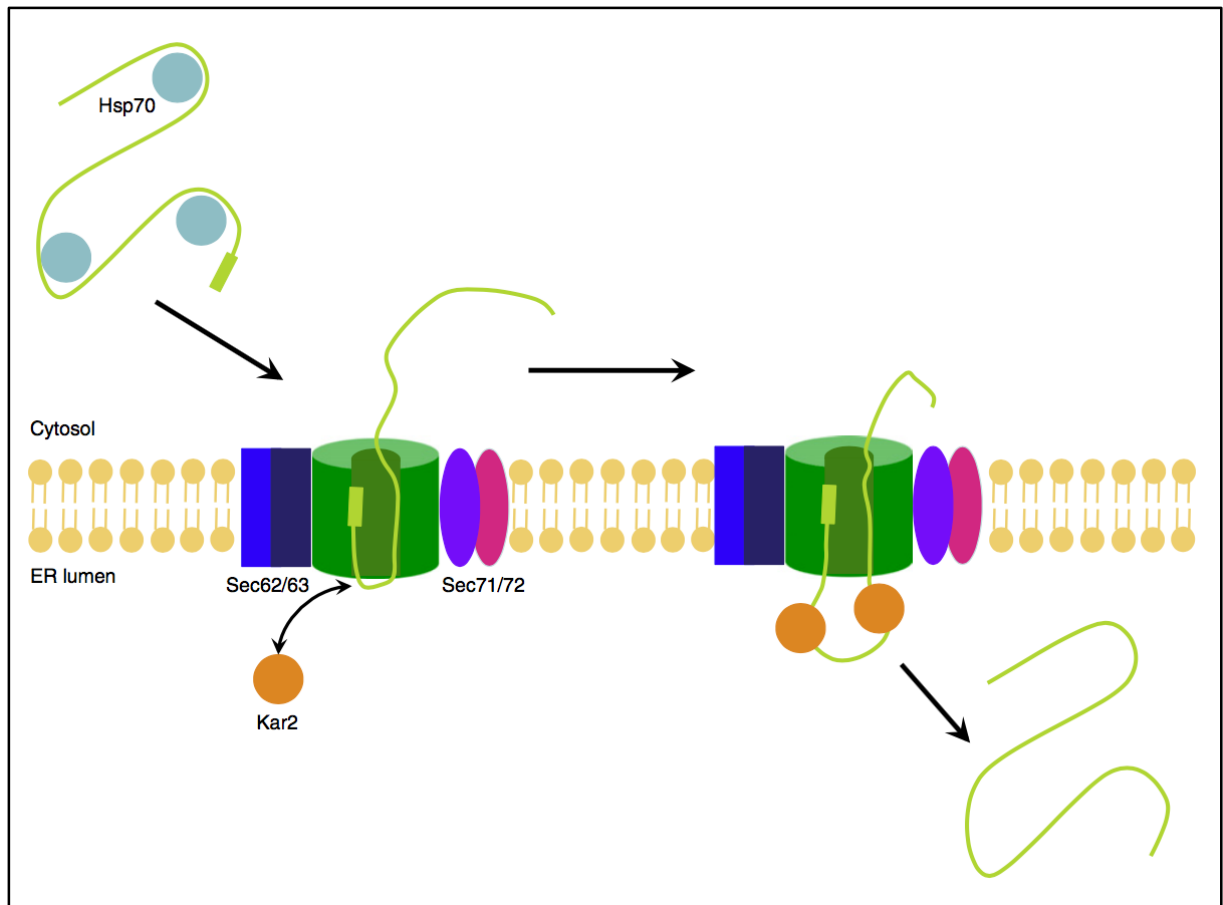


Figure 1.3. Post-translational protein translocation into the yeast ER. Hsp70s keep post-translational precursors in a translocation-competent state prior to them encountering the ER membrane. The polypeptide binds the Sec complex and inserts into the ER translocation channel. Sec63p recruits the luminal chaperone Kar2p to the luminal face of the ER membrane where it promotes the unidirectional movement of the imported protein acting as a molecular ratchet (Johnson et al., 2013).

1.3. ER quality control and ERAD

The QC system in the ER prevents the premature exit of folding intermediates and incompletely assembled proteins from the ER, thus extending the exposure of the folding substrates to the folding machinery in the ER lumen and increasing the chances of correct maturation (Ellgaard and Helenius, 2003). ERQC is based on common structural and biological features that distinguish native from non-native protein conformations, such as the exposure of hydrophobic patches normally hidden once proteins acquire native structures,

unpaired cysteine residues, hydrophilic residues in TM domains, and the tendency to aggregate (Ellgaard and Helenius 2003; Ruggiano et al., 2014). A prolonged interaction between ER-luminal chaperones and misfolded proteins is, however, not sufficient for substrate selection, as additional biochemical signatures have been proposed to be necessary for mediating ER retention (Thibault and Ng, 2012). The best-characterized QC system in yeast exploits the structure of N-linked glycans (Knop et al., 1996). As soon as polypeptides enter the ER through the Sec61 channel, the core GlcNAc₂-Man₉-Glc₃ glycan (where Glc is glucose, Man is mannose, and GlcNAc₂ is N-acetylglucosamine, Fig. 1.4) is transferred by oligosaccharyl transferase from a lipid-linked oligosaccharide donor to the side-chain nitrogen of asparagine residues part of the consensus sequence Asn-X-Ser/Thr (where X is any amino acid except proline) (Burda and Aepli, 1999; Thibault and Ng, 2012). Subsequently, the three glucose residues are sequentially removed by glucosidase I and II, generating GlcNAc₂-Man₉ (Fig. 1.4) (Thibault and Ng, 2012). Mannosidase I next cleaves the most distal mannose of branch B of the glycan to produce GlcNAc₂-Man₈ (Fig. 1.4) (Thibault and Ng, 2012). These sequential steps provide a time window for the glycoprotein to fold, and properly folded and glycosylated proteins can leave the yeast ER at this stage (Gauss et al., 2011). On the other hand, if the GlcNAc₂-Man₈ substrate is attached to an unfolded protein segment it is recognized by the Htm1p-Pdi1p complex, which specifically cleaves the terminal mannose residue from the C branch of the glycan (Xie et al., 2009; Gauss et al., 2011). The resulting exposed terminal α 1,6-linked mannose is the ligand for the ERAD substrate receptor Yos9p that targets misfolded glycoproteins for degradation (Szathmary et al., 2005; Quan et al., 2008). In this process the glycan substrate therefore functions as an intrinsic sensor for protein folding: if the protein folds by the time the signal glycan is processed to GlcNAc₂-Man₈, it escapes Htm1p-Pdi1p recognition and is free to leave the ER (Xu and Ng, 2015). The mechanism might seem wasteful, but given the toxicity of

irreversibly misfolded proteins, the degradation of a small number of slow but potentially folding proteins is definitely an acceptable cost.

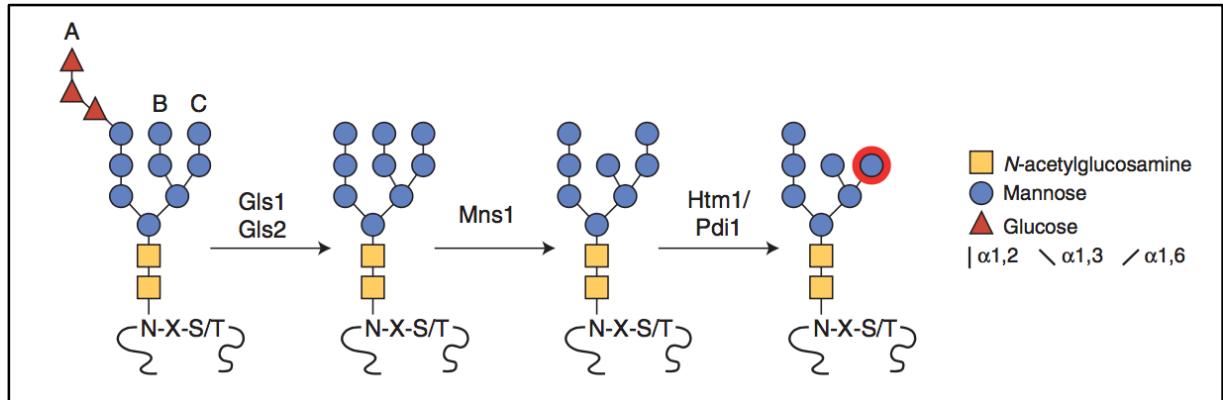


Figure 1.4. N-linked glycan processing in the yeast ER. The core $\text{GlcNAc}_2\text{-Man}_9\text{-Glc}_3$ glycan is added to the side-chain nitrogen of Asn (N) residues part of the consensus sequence Asn-X-Ser/Thr as soon as polypeptides enter the ER. Subsequently, the 3 glucoses of branch A are removed by glucosidase I (Gls1) and glucosidase II (Gls2) to generate $\text{GlcNAc}_2\text{-Man}_9$. Mannosidase I (Mns1) cleaves the $\alpha 1,2$ -linked mannose of branch B to produce $\text{GlcNAc}_2\text{-Man}_8$. At this point, folded and glycosylated proteins can leave the ER. Glycosylated proteins that fail to fold are recognized by Htm1p-Pdi1p which cleaves the $\alpha 1,2$ -linked mannose of branch C to yield the terminal $\alpha 1,6$ -linked mannose residue as the Yos9p ligand (red circle) (Thibault and Ng, 2012).

In mammalian cells, after transfer of the core oligosaccharide to the nascent chain of the protein, 2 glucoses are trimmed by glucosidases I and II (Ellgaard and Helenius, 2003). The folding of the resulting monoglucosylated glycoprotein is assisted by the lectins calnexin and calreticulin (Ellgaard and Helenius, 2003). Both proteins associate with the thiol-disulphide oxidoreductase ERp57, which forms interchain disulphide bonds with bound glycoproteins (Hebert and Molinari, 2012). Cleavage of the remaining glucose by glucosidase II releases the protein from the interaction with calnexin and calreticulin, so that, if properly folded, it can leave the ER (Ellgaard and Helenius, 2003). In yeast, the ER integral membrane protein Cne1p shares some sequence motifs with calnexin and calreticulin, and seems to function as a constituent of the ERQC apparatus (Parlati et al., 1995). Unfolded proteins can be

reglycosylated by UDP-glucose:glycoprotein glucosyltransferase (not present in *S. cerevisiae*), which reinduces association with calnexin and calreticulin (Ellgaard et al., 1999). This cycle is repeated until substrate proteins are either properly folded or degraded (Ellgaard et al., 1999).

All ERAD substrates have to be retrotranslocated to the cytosol, where in nearly all cases they are modified with polyubiquitin chains and thus designated for proteasomal degradation (Hiller et al., 1996). Potential ERAD substrates do not only include ER-luminal soluble proteins that have failed to fold, assemble, or become post-translationally modified, but also membrane proteins with luminal, intramembrane, or cytoplasmic lesions (Vembar and Brodsky, 2008). The location of a misfolded lesion determines the factors required for ERAD substrate targeting and the E3 ubiquitin ligase that transfers ubiquitin to the target protein (Vembar and Brodsky, 2008). While more classes of E3 ubiquitin ligases are present in mammals, yeast E3 ubiquitin ligases all fall into two major classes: RING (really interesting new gene) domain E3s and HECT (homologous with E6-associated protein C-terminus) domain E3s (Finley et al., 2012). Proteins with lesions in the cytoplasmic, luminal, and membrane-spanning domain enter the ERAD-C, ERAD-L, and ERAD-M pathways, respectively (Fig. 1.5) (Vashist and Ng, 2004; Carvalho et al., 2006). These three pathways have only been defined in yeast. It is likely that distinctions between these pathways became blurred as higher eukaryotes evolved larger numbers of and more complex secretory pathway residents (Vembar and Brodsky, 2008). ERAD-L and ERAD-C substrates are targeted to different E3 ligase complexes (Stolz and Wolf, 2010). After carbohydrate trimming and the mannosidase reaction mediated by the Htm1p-Pdi1p complex, ERAD-L substrates are scanned by Yos9p and delivered to its interacting partner Hrd3p, a type I TM protein that together with Hrd1p (a RING domain E3 ligase also known as Der3p) is part of an ER

membrane-embedded E3 ubiquitin ligase complex (Fig. 1.5) (Gauss et al., 2006). Hrd3p can also bind misfolded proteins independently of Yos9p (Gauss et al., 2006). In addition, despite their apparently glycan-specific function, Hrd3p and Yos9p also bind non-glycosylated misfolded proteins and the Hrd1 complex is also involved in the glycan-independent ERAD-L pathway (Bhamidipati et al., 2005; Kanehara et al., 2010). Proteins targeted for degradation are delivered to a channel that mediates retrotranslocation to the cytosol with the energy provided by the Cdc48 AAA-ATPase complex or by the 19S regulatory particle (RP) of the proteasome, which also harbors a ring of AAA-ATPases (Kalies et al., 2005; Xie and Ng., 2010; Kaiser and Römisch, 2015). The identity of the retrotranslocation channel is still a matter of debate, but Sec61p, Der1p and, more recently, Hrd1p have been proposed as channel candidates (Pilon et al., 1997; Ye et al., 2004; Carvalho et al., 2010). As proteins exit the retrotranslocon they are polyubiquitylated on the cytosolic side of the ER by the Hrd1 or Doa10 complexes, named for the E3 ubiquitin ligases that differentiate them (Fig. 1.5) (Stolz and Wolf, 2010; Thibault and Ng, 2012). This process promotes further retrotranslocation of the polyubiquitinated substrates and their recognition and subsequent degradation by the proteasome (Hiller et al., 1996). ERAD-C substrates require the ER membrane-integrated RING domain E3 ubiquitin ligase Doa10p that recognizes misfolded cytosolic domains (Fig. 1.5) (Plempner and Wolf, 1999; Vembar and Brodsky, 2008; Hirsch et al., 2009). After polyubiquitylation of misfolded membrane proteins, the ERAD-C pathway often merges with the ERAD-L pathway at the Cdc48 machinery level (Fig. 1.5) (Stolz and Wolf, 2010). The proteasome 19S RP on its own can also promote misfolded protein export from both yeast and mammalian ER (Lee et al., 2004; Wahlman et al., 2007; Kaiser and Römisch, 2015). In mammals, the 19S RP can also cooperate with Cdc48p both during proteasomal degradation of substrates that are difficult to unfold and during extraction of ERAD-M substrates, like 3-hydroxy-3-methylglutaryl coenzyme A (CoA) reductase (Isakov and Stanhill, 2011; Morris et

al., 2014). Little else is known about the pathway followed by ERAD-M substrates, but they also seem to be ubiquitylated by the Hrd1 complex (Carvalho et al., 2006).

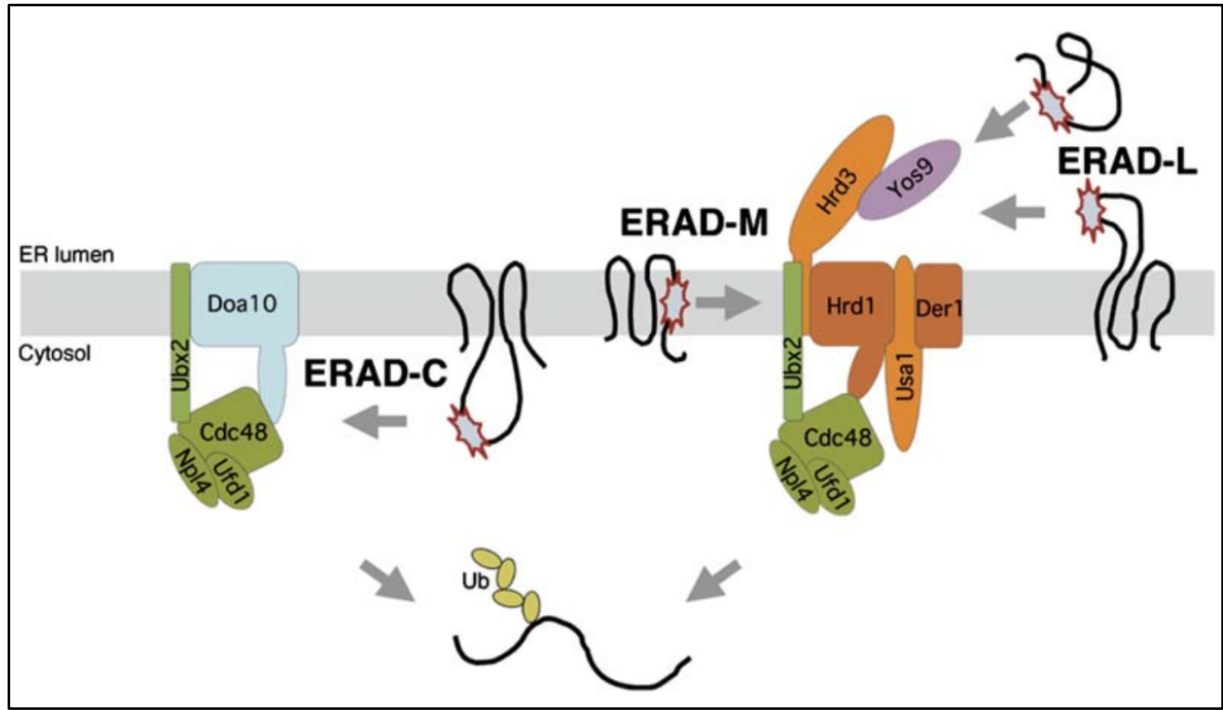


Figure 1.5. ERAD pathways in yeast. Ubiquitin ligase complexes involved in the ERAD-L, ERAD-M, and ERAD-C pathways. Components in orange and green belong to the Hrd1 and Cdc48 complexes, respectively. Stars show the location of the misfolded domain of a substrate. Der1p and Usa1p are membrane proteins part of the Hrd1 complex. Npl4p and Ufd1p are part of the Cdc48 complex. Ubx2p recruits the Cdc48 complex to the E3 ligases. Ub is ubiquitin (Carvalho et al., 2006).

1.4. The Unfolded Protein Response

Multiple physiological and pathological conditions can interfere with ERQC and lead to the accumulation of misfolded proteins in the ER (Gardner et al., 2013). To cope with the accumulation of misfolded proteins in the ER (termed “ER stress”) and maintain protein homeostasis, eukaryotic cells activate a series of adaptive mechanisms together known as the UPR (Hetz, 2012). The UPR mediates an increase in ER-folding capacity through the transcriptional up-regulation of ER folding, lipid biosynthesis, and ERAD machinery and, in mammals, at the same time a decrease in folding load through selective mRNA degradation

and translational repression (Travers et al., 2000; Hollien and Weissman, 2006; Gardner et al., 2013; Wu et al., 2014). If homeostasis in the ER cannot be reached again, the UPR can become cytotoxic and induce apoptosis (Lin et al., 2007).

In yeast, the only UPR transducer is the inositol requiring protein 1 (Ire1p), an ER-localized type I TM Ser/Thr kinase and site-specific endoribonuclease (Vembar and Brodsky, 2008). Under unstressed conditions, Kar2p binds to Ire1p on the luminal side of the ER membrane and contributes to maintaining the enzyme in an inactive state (Fig. 1.6) (Vembar and Brodsky, 2008). In the presence of ER stress, Kar2p is titrated away to bind to misfolded proteins and Ire1p, upon interaction with misfolded proteins, forms oligomeric assemblies triggered by self-association of the luminal domain (Fig. 1.6) (Gardner et al., 2013). At this stage, Ire1p activation involves the transphosphorylation of its cytosolic domain, which triggers endoribonuclease activity and splices an intron in the mRNA that encodes Hac1p, an UPR-specific transcriptional activator (Fig. 1.6) (Cox and Walter, 1996; Vembar and Brodsky, 2008). After Ire1p has removed the intron, the severed exons are ligated by tRNA ligase and the mRNA is translated to produce a transcription factor that up-regulates genes containing a conserved UPR element in their promoters (Fig. 1.6) (Travers et al., 2000; Gardner et al., 2013). In mammals, both the spliced and unspliced mRNAs for XBP1, the mammalian Hac1p homolog, are translated (Yoshida et al., 2001). The spliced form of XBP1 has higher transcriptional activator activity than the unspliced one (Yoshida et al., 2001). In higher eukaryotes, the UPR is mediated by three different ER-resident TM sensors: IRE1, the Ire1p homologue, PERK, a kinase that phosphorylates the translation initiation factor eIF2 α inhibiting global translation, and ATF6, which upon UPR activation travels to the Golgi where it is proteolytically released from the membrane and can thus translocate into the

nucleus to up-regulate genes to increase the folding capacity in the ER (van Anken and Braakman, 2005; Kimata and Kohno, 2011; Hetz, 2012).

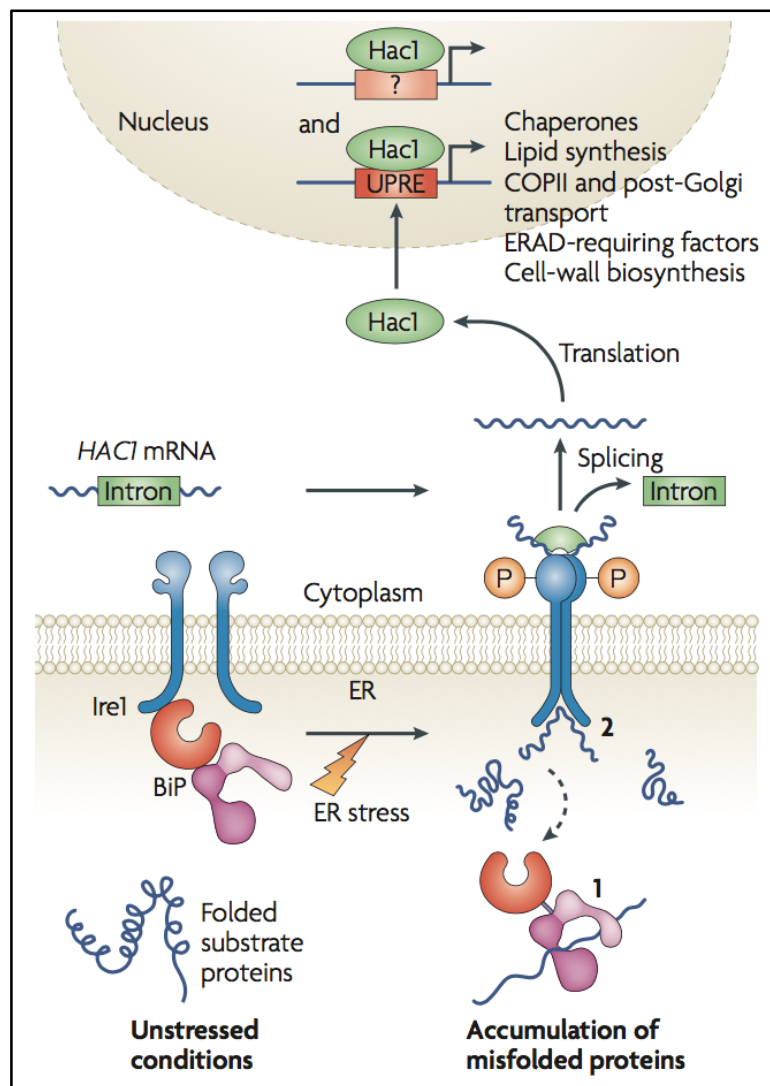


Figure 1.6. The UPR in yeast. Under unstressed conditions, Kar2p (BiP) binds to Ire1p in the ER lumen and maintains the enzyme in an inactive state. When the ER is stressed, Kar2p is titrated away to bind misfolded substrates, activating Ire1p (1). Ire1p dimerizes and might directly bind to misfolded proteins on the ER-luminal side, thus resulting in further activation (2). Ire1p activation involves the transphosphorylation of its cytosolic domain, which triggers endoribonuclease activity and splices an intron in the mRNA that encodes Hac1p. The processed mRNA is translated and Hac1p subsequently translocates into the nucleus, binds to UPR elements (UPREs) and up-regulates the expression of target genes (Vembar and Brodsky, 2008).

1.5. The Sec61 complex

The Sec61 channel translocates proteins across and integrates proteins into the ER membrane (Park and Rapoport, 2012). The identity of the retranslocation channel for ERAD substrates has been under intense investigation for 20 years. The Sec61 channel was the first proposed retrotranslocation channel (Wiertz et al., 1996). Sec61p was found to interact with ERAD substrates both in yeast and mammalian cells as well as with the yeast proteasome (Wiertz et al., 1996; Kalies et al., 2005; Römisch, 2005; Ng et al., 2007; Scott and Schekman, 2008; Schäfer and Wolf, 2009). The Sec61 channel consists of three proteins, Sec61p, Sbh1p, and Sss1p in yeast (Sec61 α , β , γ in mammals) (Johnson and van Waes, 1999). Sec61p and Sss1p are significantly conserved and essential (Wilkinson et al., 1996; Wilkinson et al., 1997). Sec61p forms the hourglass-shaped pore of the channel and surrounds the polypeptide chain during its passage across the ER membrane (Mothes et al., 1994). Sec61p is characterized by a compact bundle of 10 TM helices spanning the ER membrane with both termini in the cytoplasm (Fig. 1.7) (Mandon et al., 2013). The two symmetrical halves of the protein form an aqueous pore in the ER membrane, and the loop between TM domains 5 and 6 serves as a hinge allowing Sec61p to open at the front and form the lateral gate (Fig. 1.7) (Park and Rapoport, 2012; Mackinnon et al., 2014). At its narrowest point, the channel is lined by a pore ring of six hydrophobic residues that forms an opening of about 5-8 Å (Fig. 1.7) (van den Berg et al., 2003). Some of the Sec61p TM domains are not perpendicular to the plane of the membrane (TM domains 2, 5, 7), and some do not entirely span the membrane (TM domains 9, 10) (van den Berg et al., 2003). The segment following TM domain 1 continues as a long loop that runs along the external side of the molecule before leading back into the center of the molecule and ending in a short distorted helix called 2a, commonly referred to as the plug domain (Fig. 1.7) (van den Berg et al., 2003). This helix was predicted to be not particularly hydrophobic and localized in the external aqueous phase (Park and Rapoport,

2012). The N-terminus of Sec61p is oriented towards the cytosol and residues 3-21 have the potential to form an amphipathic α -helix (Wilkinson et al., 1996). Two evolutionarily conserved large loops of Sec61p, L6 and L8, protruding from the cytoplasmic side of the ER membrane are involved in ribosome binding during co-translational import into the ER (Cheng et al., 2005). The cytosolic C-terminus of Sec61p has also been shown to contact the ribosome and is functionally important (Harty and Römisch, 2013). The cytosolic face of the Sec61 channel also interacts with proteasomes in an ATP-dependent manner (Kalies et al., 2005). Proteasomes bind the Sec61 channel via the AAA-ATPases of the 19S RP and *in vitro* compete with ribosomes for ER membrane binding (Ng et al., 2007). The AAA-ATPase Cdc48p, involved in the delivery of both misfolded ERAD substrates and partially translocated proteins to the proteasome, can also bind to the Sec61 channel (Braunstein et al., 2015). The specific cytosolic domains of the Sec61 channel responsible for the interaction with AAA-ATPases, however, still remain to be determined (Ng et al., 2007).

Sbh1p and Sss1p are tail-anchored membrane proteins with single TM spans and both their N-termini in the cytosol (Fig. 1.7) (Toikkanen et al., 1996; van den Berg, 2003; Mandon et al., 2013). The cytosolic segment of Sbh1p is disordered and followed by a loop that crosses over the N-terminus of Sec61p (Fig. 1.7) (van den Berg et al., 2003). Its TM domain is perpendicular to the plane of the membrane and comes close to the C-terminus of Sss1p at the external side of the membrane (Fig. 1.7) (van den Berg et al., 2003). The Sbh1p TM domain is also close to transmembrane domain 4 of Sec61p (Zhao and Jääntti, 2009). Sss1p consists of two helices: the N-terminal helix is amphipathic and its hydrophobic surface is oriented towards the membrane, contacting the C-terminal part of Sec61p; the TM helix is curved and extends diagonally across the membrane clamping together the two halves of Sec61p (Fig. 1.7) (van den Berg et al., 2003; Park and Rapoport, 2012). A short β -strand

following the N-terminal helix of Sss1p forms a sheet with the segment between TM domains 6 and 7 of Sec61p (Wilkinson et al., 1997; van den Berg et al., 2003). Via its small subunits the Sec61 complex interacts with other TM protein complexes: the mammalian orthologue of Sbh1p, Sec61 β , mediates interaction with the signal peptidase complex, and its yeast homologue, Sbh2p (part of the Ssh1 complex described below), binds to the SRP receptor (Kalies et al., 1998; Jiang et al., 2008). Sbh1p and Sss1p also make contact with the oligosaccharyl transferase complex and the ribosome (Levy et al., 2001; Scheper et al., 2003; Chavan and Lennarz, 2005; Voorhees et al., 2014).

Crystal structures and crosslinking experiments indicated that the pore of the channel is formed by a single copy of the Sec61 channel (Osborne and Rapoport, 2007). Both in its resting state and when translocating a peptide, the Sec61 channel must prevent the free movement of small molecules, such as ions and metabolites (Park and Rapoport, 2012). In the resting state, the seal is provided by the interaction between the pore ring and the plug domain (Li et al., 2007). During translocation, the plug is displaced and the pore ring forms a gasket-like seal around the translocating peptide, which is itself the major obstacle for small molecules passing through the channel (Park and Rapoport, 2012). After termination of translocation across or integration into the ER membrane, the plug can return to the center of the Sec61 channel and reseal the channel restoring its interaction with the pore ring (Rapoport, 2007).

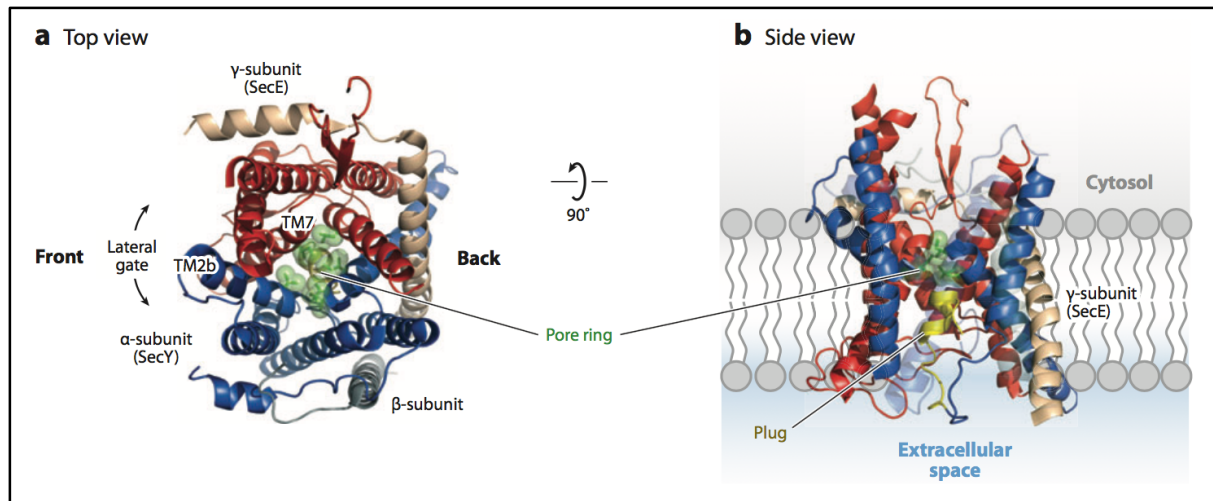


Figure 1.7. The Sec61p subunit. Crystal structure of the *Methanococcus jannaschii* SecY channel. (a) Channel viewed from the cytosol (top view). The N-terminal 1-5 TM segments of Sec61p (SecY in prokaryotes) are depicted in blue, and the C-terminal 6-10 TM segments in red. Sbh1p (β subunit) is depicted in gray and Sss1p (SecE in prokaryotes) in beige. Pore residues are shown as transparent spheres with side chains in green. The lateral gate is indicated. (b) Side view of the channel. The plug helix underneath the pore ring is depicted in yellow (Park and Rapoport, 2012).

In yeast a non-essential homolog of Sec61p, Ssh1p, forms a complex homologous to the Sec61 complex that contains the homolog of Sbh1p, Sbh2p, and Sss1p (Finke et al., 1996; Römisch, 1999). The expression levels of Ssh1p are comparable to the ones of Sec61p (Finke et al., 1996). The Ssh1 complex interacts with ribosomes, and only plays roles in co-translational protein translocation across the ER membrane (Wilkinson et al., 2001). The Ssh1 complex does not form heptameric Sec complexes with the Sec63 complex (Harty and Römisch, 2013). In addition, $\Delta ssh1$ cells displayed strong defects in the dislocation of a misfolded soluble ERAD substrate (Wilkinson et al., 2001). Given that a large amount of Sec61p is part of the heptameric Sec complex required for post-translational import into the ER, it is likely that under normal conditions Ssh1p contributes to the capacity of the ER in respect to both co-translational protein translocation and dislocation functions (Wilkinson et al., 2001). More recent data showed that specific co-translational import substrates can be delivered to the Ssh1 translocon in preference to the Sec61 channel (Spiller and Stirling,

2011). This suggests that the two translocons offer the potential for differential regulation that might favor the translocation of distinct subsets of precursors under certain physiological conditions (Spiller and Stirling, 2011).

1.6. The Sec61p N-terminus

Despite the fact that Sec61p structure and function have been extensively characterized, the role of its N-terminus in yeast is still unknown. In higher eukaryotes, the cytosolic N-terminus of Sec61 α contains a sequence motif, referred to as the IQ motif, which is recognized by calmodulin in a calcium-dependent manner during calcium signaling (Erdmann et al., 2011). After the binding of Ca²⁺, activated calmodulin binds to the Sec61 α IQ motif and induces channel closure, minimizing further calcium leakage (Erdmann et al., 2011). In mammalian cells, channel closure is also mediated by binding of Exotoxin A to the Sec61p N-terminus (Schäuble et al., 2014). In yeast cells, however, the vacuole, and not the ER, is the major site of intracellular calcium storage, and therefore there is no physiological need for translocon regulation dependent on calcium influx (Forster and Kane, 2000). Accordingly, the IQ motif is not conserved in yeast (Erdmann et al., 2011). The N-terminal region of yeast Sec61p is, however, likely to be functionally important, given that a 6-histidine tag at the Sec61p N-terminus in combination with point mutations elsewhere in the protein interferes with ER import, whereas the phenotype is much less severe in the absence of the tag (Pilon et al., 1998). The N-terminus of Sec61p is oriented towards the cytosol and residues 3-21 have the potential to form an amphipathic α -helix that may be partially embedded in the plane of the bilayer (Wilkinson et al., 1996). Together with the Sbh1p N-terminus, the Sec61p N-terminus is exposed at one side of the TM helix bundle forming the TM channel and thus poised to make contact with other proteins (van den Berg et al., 2003). This domain might therefore play an important role in mediating Sec61p interactions with

other proteins, besides stabilizing the translocon during channel opening via interaction with the cytosolic side of the ER membrane.

1.7. The Sec complex

To mediate post-translational translocation into the ER, the yeast Sec61 complex associates with the tetrameric Sec63 complex to form the heptameric Sec complex (Fig. 1.3) (Johnson and van Waes, 1999). The Sec63 complex is composed of Sec62p, Sec63p, Sec71p and Sec72p (Delic et al., 2013). Sec62p and Sec63p are essential (Wittke et al., 2000). Sec62p consists of two membrane-spanning regions that direct its N- and C- terminal domains into the cytosol (Deshaies and Schekman, 1990). Its N-terminal domain binds directly to Sec63p (Wittke et al., 2000). Sec62p has been proposed to recognize and bind to the signal peptide of nascent proteins destined for post-translational translocation (Wittke et al., 2000). In mammals, Sec62p interacts with ribosomes, suggesting an involvement in co-translational import into the ER (Müller et al., 2010). Sec63p is a TM ER protein with three TM domains, its N-terminus in the ER lumen and its long C-terminus in the cytosol (Feldheim et al., 1992; Servas and Römisch, 2013). The C-terminus is essential for the association with Sec62p and therefore for stabilizing the Sec complex (Brodsky et al., 1995; Wittke et al., 2000). The Sec63p C-terminus also mediates its association with Sec61p (Jermy et al., 2006). The Sec63p luminal J-domain between TM domains 2 and 3 is essential for recruiting Kar2p during post-translational translocation and also acts as a co-chaperone for Kar2p enhancing its ATP hydrolysis (Feldheim et al, 1992; Lyman and Schekman, 1995). Recent data also showed that the J-domain of Sec63p is required for ERAD of soluble proteins (Servas and Römisch, 2013). In yeast, Sec63p is also essential for co-translational protein import into the ER via both the Sec61 and the Ssh1 translocons (Brodsky et al., 1995; Young et al., 2001; Spiller and Stirling, 2011). In mammals, Sec63p is not essential for co-translational import

and seems to be involved in the regulation of polytopic protein integration in order to prevent ER membrane overload (Mades et al., 2012). Sec71p is a non-essential protein spanning the ER membrane one time (Feldheim et al., 1993). It was proposed to interact with the signal peptide of secretory precursors and contribute to transfer them to the translocation pore during post-translational translocation (Feldheim et al., 1993). Sec71p interacts with the non-essential peripheral membrane protein Sec72p, localized on the cytoplasmic side of the ER membrane (Feldheim and Schekman, 1994; Agarraberes and Dice, 2001). Sec72p may be also involved in signal peptide recognition for a defined subset of signal peptides or increase the efficiency of transfer of “difficult” post-translational secretory precursors to the translocation pore (Feldheim and Schekman, 1994). Deletion of both *SEC71* and *SEC72* causes temperature-sensitivity (Feldheim and Schekman, 1994). Neither gene has a homolog in mammals (Lakkaraju et al., 2012).

1.8. Protein N-terminal acetylation

Eukaryotic proteins are subjected to N-terminal acetylation (Fig. 1.8) (Arnesen et al., 2009). N-terminal acetylation can occur both co- and post-translationally, and about 50% of proteins in yeast, including Sec61p, Sbh1p, and Sec62p, and 80% of proteins in human cell lines are N-terminally acetylated (Helbig et al., 2010; Helsens et al., 2011; Soromani et al., 2012; Starheim et al., 2012). Several N-terminal acetyltransferases (NATs) with different specificities, NatA to NatE in yeast and NatA to NatF in humans, catalyze N-terminal acetylation of the different types of N-termini occurring in the proteome (Starheim et al., 2012). Due to its distinct substrate preference, NatF is responsible for the overall increase in protein acetylation observed in higher eukaryotes when compared to lower eukaryotes (Van Damme et al., 2011). NatA has specificity towards A-, S-, T-, V-, C-, and G-starting N-termini, whose initiator methionine has been removed by methionine amino peptidases

(Arnesen et al., 2009). NatD also acts on N-termini after removal of the initiator methionine, and, specifically, acetylates histones H2A and H4 (Song et al., 2003). N-termini that retain the initiator methionine are modified by NatB, NatC, NatE, NatF (Polevoda et al., 1999). NatB acetylates MD-, ME-, MN-, and MQ-starting N-termini, whereas NatC, NatE, and NatF act on Met-hydrophobic/amphipathic-type N-termini (ML-, MI-, MF-, MY-, and MK-starting) (Evjent et al., 2009; Starheim et al., 2009; Van Damme et al., 2011; Starheim et al., 2012).

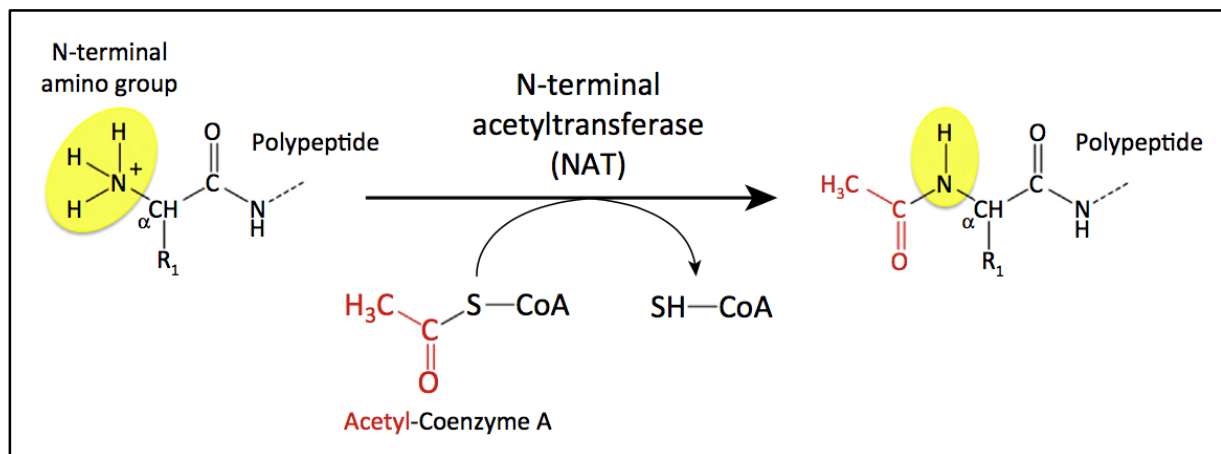


Figure 1.8. N-terminal acetylation of proteins by NATs. The reaction is enzymatically catalyzed by NATs that transfer the acetyl group (-COCH₃, in red) from acetyl CoA onto the N α -group (NH₃⁺, in yellow) of the first amino acid residue of the substrate protein (Aksnes et al., 2016).

The significance of N-terminal acetylation is only beginning to be understood. N-terminal acetylation of the Golgi-associated Arf-like GTPase Arl3p is essential for its subcellular localization (Behnia et al., 2004). Stirling and colleagues proposed that N-terminal acetylation constitutes a cytosol retention signal and inhibits post-translational protein translocation into the ER (Forte et al., 2011). In addition, several proteins showed increased affinity for their binding partners after undergoing this modification (Scott et al., 2011). N-terminal acetylation was also shown to increase helicity of the amphipathic N-terminus of α -

synuclein and its affinity for biological membranes (Dikiy and Eliezer, 2013). The most prominent (and controversial) effect of N-terminal acetylation, however, is related to protein stability. Despite being originally considered as a protection signal from N-terminal ubiquitylation and subsequent degradation, N-terminal acetylation recently emerged as a QC mechanism to target unfolded or misfolded proteins for degradation by the Ac/N-end rule pathway (Ciechanover and Ben-Saadon, 2004; Shemorry et al., 2013). Both scenarios might represent real events in the cell, with each applying to specific proteins under specific conditions (Starheim et al., 2012). These listed are only some examples of the many effects N-terminal acetylation has on proteins; nevertheless, our understanding of the cellular and physiological significance of this modification is still limited.

1.9. Aim of this study

The aim of this study was to gain insight into the function of the Sec61p N-terminus in yeast. Indeed, despite the fact that Sec61p structure and function have been extensively characterized, the role of its N-terminus is still unknown. In addition, Sec61p is N-terminally acetylated and a *sec61* mutant carrying a serine to tyrosine substitution in position 2 (*sec61S2Y*), which results in a non-cleavable and acetylated initiator methionine, is temperature-sensitive at 37°C (Soromani et al., 2012). The *sec61S2Y* substitution also results in a 2-fold increase in the half-life of the commonly used soluble ERAD substrate CPY* (Knop et al., 1996; KR, unpublished). I therefore investigated the effects of altering the sequence context or position of the N-acetylation site by further characterizing the *sec61S2Y* strain and generating a mutant carrying the deletion of the N-terminal residues 4-22 forming the amphipathic helix (*sec61ΔHI*). In addition, I generated a mutant lacking both the N-terminal acetylation site and the N-terminal residues 4-22 (*sec61ΔN21*). I investigated the effects of these mutations on co- and post-translational import into the ER and ERAD.

Furthermore, I asked whether the deletion of the N-terminal helix affected heptameric Sec complex formation and integrity of Sec61 complexes.

2. Materials and Methods

2.1. Materials

2.1.1. Laboratory equipment

The laboratory equipment used in this study is listed in Table 2.1.

Table 2.1. Laboratory equipment used in this study.

Company	Product
AGFA Healthcare GmbH	CP1000 X-ray film processor
Beckman Coulter Inc.	Optima L-90K ultracentrifuge Optima MAX-XP benchtop ultracentrifuge
Bio-Rad Laboratories Inc.	583 gel dryer PowerPac HC power supply Trans-Blot electrophoretic transfer cell
BioSpec Products Inc.	Mini-BeadBeater -24
Eppendorf AG	Microcentrifuge 5415R Thermomixer Comfort
GE Healthcare	Amersham autoradiography Hypercassettes Amersham Ultrospec 2100 pro UV/VIS spectrophotometer ImageQuant TL software Storage Phosphor Screens and cassettes Typhoon TRIO phosphorimager
Gilson Inc.	Pipette set
Hellma Analytics	Quartz cuvettes
Hirschmann GmbH & Co. KG	Pipet-Aid pipette controller
IKA-Werke GmbH & Co. KG	EUROSTAR power-b overhead stirrer RCT basic magnetic stirrer
Infors AG	Multitron Standard incubation shaker
Merck KGaA	Millipore MilliQ water purification system
neoLab Migge gmbH	Overhead rotator Rocking shaker
Roth GmbH & Co. KG	Neubauer Hemocytometer
Sartorius AG	Analytical balance
Scientific Industries Inc.	Vortex-Genie 2
Sigma Laborzentrifugen GmbH	4K15 refrigerated centrifuge
System	DX-150 autoclave

Thermo Fisher Scientific Inc.	XCell SureLock Mini-Cell electrophoresis system Sorvall Evolution RC centrifuge
VWR/PEQLAB	E-BOX VX2 gel documentation system peqSTAR 2X gradient thermocycler PerfectBlue Gelsystem Mini S
Zeiss Microscopy GmbH	Axioskop microscope
Wheaton	55 ml tissue grinder, Potter-ELV

2.1.2. Reagents, chemicals and consumables

The reagents, chemicals, and consumables used in this study are listed in Table 2.2. Chemicals not listed in Table 2.2 but mentioned in other sections of this thesis were purchased from the Zentrales Chemikalienlager at the University of Saarland.

Table 2.2. Reagents, chemicals and consumables used in this study.

Company	Product
AGFA Healthcare GmbH	G153 developer G354 rapid fixer
Agilent Technologies GmbH & Co. KG	QuikChange II Site Directed Mutagenesis Kit
Applichem GmbH	Ammonium acetate Ampicillin sodium salt HEPES – sodium salt Magnesium acetate Magnesium chloride Sodium acetate Sodium chloride Tunicamycin
Beckman Coulter GmbH	13 x 51 mm polycarbonate thick wall tubes 13 x 51 mm Ultra-Clear tubes
Becton, Dickinson & Company	Bacto peptone Bacto yeast extract Difco Yeast Nitrogen Base without amino acids Difco Yeast Nitrogen Base without amino acids and ammonium sulphate
Bio-Rad Laboratories Inc.	Nitrocellulose membrane, 0.2 µm
Biozym Scientific GmbH	Pipette tips
Corning Inc.	2 ml polypropylene cryogenic vials

	5-25 ml sterile pipettes
Formedium	Synthetic Complete dropout medium (-Ade, -His, -Leu, -Lys, -Trp, -Ura)
Fuji	Super RX medical X-ray films
GE Healthcare	Con A sepharose 4B Protein A sepharose CL-4B Whatman paper
Greiner Bio-One International GmbH	15, 50 ml tubes Petri dishes
Invitex GmbH	Invisorb Spin Plasmid Mini Two kit
Merck KGaA	Calbiochem cycloheximide
PerkinElmer Inc.	EXPRE ³⁵ S ³⁵ S Protein Labeling Mix, [³⁵ S]-, 50 mM tricine (pH 7.4), 10 mM 2-mercaptoethanol L-[³⁵ S]-methionine
Promega GmbH	Rabbit reticulocyte lysate system nuclease treated Ribo m ⁷ G cap analog RiboMAX large scale RNA production system – SP6 RNasin ribonuclease inhibitor Wizard DNA clean-up system
Roche Life Science	cOMplete, EDTA-free, protease inhibitor cocktail Creatine phosphate Creatine kinase from rabbit muscle
Rockland Immunochemicals Inc.	Horseradish peroxidase-conjugated anti-rabbit IgG (goat)
Roth GmbH & Co. KG	β-mercaptoethanol 2-nitrophenyl-β-D-galactopyranoside Agar-agar Glycerol Glycine Peptone from casein PMSF RNase AWAY Triton X-100 Yeast extract
Sarsedt	0.5-2 ml tubes PCR tubes
Sigma-Aldrich Co. LLC.	Adenine Bromophenol blue sodium salt D-(+)-glucose Deoxyribonucleic acid sodium salt from salmon testes DEPC-treated and sterile filtered water

	<p>Digitonin DL-diothiothreitol DMSO EDTA dianhydride Genelute HP plasmid maxiprep kit Glass beads, acid-washed 425-600 µm L-histidine L-leucine L-lysine L-tryptophan Lithium acetate dihydrate Nourseothricin sulfate Polyethylene glycol 4000 Sodium azide Sucrose Trizma base Tryptone enzymatic digest from casein Tween 20 Uracil Urea</p>
Sucofin	Skimmed milk powder
Thermo Fisher Scientific Inc.	<p>20X NuPAGE MES SDS running buffer 20X NuPAGE MOPS SDS running buffer 5-fluoroorotic acid FastDigest <i>Xba</i>I GeneRuler 1 kb DNA ladder NuPAGE Novex 4-12% bis-tris mini-gels, 1.5 mm, 10 wells Nalgene polypropylene 50, 500 ml centrifuge tubes Nalgene Rapid-Flow sterile disposable 250, 500 ml filters PageRuler prestained protein ladder SuperSignal West Dura extended duration chemiluminescent substrate</p>
VWR/PEQLAB	<p>Ethanol absolute KAPA HiFi HotStart PCR kit Latex and nitrile gloves</p>

2.1.3. *E. coli* and *S. cerevisiae* strains

Genotypes and origins of the *E. coli* and *S. cerevisiae* strains used in this study are listed in Tables 2.3 and 2.4, respectively.

Table 2.3. *E. coli* strains used in this study.

Strain	Genotype	Reference/source
DH5 α	<i>F</i> - <i>endA1 glnV44 thi-1 recA1 relA1 gyrA96 deoR nupG Φ 80dlacZΔM15 Δ(lacZYA-argF)U169, hsdR17(rK- mK+), λ-</i>	Hanahan, 1983
HB101	<i>F</i> <i>mcrB mrr hsdS20(r_B⁻ m_B⁻) recA13 leuB6 ara-14 proA2 lacY1 galK2 xyl-5 mtl-1 rpsL20(Sm^R) glnV44 λ-</i>	Boyer and Roulland-Dussoix, 1969
KRB3	<i>E. coli</i> DH5 α carrying the YCpG1S plasmid for lyticase expression	Shen et al., 1991
KRB38	<i>E. coli</i> HB101 carrying the pDJ100 plasmid	Hansen et al., 1986
KRB733	<i>E. coli</i> DH5 α carrying the pJC30 plasmid	Ng lab
KRB734	<i>E. coli</i> DH5 α carrying the pJC31 plasmid	Ng lab
KRB764	<i>E. coli</i> DH5 α carrying the pRS424- <i>SBH1</i> plasmid	Römisch lab
KRB785	<i>E. coli</i> DH5 α carrying the pRS414 empty plasmid	Römisch lab
KRB787	<i>E. coli</i> DH5 α carrying the pRS414- <i>SBH1</i> plasmid	Römisch lab
KRB1003	<i>E. coli</i> DH5 α carrying the pRS315- <i>sec61ΔH1</i> plasmid	This study
KRB1004	<i>E. coli</i> DH5 α carrying the pRS315- <i>sec61ΔN21</i> plasmid	This study
KRB1074	<i>E. coli</i> DH5 α carrying the pMS529 plasmid	Schuldiner lab
XL1-Blue	<i>endA1 gyrA96(nal^R) thi-1 recA1 relA1 lac glnV44 F' [::Tn10 proAB⁺ lacI^q Δ(lacZ)M15] hsdR17(r_K⁻ m_K⁺)</i>	Agilent Technologies (QuikChange kit)

Table 2.4. *S. cerevisiae* strains used in this study.

Strain	Genotype	Source
KRY49	<i>ura3-52 leu2-3,112 pep4::URA3</i>	Römisch lab
KRY461	<i>SEC61::HIS3 ade2-1 leu2-3, 112 trp1-1 prc1-1 his3-11, 15 ura3-1 [pGALSEC61-URA3]</i>	Römisch lab
KRY588	<i>seb1::KanMX seb2::hphMX leu2-3, 112 ura3-52 GAL+</i>	Römisch lab
KRY904	<i>SEC61::HIS3 ade2-1 leu2-3, 112 trp1-1 prc1-1 his3-11, 1 ura3-1 [sec61S2Y-LEU2]</i>	Römisch lab
KRY992	<i>SEC61::HIS3 ade2-1 leu2-3, 112 trp1-1 prc1-1 his3-11, 15 ura3-1 [sec61ΔH1-LEU2]</i>	This study
KRY993	<i>SEC61::HIS3 ade2-1 leu2-3, 112 trp1-1 prc1-1 his3-11, 15 ura3-1 [sec61ΔN21-LEU2]</i>	This study

2.1.4. Plasmids

Plasmids used in this study are listed in Table 2.5.

Table 2.5. Plasmids used in this study.

Plasmid	Characteristics	Source
pDJ100	ppαF gene cloned into pSP65 behind SP6 promoter	Schekman lab
pJC30	CYC1 TATA box fused to <i>LacZ</i> in pRS314	Ng lab
pJC31	<i>UPRE-LacZ</i> reporter construct in pRS314	Ng lab
pMS529	PDI-DHFR-3Gly-3HA fusion protein under the control of a <i>GAL1</i> promoter in pYM-24	Schudiner lab
pRS315- <i>SEC61</i>	<i>SEC61</i> in pRS315	Römisch lab
pRS315- <i>sec61ΔH1</i>	<i>sec61ΔH1</i> in pRS315	This study
pRS315- <i>sec61ΔN21</i>	<i>sec61ΔN21</i> in pRS315	This study
pRS414	Empty plasmid; control for pRS414- <i>SBH1</i>	Römisch lab
pRS414- <i>SBH1</i>	<i>SBH1</i> in pRS414	Römisch lab
pRS424- <i>SBH1</i>	<i>SBH1</i> in pRS424 for overexpression	Römisch lab

2.1.5. Primers

Primers used in this study and their applications are listed in Table 2.6.

Table 2.6. Primers used in this study.

Primer	Sequence (5'-3')	Application
Clogging-HOClone-F	AAATCCATATCCTCATAAGCAGCAATCAATT CTATCTATACGTACGCTGCAGGTCGAC	Amplification of the integrative clogger construct from pMS529 plasmid
Clogging-HOClone-R	AAATTTTACTTTTATTACATACTTTTAA ACTAATATGCCTTTTACGGTTCCTGGCC	Amplification of the integrative clogger construct from pMS529 plasmid
dh-fwd	CGCTTACTTTGAAAATGTCCTCCCCAGAAA GGAAGGTTCCATAACAACC	Generation of the pRS315- <i>sec61</i> Δ <i>H1</i> plasmid from pRS315- <i>SEC61</i>
dh-rev	GGTTGTATGGAACCTTCCTTTCTGGGGAGGA CATTTTCAAAGTAAAGCG	Generation of the pRS315- <i>sec61</i> Δ <i>H1</i> plasmid from pRS315- <i>SEC61</i>
dhdnac-fwd	CGCTTACTTTGAAAATGCCAGAAAGGAAGG TTCC	Generation of the pRS315- <i>sec61</i> Δ <i>N21</i> plasmid from pRS315- <i>SEC61</i>
dhdnac-rev	GGAACCTTCCTTTCTGGCATTTCAAAGTAAA GCG	Generation of the pRS315- <i>sec61</i> Δ <i>N21</i> plasmid from pRS315- <i>SEC61</i>

2.1.6. Antibodies

Antibodies used in this study are listed in Table 2.7.

Table 2.7. Antibodies used in this study and their working dilutions.

Antibody	Dilution	Source
anti- α factor (rabbit)	Western blot: 1:2000	Römisch lab
anti-CPY (rabbit)	Western blot: 1:2000 IP: 1:100	Römisch lab
anti-DPAPB (rabbit)	IP: 1:100	Stevens lab
anti-HA (rabbit)	Western blot: 1:5000	Rockland Inc.
anti-Pdi1p (rabbit)	Western blot: 1:5000	Römisch lab
anti-Rpn12p (rabbit)	Western blot: 1:2000	Römisch lab
anti-Sbh1p (rabbit)	Western blot: 1:2000	Römisch lab
anti-Sec61p (C-terminus) (rabbit)	Western blot: 1:2000	Römisch lab
anti-Sec61p (N-terminus) (rabbit)	Western blot: 1:2000	Römisch lab
anti-Sec63p (rabbit)	Western blot: 1:2500	Schekman lab
anti-Sss1p (rabbit)	Western blot: 1:2500	Schekman lab
Horseradish peroxidase-conjugated anti-rabbit (goat)	Western blot: 1:2500	Rockland Inc.

2.1.7. Growth media

S. cerevisiae cells were routinely grown in YPD or YPG (1% yeast extract, 2% peptone, 2% glucose or galactose, respectively) or minimal medium [0.67% Yeast Nitrogen Base without amino acids, 0.13% Synthetic Complete dropout medium (-Ade, -His, -Leu, -Lys, -Trp, -Ura), 2% glucose or galactose, individual amino acids according to auxotrophies (concentrations shown in Table 2.8)]. *E. coli* cells were routinely grown in LB (0.5% yeast extract, 1% tryptone) in the absence or presence of 100 μ g/ml ampicillin. All media were autoclaved (YPD, YPG, LB) or filter sterilized (minimal medium). Glucose, galactose, and ampicillin were filter-sterilized and added to the respective medium prior to use. Solid growth media were prepared by dissolving 2% agar-agar into each medium.

Table 2.8. Concentrations of Ade, His, Leu, Lys, Trp and Ura in minimal medium.

Component	Concentration (mg/l)
Adenine	18
L-histidine	76
L-leucine	380
L-lysine	76
L-tryptophan	76
Uracil	76

2.2. Methods

2.2.1. Sterilization

All glassware and media were sterilized by autoclaving at 100 kPa and 121°C for 20 min unless otherwise stated.

2.2.2. Growth of *E. coli*

E. coli cells were grown at 37°C in LB medium with continuous shaking at 200 rpm or on LB plates unless otherwise stated.

2.2.3. Growth of *S. cerevisiae*

S. cerevisiae cells were grown at 30°C in YPD or YPG (KRY461) with continuous shaking at 200 rpm or on YPD or YPG (KRY461) plates unless otherwise stated.

2.2.4. Polymerase chain reaction

The polymerase chain reaction (PCR) was employed in this study to generate the *sec61ΔHI* and *sec61ΔN2I* mutations and to amplify from the pMS529 plasmid an integrative construct that encodes a post-translational ER import substrate that clogs the Sec61 channel (Ast et al.,

2016). The sequences of the primers used are listed in Table 2.6. The *sec61ΔH1* and *sec61ΔN21* mutations were obtained by PCR-mediated DNA deletion of a pRS315 plasmid carrying the *SEC61* gene using the QuikChange kit (Agilent Technologies) according to the manufacturer's instructions (Hansson et al., 2008). Reaction parameters were as follows: initial denaturation at 95°C for 30 sec; 18 cycles each of denaturation at 95°C for 30 sec, annealing at 43°C for 1 min, and extension at 68°C for 8 min. Samples were stored at 4°C until further use. Deletions of the N-terminal residues 4-22 and 2-22 of Sec61p, respectively, were confirmed by DNA sequencing (LGC Genomics). The pRS315-*sec61ΔH1* and pRS315-*sec61ΔN21* plasmids were transformed into *E. coli* DH5α competent cells (see 2.2.7) and added to our recombinant strain collection (KRB1003 and KRB1004, respectively). Amplification of the clogger construct from the pMS529 plasmid was performed using the KAPA HiFi HotStart PCR kit (VWR). Reaction parameters were as follows: initial denaturation at 95°C for 5 min; 35 cycles each of denaturation at 98°C for 20 sec, annealing at 58.5°C for 15 sec, and extension at 72°C for 2 min; final extension at 72°C for 5 min. Success of the amplification reaction was assessed by agarose gel electrophoresis. Samples were stored at 4°C until further use.

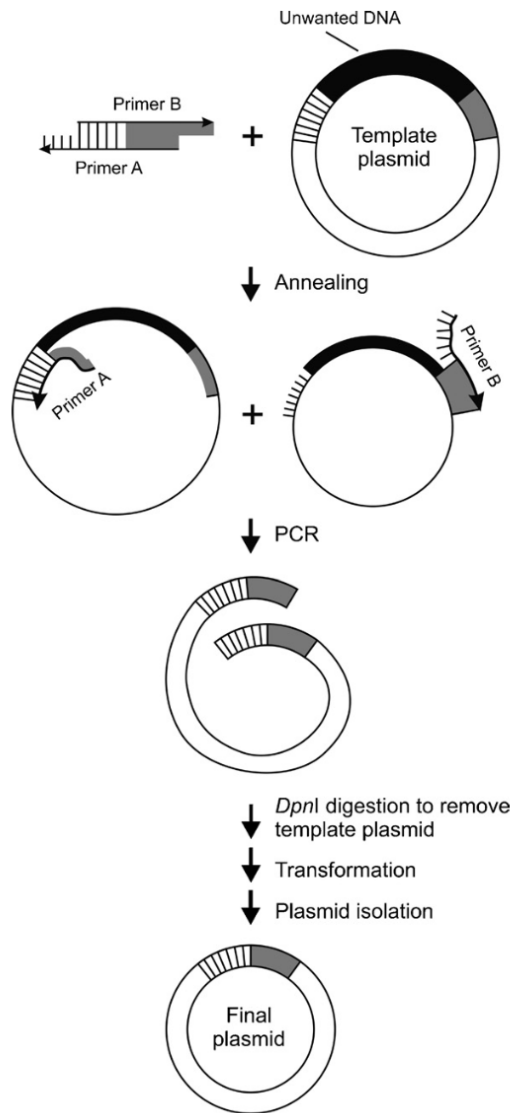


Figure 2.1. Schematic representation of the PCR-mediated plasmid DNA deletion method. DNA to be deleted is depicted in black. The complementary features of the A and B primers and the plasmid are indicated by gray and striped segments. The steps resulting in the final construct are indicated by arrows (Hansson et al., 2008).

2.2.5. Agarose gel electrophoresis

Agarose gel electrophoresis was performed to separate DNA fragments. DNA samples were mixed with loading buffer (6X: 50% sucrose, 0.15% bromophenol blue, 0.02 M EDTA) and loaded onto 1% agarose gels (2% 50X TAE, 90% dH₂O, 0.5 µg/ml ethidium bromide). Electrophoresis was carried out at 100 V for approximately 1 h using a PowerPac HC power

supply (Bio-Rad) and a PerfectBlue Gelsystem Mini S (PEQLAB) containing 1X Tris acetate EDTA buffer (TAE; 50X: 20 M Tris-HCl, pH 8.4, 10 M acetic acid, 0.05 M EDTA). Five μ l of GeneRuler 1 kb DNA ladder (Thermo Fisher Scientific) were routinely loaded as a size standard. Data were acquired using the E-BOX VX2 gel documentation system (PEQLAB) in UV mode.

2.2.6. Preparation of chemically competent competent *E. coli* cells

E. coli DH5 α cells were grown to an OD₆₀₀ of approximately 0.5-0.7 and subsequently centrifuged at 4000 rpm at 4°C for 6 min (Sorvall Evolution RC centrifuge, SLA3000 rotor). The pellet was resuspended in 8.5 ml of cold and sterile TFPI buffer at pH 5.8 (30 mM KOAc, 100 mM KCl, 10 mM CaCl₂, 50 mM MnCl₂, 10% glycerol) and incubated on ice for 10 min. After centrifugation at 4000 rpm at 4°C for 6 min, the pellet was resuspended in 1 ml of cold and sterile TFPII buffer at pH 6.5 (10 mM KCl, 75 mM CaCl₂, 10% glycerol, 10 mM MOPS) and incubated on ice for 30 min. The sample was then divided into small volume aliquots that were flash frozen in liquid nitrogen and stored at -80°C until use.

2.2.7. Transformation of chemically competent *E. coli* cells

To generate recombinant bacteria, 10-100 ng of plasmid DNA were added to 100 μ l of chemically competent *E. coli* DH5 α cells. Cells were incubated for 20 min on ice and subsequently heat-shocked at 42°C for 2 min. Next, 700 μ l of prewarmed LB medium were added and cells were incubated for 1 h at 37°C under shaking at 900 rpm. After centrifugation (1 min, 10000 rpm; Eppendorf 5415 R microcentrifuge), the supernatant was discarded by decanting and cells were resuspended in the residual LB medium. Cells were

finally plated onto LB agar plates containing the appropriate selection marker (100 µg/ml ampicillin).

2.2.8. Transformation of *S. cerevisiae*

Two ml of an overnight (ON) *S. cerevisiae* culture were harvested at 3000 rpm for 2 min (Eppendorf 5415 R microcentrifuge). Cells were washed with 1 ml of LiAc/TE buffer (100 mM LiAc, 10 mM Tris-HCl, pH 7.5, 1 mM EDTA) and after centrifugation at 3000 rpm for 2 min resuspended in 100 µl of LiAc/TE buffer. Subsequently, 20 µl of 10 mg/ml denatured carrier DNA (from salmon testes), 1 µg of plasmid or integrative DNA and 600 µl of PEG buffer (50% PEG 4000, 100 mM LiAc, 10 mM Tris-HCl, pH 7.5, 1 mM EDTA) were added to the suspension. Next, 50 µl of 1 M LiAc (pH 7.5) were added to the suspension and cells incubated for 1 h at 30°C. After incubation, 20 µl of DMSO were added to the suspension and cells heat-shocked at 42°C for 15 min. Cells were then centrifuged at 3000 rpm for 2 min and washed 2 times with 1 ml of TE buffer. The pellet was resuspended in 100 µl of TE buffer and plated onto agar plates with the appropriate selection medium. More specifically, cells transformed with the pRS314, pRS414, and pRS424 plasmids were selected on minimal medium without triptophan; cells transformed with the integrative clogger construct were selected on YPD or YPG in the presence of 100 µg/ml nourseothricin; KRY461 (genotype in Table 2.4) cells transformed with the pRS315-*sec61ΔH1* and pRS315-*sec61ΔN21* plasmids were selected on minimal medium without leucine at 30°C, and subsequently selected on minimal medium without leucine at 30°C in the presence of 1 g/l 5-fluoroorotic acid.

2.2.9. Drop test

To test temperature-sensitivity, serial dilutions of yeast cultures were prepared and 5 μ l of each dilution containing 10^4 - 10^7 cells were dropped onto YPD, YPG (KRY461), or minimal medium plates and incubated at the indicated temperatures for 3 or 3.5 days. To test tunicamycin sensitivity, serial dilutions were prepared and 5 μ l of each dilution containing 10^4 - 10^7 cells were dropped onto YPD or YPG (± 0.25 μ g/ml tunicamycin) plates. Plates were incubated at the indicated temperatures for 3.5 days.

2.2.10. β -galactosidase assay

The investigated strains were transformed with the plasmids pJC31, a pRS314 plasmid carrying the *UPRE-LacZ* reporter construct, and the control plasmid pJC30, a pRS314 plasmid carrying the *LacZ* gene (Cox et al., 1993). Cells were grown in synthetic complete medium without tryptophan to an OD₆₀₀ of approximately 0.5 and aliquots of 1 ml were harvested by centrifugation and resuspended in 1 ml of Z buffer (60 mM Na₂HPO₄, 40 mM NaH₂PO₄, 10 mM KCl, 1 mM MgSO₄, 0.27% β -mercaptoethanol). Subsequently, 100 μ l of chloroform and 50 μ l of 0.1% SDS were added to each sample; after 10 s of vortexing, samples were pre-incubated for 5 min at 28°C in a water bath, and reactions were induced with 200 μ l of 4 mg/ml 2-nitrophenyl- β -D-galactopyranoside Z buffer. After 20 min of incubation at 28°C, reactions were stopped by adding 500 μ l of 1 M Na₂CO₃, samples centrifuged, and supernatants analyzed photometrically at 420 nm to calculate β -galactosidase units using the following formula:

$$\beta\text{-gal units: } 1000 \times [\text{OD}_{420}/(\text{OD}_{600} \times v \times t)]$$

where OD₄₂₀ is the optical density of the reaction product, OD₆₀₀ is the optical density of each culture, v is the volume of culture used in the assay, and t is the time of the assay.

2.2.11. Preparation of yeast cell extracts and cycloheximide chase

An equal amount of cells (1 OD₆₀₀) was taken from each fresh ON culture, washed with sterile water, resuspended in 50 µl of 2x SDS-buffer (100 mM Tris-HCl, pH 6.8, 4% SDS, 0.2% bromophenol blue, 20% glycerol, 200 mM DTT) and lysed with glass beads (Sigma) in a Mini-Beadbeater-16 (BioSpec; two 1 min disruption cycles at 4°C with 1 min of incubation at 4°C between cycles). Lysates were heated for 10 min at 65°C in a Thermomixer Comfort (Eppendorf) before Western blot analysis as described in 2.2.13. For CHX chases, ON cultures were treated with 200 µg/ml CHX (Merck) and equal amounts of cells (1 OD) were taken at the indicated time points before lysis and Western blotting.

2.2.12. Protein gel electrophoresis

SDS-polyacrylamide gel electrophoresis (SDS-PAGE) was routinely employed to resolve proteins based on their electrophoretic mobility. Samples were resuspended in 2x SDS-buffer, heated for 5 min at 95°C (10 min at 65°C when investigating membrane proteins), and loaded onto NuPAGE Novex 4-12% Bis-Tris protein gels (Thermo Fisher Scientific). Electrophoresis was carried out at 100 V for approximately 1 h using a PowerPac HC power supply (Bio-Rad) and an XCell SureLock Mini-Cell electrophoresis system (Thermo Fisher Scientific) containing 1X MOPS (Thermo Fisher Scientific) or 1X MES buffer (Thermo Fisher Scientific) when smaller proteins were investigated. Six µl of PageRuler prestained protein ladder were routinely loaded as a size standard.

2.2.13. Western blot analysis

Western blot analysis was employed to detect proteins of interest using specific antibodies. Following SDS-PAGE, proteins were transferred to nitrocellulose membranes (0.2 µm; Bio-

Rad) using a PowerPac HC power supply and Trans-Blot electrophoretic transfer cell (Bio-Rad) filled with transfer buffer (0.2% SDS, 20% methanol, 25 mM Tris, 200 mM glycine). The transfer was carried out at 4°C either at 100 V for 1.5 h or at 300 mA ON. After the transfer, membranes were blocked with 5% milk powder TBS-T (50 mM Tris-HCl, pH 7.4, 150 mM NaCl, 0.1% Tween 20, 5 mM sodium azide) under shaking at RT for 1 h or ON at 4°C on a standard rocking shaker (neoLab) and subsequently incubated with the primary antibody diluted in 5% milk powder TBS-T under shaking at RT for 2 h or ON at 4°C. Membranes were then washed 2 times for 10 min with 5% milk powder TBS-T and 2 times for 10 min with TBS-T and incubated with the secondary antibody diluted in TBS-T under shaking at RT for 1 h. After 5 or 6 5-min washes with TBS-T, signals were developed using the SuperSignal West Dura extended duration chemiluminescent substrate (Thermo Fisher Scientific) and acquired on Super RX medical X-ray films (Fuji) by autoradiography. Quantitations were performed using the ImageQuant TL software (GE Healthcare).

2.2.14. Pulse-labeling and immunoprecipitation

Cells were grown ON in YPD or YPG to an OD₆₀₀ of 0.5-1 and washed 2 times with labeling medium (5% glucose or galactose, 0.67% yeast nitrogen base without amino acids and ammonium sulfate) supplemented with auxotrophy-complementing amino acids and concentrated to 6 OD/ml. Each 250- μ l cell suspension was preincubated at 30°C (unless otherwise stated) under shaking at 600 rpm for 15 min, and subsequently labeled for 5 min adding 55 μ Ci of EXPRE³⁵S³⁵S Protein Labeling Mix (PerkinElmer). Labeling was stopped by adding 750 μ l of ice-cold Tris-azide (20 mM Tris, pH 7.5, 20 mM sodium azide); cells were subsequently washed with 1 ml of Tris-azide and incubated for 10 min at room temperature (RT) in resuspension buffer (100 mM Tris, pH 9.4, 10 mM DTT, 20 mM sodium azide). After centrifugation, cells were lysed with glass beads (Sigma) in 150 μ l of lysis

buffer (20 mM Tris, pH 7.5, 2% SDS, 1 mM DTT, 1 mM PMSF) and the lysate denatured for 10 min at 65°C. Glass beads were washed and the collected supernatant was used for immunoprecipitation with 60 µl of a 20% suspension of Protein A Sepharose beads CL-4B (GE Healthcare) and 10 µl of polyclonal rabbit antisera against CPY or DPAPB in IP buffer (15 mM Tris, pH 7.5, 150 mM NaCl, 1% Triton X-100, 0.1% SDS, 2 mM sodium azide) for 2 h at 4°C. Precipitates were washed in IP buffer, urea wash (100 mM Tris, pH 7.5, 2 M urea, 200 mM NaCl, 1% Triton X-100, 2 mM sodium azide), Con A wash (20 mM Tris, pH 7.5, 500 mM NaCl, 1% Triton X-100, 2 mM sodium azide), Tris-NaCl wash (10 mM Tris, pH 7.5, 50 mM NaCl, 2 mM sodium azide), incubated for 10 min at 65°C in 2x SDS-buffer and resolved by gel electrophoresis. Gels were dried for 2 h at 80°C using a 583 gel dryer (Bio-Rad) and signals were acquired by autoradiography on Storage Phosphor Screens (GE Healthcare) and developed using a Typhoon Trio imager (GE Healthcare).

2.2.15. Lyticase preparation

A 10-l culture (8 flasks, each containing 1.25 l of culture) of the KRB3 strain was grown to an OD_{600} of 0.5 and subsequently induced with 0.5 mM IPTG. After 5 h, cells were centrifuged for 5 min at 8000 rpm at 4°C (Sorvall Evolution RC centrifuge, GSA rotor) and resuspended in 400 ml of 25 mM Tris-HCl, pH 7.4. Cells were then centrifuged for 5 min at 8000 rpm at 4°C and pellets resuspended in 200 ml of 25 mM Tris-HCl, 2 mM EDTA, pH 7.4. Next, 200 ml of 40% sucrose 25 mM Tris-HCl, pH 7.4 were added to the suspension, which was gently stirred for 20 min at RT on an RCT basic magnetic stirrer (IKA). The suspension was centrifuged for 10 min at 8000 rpm at 4°C and the supernatant completely discarded. The pellet was resuspended in 150 ml of ice-cold 0.5 mM $MgSO_4$, gently stirred at 4°C for 20 min and centrifuged for 10 min at 8000 rpm at 4°C (SS34 rotor). The supernatant (containing lyticase) was collected in 10-ml aliquots, flash frozen in liquid nitrogen and

stored at -80°C until use. The activity of the enzyme was tested on the KRY49 yeast strain. The strain was grown to an OD_{600} of approximately 2, centrifuged for 5 min at 4200 rpm at RT (SS34 rotor) and resuspended in 100 mM Tris-HCl, pH 9.4, 10 mM DTT (freshly added) to an OD_{600} of approximately 2. After 10 min of incubation at RT, cells were harvested by centrifugation for 5 min at 4200 rpm at RT and resuspended in 50 mM Tris-HCl, pH 7.4, 10 mM DTT (freshly added) to an OD_{600} of approximately 2. Aliquots (1 ml) of the suspension were incubated with different amounts of lyticase (0, 0.1, 0.25, 0.5, 1, 2 μl) at 30°C for 30 min and their OD_{600} measured immediately after incubation. One unit of lyticase was defined as the amount of enzyme inducing a 10% decrease in the OD_{600} of the cell suspension after the 30-min incubation. A successful preparation protocol was considered to yield a lyticase concentration of 30000 U/ml or higher.

2.2.16. Preparation of rough yeast microsomes

Five l of a yeast culture were grown to an OD_{600} of approximately 2-3. Cells were harvested at 5000 rpm for 3 min at RT (Sorvall Evolution RC centrifuge, SLA3000 rotor), resuspended in 100 mM Tris-HCl, pH 9.4, 10 mM DTT to 100 $\text{OD}_{600}/\text{ml}$ and incubated for 10 min at RT. Cells were then centrifuged for 3 min at 5000 rpm and resuspended in lyticase buffer (50 mM Tris-HCl, pH 7.5, 0.75x YP, 700 mM sorbitol, 0.5% glucose, 10 mM DTT) to 100 $\text{OD}_{600}/\text{ml}$. Subsequently, 40 U/ OD_{600} lyticase was added, and the cell suspension was incubated under shaking at 80 rpm for 20 min at 30°C (Infors Multitron Standard incubation shaker). Cultures were transferred to ice and cells harvested at 5000 rpm for 5 min at 4°C . Spheroplasts were then gently resuspended in cold 2x JR lysis buffer (40 mM HEPES-KOH, pH 7.4, 400 mM sorbitol, 100 mM KOAc, 4 mM EDTA) to 250 $\text{OD}_{600}/\text{ml}$ and centrifuged at 10000 rpm for 5 min at 4°C (Sorvall Evolution RC centrifuge, SS34 rotor). Next, spheroplasts were gently resuspended in cold 2x JR lysis buffer to 500 $\text{OD}_{600}/\text{ml}$ and incubated at -80°C for at least 45

min. Spheroplasts were then thawed in a water bath at RT and an equal volume of cold Milli-Q water containing 1 mM DTT and 1 mM PMSF was added to the suspension. Spheroplasts were disrupted with 10 strokes of an EUROSTAR power-b homogenizer (IKA) at 4°C and the lysate was centrifuged at 3000 rpm for 5 min at 4°C; the supernatant was transferred to a new tube and centrifuged at 17500 rpm for 15 min at 4°C (Sorvall Evolution RC centrifuge, SS34 rotor). The pellet was resuspended in 100 µl of cold B88 (20 mM HEPES-KOH, pH 6.8, 250 mM sorbitol, 150 mM KOAc, 5 mM Mg(OAc)₂), homogenized on ice with a small teflon pestle, and loaded onto a 1.2/1.5 M sucrose gradient (20 mM HEPES-KOH, pH 7.5, 50 mM KOAc, 2 mM EDTA, 1 mM DTT, 1.2 or 1.5 M sucrose). The gradient was centrifuged at 44000 rpm for 70 min at 4°C in an Optima L-90K ultracentrifuge (Beckman Coulter) using an SW 60 Ti rotor (Beckman Coulter). Microsomes were collected at the 1.2/1.5 M sucrose interface, transferred to a fresh tube, resuspended in approximately 25 ml of cold B88, and centrifuged at 17500 rpm for 15 min at 4°C (Sorvall Evolution RC centrifuge, SS34 rotor). The pellet was resuspended in a minimal volume of B88 (approximately 300 µl) and the OD₂₈₀ of a 1:200 dilution in 2% SDS of the suspension was measured. The concentration of the microsome suspension was adjusted to an OD₂₈₀ of 30 and the sample was then divided into 20-µl aliquots that were flash frozen in liquid nitrogen and stored at -80°C until use.

2.2.17. *In vitro* transcription

All of the following steps were performed under RNase-free conditions. The pDJ100 plasmid was linearized with the *Xba*I restriction enzyme (Thermo Scientific) for 5 min at 37°C. After digestion, the linearized plasmid was cleaned up with the Wizard DNA clean-up system (Promega) according to the manufacturer's instructions. The ppαF RNA was transcribed from the linearized pDJ100 plasmid using the RiboMAX large-scale RNA production system - SP6 (Promega) kit according to the manufacturer's instructions. To produce capped

transcripts that could mimic the structure of mRNA and to prevent their degradation by ribonucleases, the Ribo m⁷G cap analog (Promega; final concentration: 0.25 mM) and the RNasin ribonuclease inhibitor (Promega; final concentration: 1.2 U/μl), respectively, were added to the reaction mixture. To remove unincorporated nucleotides and chloride ions that could interfere with translation, transcripts were precipitated by adding 0.1 ml of cold 100% ethanol and 4 μl of 3 M NaAc and incubated at -20°C for 30 min. Transcripts were centrifuged for 10 min at 4°C at full speed (Eppendorf 5415 R), the supernatant was discarded and 150 μl of cold 70% ethanol were added to the pellet. After 10 min of centrifugation at full speed at 4°C, the supernatant was discarded and the pellet was air-dried at RT for approximately 5 min. The pellet was then resuspended in 20 μl of DEPC-treated and sterile-filtered water and transferred to ice. To calculate the amount of transcript obtained with the reaction, the OD₂₆₀ of a 1:200 dilution of the suspension was determined (1 OD₂₆₀ = 40 μg/ml RNA). The purity of the sample was considered sufficient and devoid of significant protein contamination if OD₂₆₀/OD₂₈₀ > 2.

2.2.18. *In vitro* post-translational translocation

For *in vitro* post-translational import experiments, ppαF was translated and ³⁵S-methionine-labeled *in vitro* using the Rabbit Reticulocyte Lysate System (Promega) according to the manufacturer's instructions (2 μg RNA per 50 μl reaction) and translocated into wildtype and mutant microsomes at 20°C for the indicated times. Individual reactions were set up as follows: 3 μl of B88 (20 mM HEPES-KOH, pH 6.8, 250 mM sorbitol, 150 mM KOAc, 5 mM Mg(OAc)₂), 1 μl of 10x ATP mix (10 mM ATP, 400 mM creatine phosphate, 2 mg/ml creatine kinase in B88), 5 μl of fresh translation reaction product, 0.5 eq of microsomes (1 μl of membranes at OD₂₈₀ = 30) unless otherwise stated. To investigate translocation in the presence of limiting amounts of membranes adjusting for equal amounts of Sec61p, 0.25 eq

of wildtype and 0.7 eq of *sec61S2Y* microsomes were used for the experiment. After incubation, samples were resolved by gel electrophoresis. Gels were dried for 2 h at 80°C using a 583 gel dryer (Bio-Rad) and signals were acquired by autoradiography on Storage Phosphor Screens (GE Healthcare) and developed using a Typhoon Trio imager (GE Healthcare). Quantitation was performed using the ImageQuant TL software (GE Healthcare).

2.2.19. Fractionation of Sec complex

Fractionation of Sec complex was performed as described in Pilon et al. (1998). Briefly, microsomes (50 eq) were resuspended on ice in 100 µl of solubilization buffer (50 mM HEPES-KOH, pH 7.4, 400 mM KOAc, 5 mM Mg(OAc)₂, 10% glycerol, 0.05% β-mercaptoethanol) containing the cOmpleteMini EDTA-free Protease Inhibitor (PI) Cocktail (Roche) and 0.1 mM PMSF; subsequently, 400 µl of solubilization buffer containing 3.75% digitonin were added, resulting in a final 3% digitonin concentration, and samples were incubated on ice for 30 min and subsequently centrifuged at 110000 g in a TLA100.3 rotor (Beckman Instruments) using an Optima MAX-XP benchtop ultracentrifuge (Beckman Instruments) for 30 min at 4°C. The Sec63 complex was precipitated from the resulting supernatant at 4°C for 1 h with 100 µl of Concanavalin A (Con A) Sepharose 4B (GE Healthcare) using an overhead rotator (neoLab). Remaining beads were cleared from the supernatant by centrifugation at 13000 rpm for 1 min at 4°C to obtain the free fraction (Eppendorf 5415R centrifuge). Con A beads were washed twice with equilibration buffer (1% digitonin, 50 mM HEPES-KOH pH 7.4, 10% glycerol, 0.05% β-mercaptoethanol, 0.1 mM PMSF and PIs) and glycoproteins were subsequently released in 2x SDS-buffer for 10 min at 65°C. To obtain the ribosome-associated membrane protein (RAMP) fraction, the pellet from the 110000 g spin was dissolved in 100 µl of 50 mM HEPES-KOH (pH 7.8), 1 M

KOAc, 17.5 mM Mg(OAc)₂, 2.5% digitonin, 1 mM puromycin, 0.2 mM GTP, 5 mM dithiothreitol, 0.1 mM PMSF containing PIs. After 30 min on ice and 30 min at 30°C, RAMPs including the Sec61 complex were recovered from the supernatant after centrifugation at 100000 g for 30 min at 4°C. Equal amounts of each fraction were analyzed by gel electrophoresis on NuPAGE Novex 4-12% Bis-Tris Protein Gels (Thermo Fisher Scientific) and immunoblotting with antisera against Sec61p and Sec63p.

2.2.20. Sucrose gradient centrifugation

Sucrose gradients were prepared in 13 x 51 mm polycarbonate centrifuge tubes (Beckman) using 1 ml of 15%, 10%, 5% and 0% sucrose in 50 mM HEPES-KOH, pH 7.5, 500 mM KOAc, 1 mM EDTA, 0.1% Triton X-100, 0.05% β-mercaptoethanol, 1 mM PMSF containing PIs. Microsomes (50 eq) were centrifuged for 1 min at 10000 rpm at 4°C (Eppendorf 5415R centrifuge) and the pellet was resuspended in 100 µl of solubilization buffer (50 mM HEPES-KOH, pH 7.5, 500 mM KOAc, 1% Triton X-100, 10 mM EDTA, 0.05% β-mercaptoethanol, 1 mM PMSF, and 5x PIs) and incubated for 15 min on ice. Solubilized microsomes were loaded onto 0-15% sucrose gradients and ultracentrifuged (200000 g, 4°C, 16 h) in a TLA 100.3 rotor. After centrifugation, 13 fractions were collected from top to bottom of the gradients and precipitated with trichloroacetic acid (TCA). For TCA precipitation, an equal volume of ice-cold 20% TCA was added to each fraction. Samples were quickly vortexed and subsequently incubated on ice for 30 min and centrifuged at 13000 rpm for 30 min at 4°C (Eppendorf 5415R centrifuge). Supernatants were discarded and 500 µl of ice-cold acetone were added to the pellets. Supernatants were centrifuged at 13000 rpm for 30 min at 4°C and the pellets air-dried for approximately 5 min at RT. Samples were analyzed by gel electrophoresis and immunoblotting with antisera specific for Sec61p, Sbh1p, and Sss1p.

3. Results

To gain insight into the function of the Sec61p N-terminus, I deleted its amphipathic helix, or both the helix and the N-acetylation site, and characterized these two deletion mutants together with the *sec61S2Y* strain, which carries a mutation of the N-acetylation site previously shown in our laboratory to result in temperature-sensitivity at 37°C and in an ERAD defect (Soromani et al., 2012; KR, unpublished).

3.1. Generation of *sec61* N-terminal mutants

To investigate the function of the Sec61p N-terminus, I generated *sec61* mutants carrying a deletion of the N-terminal helix but preserving the N-terminal acetylation site in its original sequence context, *sec61ΔH1*, and lacking both the N-terminal acetylation site and the N-terminal helix, *sec61ΔN21* (Fig. 3.1).

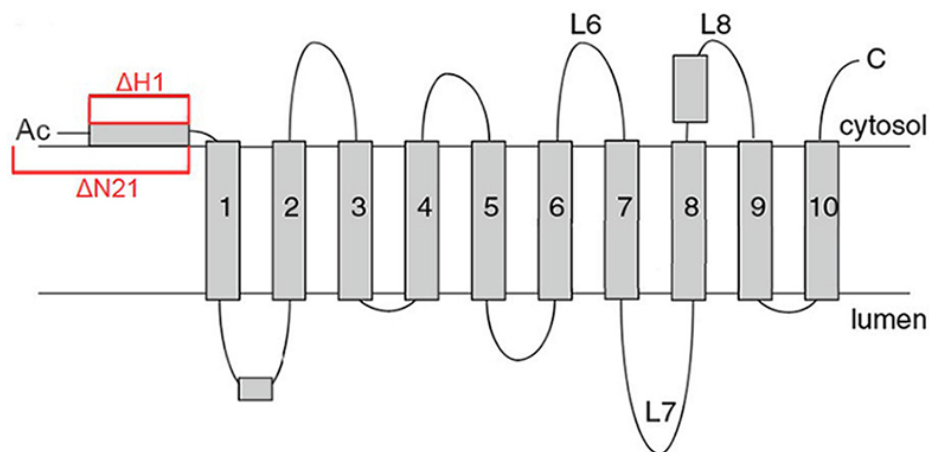


Figure 3.1. Topology of Sec61p. N-terminal mutations generated in this work are highlighted in red (adapted from Tretter et al., 2013).

I also investigated the *sec61S2Y* strain, which carries a serine to tyrosine substitution in position 2 resulting in a non-cleavable and acetylated initiator methionine, and thus in a substantially bulkier N-terminus than in the wildtype protein (Fig. 4.1) (Hoffman and Munro, 2006; Soromani et al., 2012). Preliminary data on this strain were already available at the beginning of this study. To be able to compare results, I used the same genetic background and vector of the *sec61S2Y* mutant (KRY461 [*pGALSEC61-URA3*] and pRS315, respectively) to generate the *sec61ΔH1* and *sec61ΔN21* strains. The pRS315-*SEC61* plasmid was already available in our laboratory and it was used to generate the pRS315-*sec61ΔH1* and pRS315-*sec61ΔN21* plasmids by PCR-mediated DNA deletion (Hansson et al., 2008); deletions of the N-terminal residues 4-22 and 2-22 of Sec61p, respectively, were confirmed by DNA sequencing. Plasmids were individually transformed into the KRY461 strain; transformants were selected on minimal medium without leucine and subsequently on minimal medium without leucine in the presence of 5-fluoroorotic acid, which is converted to the toxic metabolite 5-fluorouracil in cells expressing the functional *URA3* gene (Boeke et al., 1987). To confirm that the *sec61ΔH1* and *sec61ΔN21* strains were only expressing the Sec61ΔH1p and Sec61ΔN21p protein variants, cells were grown overnight (ON), cell extracts were prepared by bead-beating and analyzed by Western blotting using antibodies directed against the C- and N-termini of Sec61p (Fig. 3.2). KRY461 (*SEC61*) cell extracts were used as a control.

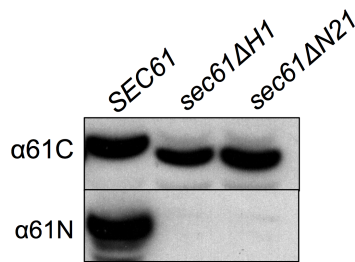


Figure 3.2. Expression of Sec61ΔH1p and Sec61ΔN21p. Cells were grown at 30°C to an $OD_{600} = 1$, extracts were prepared by bead-beating, and samples resolved by SDS-PAGE. Proteins were transferred to nitrocellulose and analyzed with polyclonal rabbit antisera directed against the C- ($\alpha 61C$) and N-termini ($\alpha 61N$) of Sec61p and enhanced chemiluminescence.

As shown in Fig. 3.2, only the C-terminal anti-Sec61p antibody could recognize the bands close to 40 kDa belonging to Sec61ΔH1p and Sec61ΔN21p, confirming the absence of the N-terminal domain in these protein variants. Moreover, the increased electrophoretic mobility of Sec61ΔH1p and Sec61ΔN21p compared to Sec61p (Fig. 3.2, $\alpha 61C$) further confirms the presence of the desired deletions.

3.2. Growth analysis of *sec61* N-terminal mutants

The *sec61S2Y* strain had been previously shown to be temperature-sensitive at 37°C, suggesting a possible role for the N-acetylation of S2 in Sec61p function (KR, unpublished). In addition, growth of the strain was affected in the presence of higher concentrations of tunicamycin (KR, unpublished). Tunicamycin interferes with N-linked glycosylation in the ER and hence tunicamycin-sensitivity is often indicative of perturbations in ER homeostasis (Xiao et al., 2016). The *sec61ΔH1* and *sec61ΔN21* mutants were tested for growth on rich medium at various temperatures both in the absence and presence of 0.25 $\mu\text{g/ml}$ tunicamycin. Cells (10^4 - 10^8) of *sec61ΔH1*, *sec61ΔN21*, and the corresponding wildtype (*SEC61*) were grown for 3.5 days on YPD or YPG plates, respectively, without or with 0.25 $\mu\text{g/ml}$ tunicamycin at 24°C, 30°C, and 37°C (Fig. 3.3). The *sec61ΔH1* and *sec61ΔN21* strains

exhibited severe growth defects at all temperatures tested, which were slightly exacerbated by tunicamycin, and no growth at all at 24°C in the presence of tunicamycin (Fig. 3.3). These results suggest that deletion of the N-terminal amphipathic helix of Sec61p highly affects Sec61p function resulting in reduced cell viability.

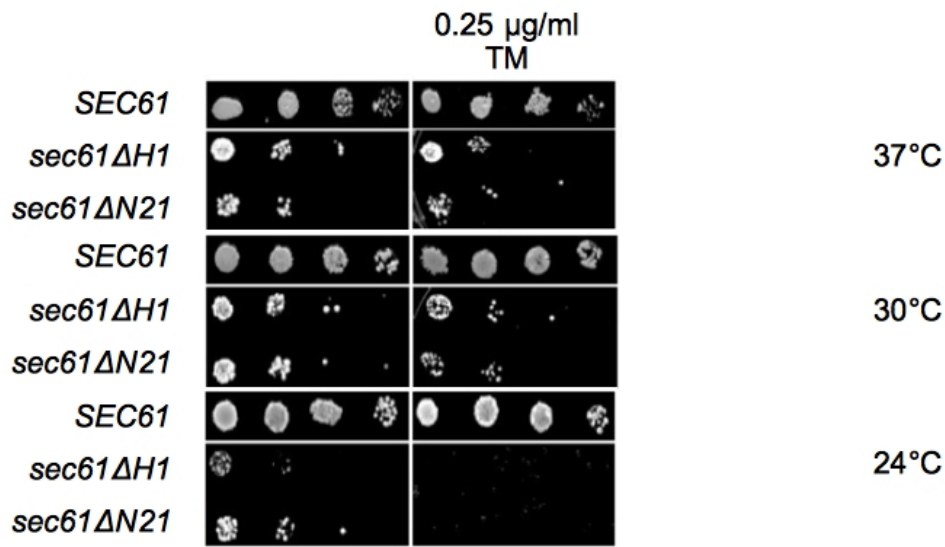


Figure 3.3. Temperature- and tunicamycin-sensitivity of the *sec61ΔH1* and *sec61ΔN21* strains. Cells (10^4 - 10) expressing *sec61ΔH1*, *sec61ΔN21*, or wildtype *SEC61* were grown for 3.5 days on YPD or YPG (*SEC61*) plates without or with 0.25 $\mu\text{g/ml}$ tunicamycin (TM) at the indicated temperatures. The experiment was performed 2 times.

3.3. Stability and expression levels of *sec61* N-terminal variants

Previously identified temperature-sensitive *sec61* alleles have been shown to affect stability of Sec61p (Pilon et al., 1998). In order to test whether the *sec61ΔH1* and *sec61ΔN21* deletions resulted in lower Sec61p stability, I monitored the steady-state levels of Sec61 Δ H1p and Sec61 Δ N21p in a cycloheximide (CHX) chase experiment conducted over 3 h (Fig. 3.4). CHX acts at the large subunit of the ribosome to inhibit translation and was therefore added to ON cultures to monitor the levels of *sec61* variants in the absence of new protein synthesis

(Hanna et al., 2003). After treatment with CHX, equal amounts of cells were taken every 30 min for 3 h, washed with sterile water, lysed with glass beads, resuspended in 50 μ l of 2x SDS-buffer and analyzed by Western blotting as described in 2.2.13.

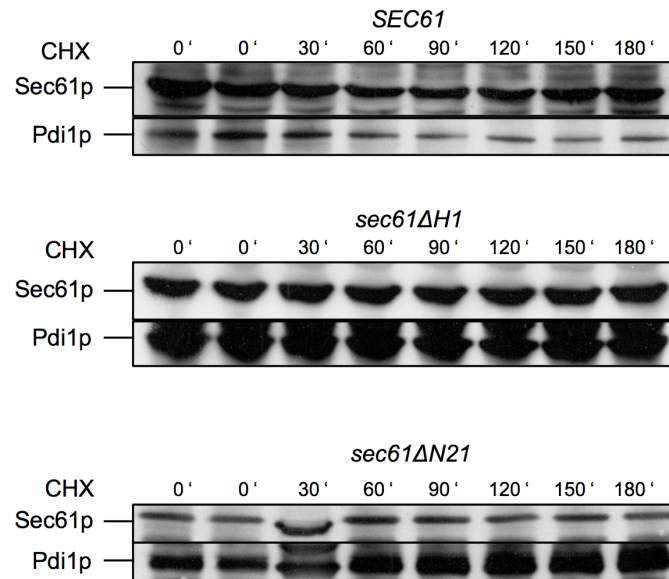


Figure 3.4. Stability of Sec61 Δ H1p and Sec61 Δ N21p. Cells were grown at 30°C to an OD₆₀₀ = 1, translation was inhibited by adding 200 μ g/ml CHX, extracts were prepared by bead-beating, and samples resolved by SDS-PAGE. The 0' samples were taken in duplicate. Proteins were transferred to nitrocellulose and Sec61p, Sec61 Δ H1p, and Sec61 Δ N21p were detected with polyclonal rabbit antiserum against the C-terminus of Sec61p and enhanced chemiluminescence. Pdi1p was used as a loading control.

The results in Fig. 3.4 show that both Sec61 Δ H1p and Sec61 Δ N21p were as stable as the wildtype protein and the Pdi1p loading control. The deletions of the N-terminal residues 4-22 and 2-22 of Sec61p do not therefore compromise the stability of the investigated *sec61* variants.

The most prominent effect of N-terminal acetylation relates to protein stability (Drazic et al., 2016). This topic, however, is controversial. Examples exist showing that N-terminal acetylation increases the stability and half-life of proteins, whereas N-terminal acetylation has also been reported to create degradation signals in some yeast proteins (Ciechanover and Ben-Saadon, 2004; Hwang et al., 2010). The two hypotheses explaining the effect of N-terminal acetylation on protein stability thus seem to apply to specific proteins. In order to test whether N-acetylation of Sec61p at its canonical acetylation site was important for Sec61p stability, I monitored the steady-state levels of Sec61S2Yp in a CHX chase experiment conducted over 3 h (Fig 3.5).

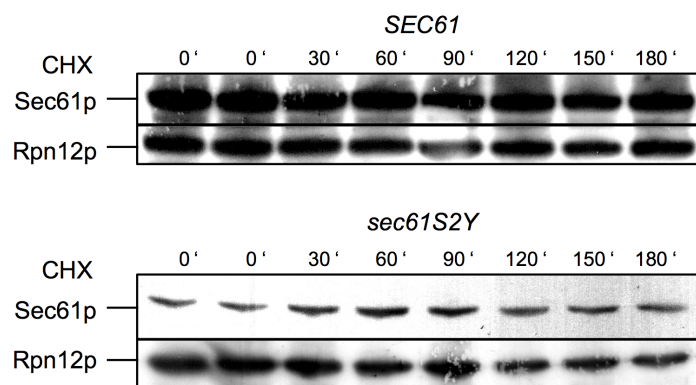


Figure 3.5. Stability of Sec61S2Yp. Cells were grown at 30°C to an $OD_{600} = 1$, translation was inhibited by adding 200 $\mu\text{g/ml}$ CHX, extracts were prepared by bead-beating, and samples resolved by SDS-PAGE. The 0' samples were taken in duplicate. Proteins were transferred to nitrocellulose and Sec61p and Sec61S2Yp were detected with polyclonal rabbit antiserum against the C-terminus of Sec61p and enhanced chemiluminescence. Rpn12p was used as a loading control.

I found that mutation of the Sec61p N-terminal acetylation site had no effect on Sec61p stability. I also quantified by densitometric analysis the amounts of Sec61 Δ H1p, Sec61 Δ N21p, and Sec61S2Yp detected by immunoblotting relative to loading controls. The densitometric analysis performed with the ImageQuant TL software revealed that

Sec61 Δ H1p was expressed at wildtype level, whereas Sec61 Δ N21p and Sec61S2Yp were expressed at approximately 60% of wildtype. The expression levels of Sec61 Δ N21p and Sec61S2Yp are similar to those of other *sec61* mutants expressed from plasmids without causing translocation defects (Trueman et al., 2012).

3.4. UPR induction in *sec61* N-terminal mutants

I next investigated the *sec61* Δ H1, *sec61* Δ N21, and *sec61*S2Y strains for UPR induction, as translocation-defective *sec61* mutants are often UPR-induced (Tretter et al., 2013). The UPR is a series of complementary adaptive mechanisms that cells activate upon ER stress to cope with protein folding alterations (Hetz, 2012). The UPR transduces information about the protein folding status in the ER lumen to the nucleus and cytosol to buffer fluctuations in unfolded protein load (Hetz et al., 2011). The *SEC61*, *sec61* Δ H1, *sec61* Δ N21, and *sec61*S2Y strains were transformed with the plasmids pJC31, a pRS314 plasmid carrying the *LacZ* gene under the control of the UPR element (UPRE), and the control plasmid pJC30, a pRS314 plasmid carrying the *LacZ* gene (Cox et al., 1993). The UPRE is a 22-bp promoter sequence found upstream of many UPR target genes that can induce *LacZ* expression as a consequence of UPR induction (Mori et al., 2000; Patil and Walter, 2001). The activity of the *LacZ* gene product, β -galactosidase, can be monitored spectrophotometrically measuring the conversion of ortho-nitrophenyl- β -D-galactopyranoside (ONPG) to ortho-nitrophenol, which absorbs light at a wavelength of 420 nm (Miller et al., 1972). Transformants were grown in minimal medium without tryptophan, lysed, pre-incubated at 28°C, and incubated with ONPG for 20 min. Reactions were stopped and supernatants analyzed photometrically at 420 nm to calculate β -galactosidase units (Fig. 3.6).

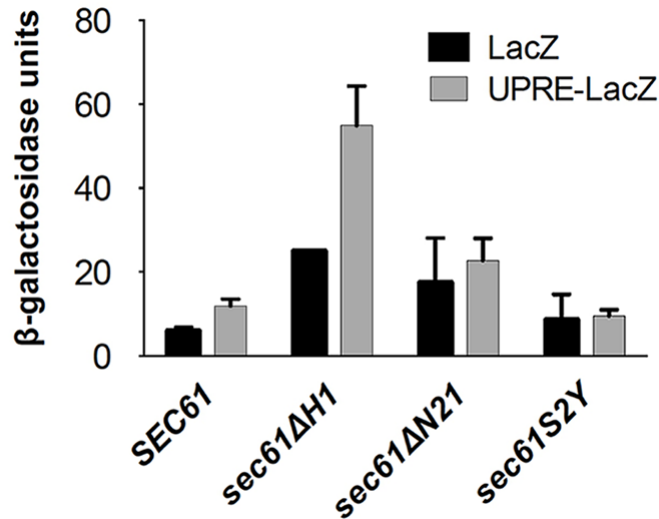


Figure 3.6. Liquid β -galactosidase assay with *sec61* N-terminal mutants. The *sec61ΔH1*, *sec61ΔN21*, and *sec61S2Y* strains were transformed with the plasmids pJC31 (UPRE-*LacZ*) and the control plasmid pJC30 (*LacZ*). Cells were harvested in early exponential phase, lysed, and β -galactosidase activity was analyzed photometrically in duplicate samples. The experiment was performed 2 times. Error bars indicate standard deviation.

The UPR was induced in the *sec61ΔH1* strain, but although the β -galactosidase activity was higher in *sec61ΔN21* than in wildtype cells, this was independent of the UPRE (Fig. 3.6). Despite its temperature- and tunicamycin-sensitivity, in the *sec61S2Y* mutant the UPR was not induced (Fig. 3.6) (KR, unpublished). Collectively, these data suggest that repositioning of the N-terminal acetylation site in *sec61ΔH1* is more detrimental to ER protein homeostasis than mutation of the N-terminal acetylation site (*sec61S2Y*) or the concomitant absence of the N-terminal acetylation site and N-terminal helix in the *sec61ΔN21* mutant.

3.5. ERAD of CPY* in *sec61* N-terminal mutants

Tunicamycin inhibits N-linked glycosylation in the ER and tunicamycin-sensitivity is often associated with defects in export of misfolded proteins from the ER to the cytosol (Travers et al., 2000). In addition, the *sec61S2Y* substitution was shown to result in a 2-fold increase in

the half-life of the commonly used soluble ERAD-L substrate CPY* (Knop et al., 1996; KR, unpublished). I therefore investigated the *sec61ΔH1* and *sec61ΔN21* strains for ERAD defects conducting CHX chase experiments (as described in 3.3) to monitor the decline of the steady-state levels of CPY* in the *sec61ΔH1* and *sec61ΔN21* strains (Fig. 3.7) (Knop et al., 1996). CPY (carboxypeptidase Y) is a vacuolar C-terminal exopeptidase that contains four Asn-X-Thr glycosylation sites and is synthesized as a precursor (ppCPY, 59 kDa) (Stevens et al., 1982). After being post-translationally imported across the ER membrane, ppCPY undergoes cleavage of the signal sequence (pCPY, 57 kDa) and receives core glycosylation in the ER giving the p1 (or ER) form of CPY (67 kDa) (Winther et al., 1991). CPY is further modified in the Golgi to obtain the p2 (or Golgi, 69 kDa) form, and is subsequently converted into the mature form (mCPY, 61 kDa) in the vacuole by proteolytic cleavage (Stevens et al., 1982). The strains characterized in this study carry a chromosomal integration of the CPY* allele (*prc1-1*), characterized by a point mutation (G255R) in the *PRC1* gene that makes CPY* unable to fold and acquire native structure upon receiving core glycosylation in the ER (Finger et al., 1993). CPY* is therefore recognized by the ERQC machinery and retrotranslocated to the cytosol in order to be degraded by the 26S proteasome (Kostova and Wolf, 2003). Post-translational import and subsequent glycosylation of CPY*, however, occur efficiently, thus making CPY* a valuable model protein to investigate ERAD of soluble substrates in *sec61* mutant strains that are not defective in post-translational protein import into the ER (Finger et al., 1993).

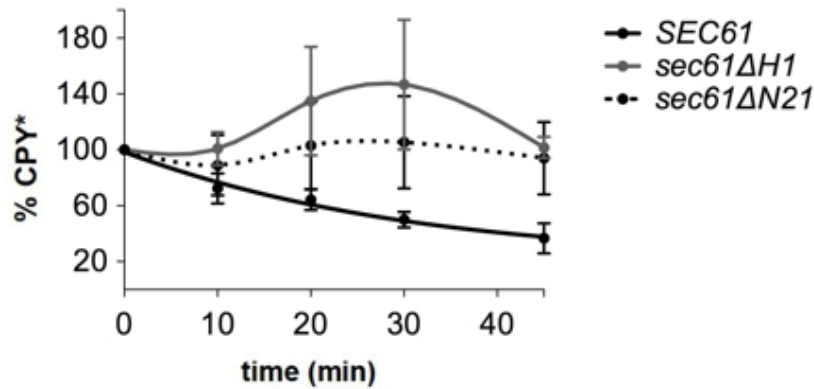
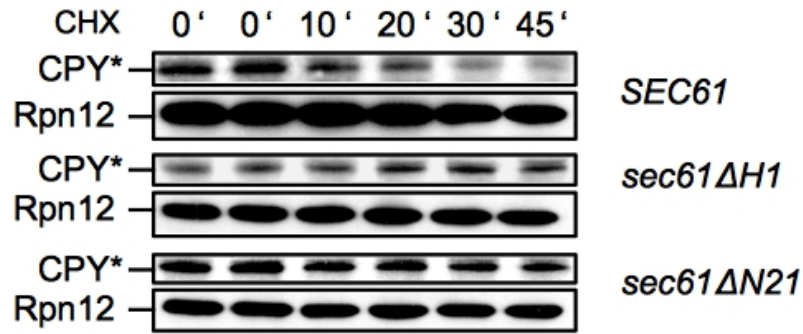


Figure 3.7. ERAD of CPY* in *sec61ΔH1* and *sec61ΔN21* cells. Cells were grown at 30°C to an $OD_{600} = 1$, translation was inhibited by adding 200 $\mu\text{g/ml}$ CHX, extracts were prepared by bead-beating, and samples resolved by SDS-PAGE. The 0' samples were taken in duplicate. Proteins were transferred to nitrocellulose and CPY* was detected with polyclonal rabbit antiserum and enhanced chemiluminescence. Bands were quantified using the ImageQuant TL software. Rpn12 was used as a loading control. Band intensities were quantified relative to loading controls. Curves represent the averages of 3 independent experiments. Error bars represent standard deviations.

Results in Fig. 3.7 show a marked accumulation of CPY* in the ER of the *sec61ΔN21* and especially *sec61ΔH1* mutants after 30 min, suggesting that post-translational import of ppCPY* into the ER was still taking place after protein biosynthesis had been inhibited with CHX. It was therefore not possible to monitor whether or not ERAD was also affected in these mutants. Due to the quality of the polyclonal rabbit CPY antiserum I used to monitor the levels of CPY* in this experiment, I was not able to identify the ppCPY* signals in the

Western blots I developed. I therefore decided to repeat the experiment using another CPY antiserum available in our laboratory. I extended the chase to 90 min to further evaluate the steady-state levels of CPY* in the two helix deletion mutants, as data shown in Fig. 3.7 might suggest that CPY* starts decaying after 30 min in the *sec61ΔH1* and *sec61ΔN21* strains at a rate comparable to wildtype (Fig. 3.8).

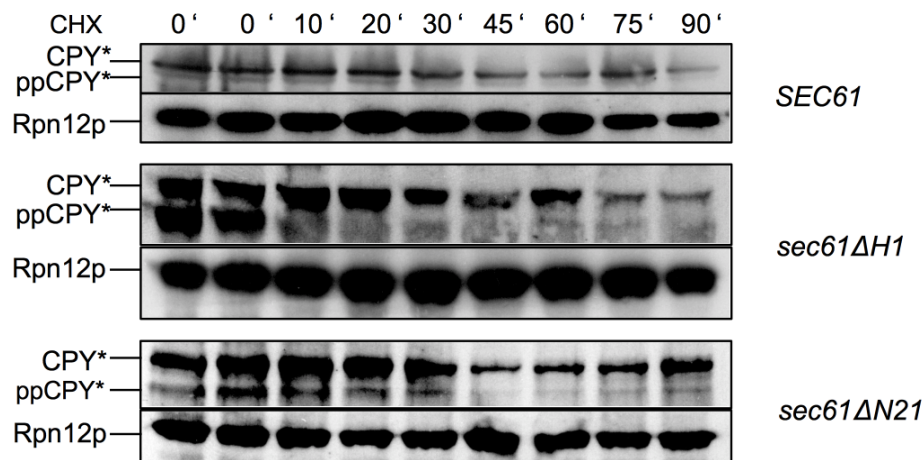


Figure 3.8. ERAD of CPY* in *sec61ΔH1* and *sec61ΔN21* cells (90 min). Cells were grown at 30°C to an $OD_{600} = 1$, translation was inhibited by adding 200 $\mu\text{g/ml}$ CHX, extracts were prepared by bead-beating, and samples resolved by SDS-PAGE. The 0' samples were taken in duplicate. Proteins were transferred to nitrocellulose and CPY* was detected with polyclonal rabbit antiserum and enhanced chemiluminescence. Rpn12 was used as a loading control. The experiment was performed 3 times.

Results in Fig. 3.8 show accumulation of ppCPY* at 0 min for both helix deletion mutants, but more dramatically for *sec61ΔH1*. Post-translational protein import of ppCPY* was therefore still taking place during the chase after protein synthesis had been inhibited. ppCPY* gradually converted into the mature form over the time of the chase as already shown in Fig. 3.7, decreasing in *sec61ΔH1* and *sec61ΔN21* cells after 30 and 45 min, respectively, and not further decaying in *sec61ΔN21* cells up to 90 min (Fig. 3.8).

I next investigated the steady-state levels of CPY* in the *sec61S2Y* strain performing the CHX chase at 37°C (Fig. 3.9). The experiment was also performed at 30°C as a control. The *sec61S2Y* strain is temperature-sensitive at 37°C and, as already mentioned, the *sec61S2Y* substitution results in a 2-fold increase in the half-life of CPY* (Soromani et al., 2012; KR, unpublished). I therefore tested whether the ERAD defect exhibited by the *sec61S2Y* strain was exacerbated at the non-permissive temperature.

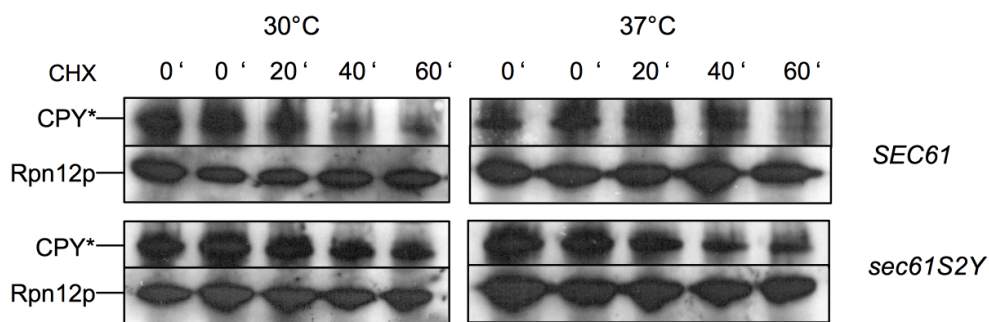


Figure 3.9. ERAD of CPY* in *sec61S2Y* cells. Cells were grown at 30°C to an $OD_{600} = 1$, translation was inhibited by adding 200 $\mu\text{g/ml}$ CHX, extracts were prepared by bead-beating, and samples resolved by SDS-PAGE. Cells tested at 37°C were moved to an incubation shaker set at 37°C immediately after addition of CHX. The 0' samples were taken in duplicate. Proteins were transferred to nitrocellulose and CPY* was detected with polyclonal rabbit antiserum and enhanced chemiluminescence. Rpn12 was used as a loading control. The experiment was performed 2 times.

Data in Fig. 3.9 confirm the defect in ERAD of CPY* found for *sec61S2Y* (KR, unpublished). Despite the temperature-sensitivity of the *sec61S2Y* strain, the defect was probably not exacerbated at 37°C.

In summary, while I could not determine whether or not ERAD was affected in the *sec61 Δ H1* and *sec61 Δ N21* strains, it can be concluded that N-acetylation of Sec61p at S2 is required for ERAD of misfolded soluble proteins.

3.6. Co-translational import in *sec61* N-terminal mutants

As the results in Fig. 3.7 and 3.8 suggest an ER import defect for *sec61ΔH1* and *sec61ΔN21*, I decided to investigate import directly. I first monitored co-translational membrane integration of diaminopeptidase B (DPAPB) in the *sec61ΔH1* and *sec61ΔN21* strains by pulse-labeling with ³⁵S-Met/Cys for 5 min, lysing the cells, and immunoprecipitation with specific polyclonal antibodies. After immunoprecipitation, samples were resolved by SDS-PAGE and detected by autoradiography (Fig. 3.10). DPAPB is a type II membrane protein with an N-terminal signal anchor sequence (Pilon et al., 1998). Upon co-translational integration into the ER membrane, the precursor protein (pDPAPB) is core-glycosylated to form the mature protein (DPAPB) (Roberts et al., 1989). DPAPB migrates as a 120-kDa species, whereas pDPAPB migrates as a 96 kDa species (Roberts et al., 1989). If DPAPB is efficiently integrated, its precursor form is undetectable by pulse-labeling.

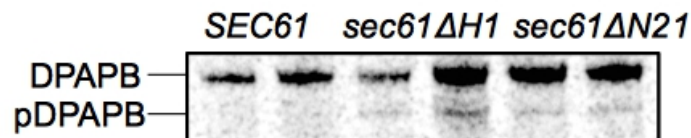


Figure 3.10. Co-translational ER import of newly synthesized DPAPB in *sec61ΔH1* and *sec61ΔN21* cells. Cells were grown at 30°C to early exponential phase, labeled with ³⁵S-Met/Cys for 5 min and lysed. Cytosolic precursor (pDPAPB) and ER-membrane integrated DPAPB were immunoprecipitated, resolved by SDS-PAGE, and detected by autoradiography. Samples were taken in duplicates. The experiment was performed 4 times.

Results in Fig. 3.10 show that the cytosolic precursor form of DPAPB could be barely detected in *sec61ΔH1* and *sec61ΔN21*, and thus that co-translational translocation into the ER is not affected in the *sec61ΔH1* and *sec61ΔN21* strains.

In order to also test whether substitution of the N-acetyl acceptor serine in position 2 of Sec61p had an effect on co-translational import into the ER, I monitored pDPAPB integration in the *sec61S2Y* strain (Fig. 3.11). Given the temperature sensitivity of the *sec61S2Y* strain at 37°C, I also performed the experiment carrying the pulse-labeling step at 37°C to verify whether co-translational import defects occurred or were exacerbated at the non-permissive temperature (Fig. 3.11).

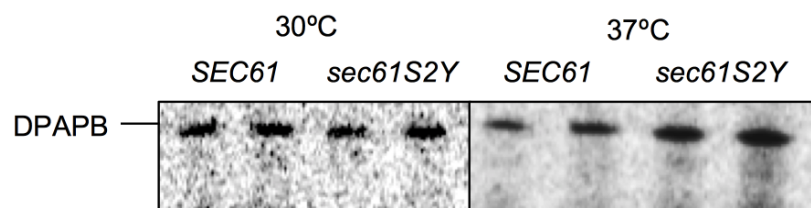


Figure 3.11. Co-translational ER import of newly synthesized DPAPB in *sec61S2Y* cells. Cells were grown at 30°C to early exponential phase, labeled with ^{35}S -Met/Cys for 5 min at 30°C (left panel) or 37°C (right panel) and lysed. DPAPB was immunoprecipitated, resolved by SDS-PAGE, and detected by autoradiography. Samples were taken in duplicates. The experiment was performed 3 times.

I found that mutation of the N-terminal acetylation site had no effect at all on pDPAPB import, even when, despite the temperature sensitivity of the *sec61S2Y* strain, the pulse-labeling step was performed at 37°C (Fig. 3.11). Collectively, these data show that none of the investigated N-terminal *sec61* mutations affects co-translational translocation into the ER.

3.7. Post-translational import in *sec61* N-terminal mutants

I next investigated the *sec61ΔH1* and *sec61ΔN21* mutants for post-translational import defects, monitoring the cytoplasmic accumulation of the post-translational import substrate prepro alpha factor (ppαF) in cell lysates by Western Blotting with specific polyclonal

antiserum (Fig. 3.12). The *sec61S2Y* mutation had been previously shown to have no effect on post-translational import of pp α F *in vivo* (KR, unpublished). pp α F (19 kDa) is the precursor protein of the mating pheromone secreted by α cells and consists of a 19-amino acid signal peptide, a 64-amino acid pro region containing three sites for N-linked glycosylation, and four tandem repeats of the mature α factor sequence preceded by a spacer peptide (Caplan et al., 1991). pp α F is post-translationally imported into the ER where its signal sequence is cleaved to produce pro alpha factor (p α F), which is subsequently glycosylated at its three sites within the pro region (3gp α F, 28 kDa) (Caplan et al., 1991). After glycosylation, 3gp α F is transported to the Golgi apparatus where it undergoes several proteolytic processing steps (Caplan et al., 1991). Mature α factor is then rapidly secreted into the extracellular medium (Caplan et al., 1991). The accumulation of pp α F in the cytosol is a sensitive marker for post-translational import defects, as the precursor is undetectable in wildtype cells because it is rapidly translocated into the ER, transported to the Golgi and processed (Soromani et al., 2012).

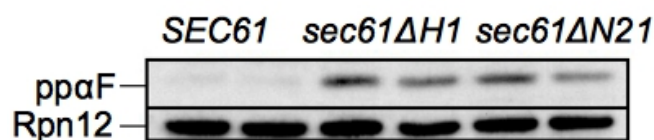


Figure 3.12. Post-translational ER import of pp α F in *sec61ΔH1* and *sec61ΔN21* cells. Cells were grown at 30°C to an OD₆₀₀ = 1, extracts were prepared by bead-beating, and samples resolved by SDS-PAGE. Proteins were transferred to nitrocellulose and the accumulation of cytosolic pp α F was analyzed by immunoblotting. Rpn12p was used as a loading control. Samples were taken in duplicates. The experiment was performed 3 times.

As shown in Fig. 3.12, post-translational import of pp α F was profoundly affected in both *sec61ΔH1* and *sec61ΔN21*. Both *sec61ΔH1* and *sec61ΔN21* robustly accumulated pp α F in the cytosol, while no cytosolic precursor could be detected in the wildtype strain as expected

(Fig. 3.12). Strong post-translational import defects were also displayed by the *sec61ΔH1* and *sec61ΔN21* mutants in a pulse-labeling experiment with ³⁵S-Met/Cys for 5 min followed by immunoprecipitation with antibodies against CPY to monitor the efficiency of post-translational ER import of newly synthesized proteins (Fig. 3.13). Precipitates were resolved by SDS-PAGE and signals detected by autoradiography.

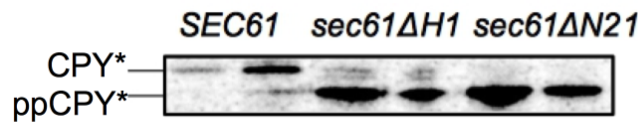


Figure 3.13. Post-translational ER import of newly synthesized ppCPY* in *sec61ΔH1* and *sec61ΔN21* cells. Cells were grown at 30°C to early log phase, labeled with ³⁵S-Met/Cys for 5 min and lysed; cytosolic ppCPY* and ER-luminal CPY* were immunoprecipitated, resolved by SDS-PAGE and detected by autoradiography. Samples were taken in duplicates. The experiment was performed 2 times.

No post-translational import of cytosolic precursor ppCPY* could be detected in *sec61ΔN21* cells during the 5 min pulse, and the *sec61ΔH1* mutant only allowed minimal ppCPY* import into the ER (Fig. 3.13). These data confirm that *sec61ΔH1* and *sec61ΔN21* cells are highly defective in post-translational protein import into the ER (see Fig. 3.12). These data also confirm that during my CHX experiment to monitor the decline of the steady-state levels of CPY* post-translational import of ppCPY* was still taking place (see Fig. 3.7). The *sec61S2Y* substitution had been previously shown in our laboratory to lead only to a marginal accumulation of newly synthesized ppCPY* in the cytosol (KR, unpublished).

Collectively, these data suggest that the N-terminal helix of Sec61p, but not its N-terminal acetylation site, is essential for post-translational import into the ER.

3.8. Post-translational protein import into *sec61S2Y*, *sec61ΔH1* and *sec61ΔN21* microsomes

As subtle translocation defects can be masked by the abundance of Sec61 channels in intact cells, to further explore a potential impact of the *sec61S2Y* mutation on protein import into the ER, we investigated the ability of *sec61S2Y* microsomes to import ppαF *in vitro* (Feng et al., 2007; Kaiser and Römisch, 2015). For an overview of the ppαF route along the secretory pathway, see 3.7. The ppαF mRNA was translated *in vitro* in the presence of ³⁵S-labeled methionine, and the resulting radiolabeled ppαF subsequently incubated at 20°C in the presence of ATP, an ATP-regenerating system, and wildtype or mutant microsomes (0.5 eq) for the indicated periods of time (McCracken and Brodsky, 1996) (Fig. 3.14). After resolving the samples by SDS-PAGE, signals were acquired by autoradiography. The efficiency of post-translational import was monitored following the formation of glycosylated 3gpαF.

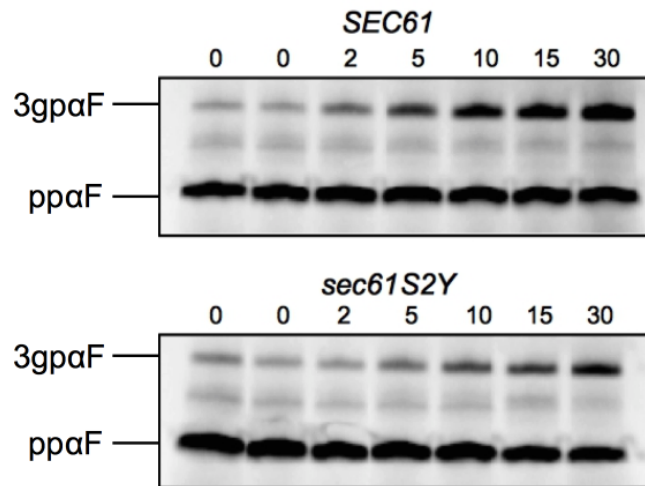


Figure 3.14. *In vitro* post-translational import of pp α F into *sec61S2Y* microsomes. The mRNA for pp α F was translated in the presence of 35 S-methionine *in vitro* and radiolabeled pp α F was translocated into wildtype and mutant microsomes at 20°C in the presence of ATP and an ATP-regenerating system. At the indicated time points (min), 2x SDS-buffer was added and samples were resolved by SDS-PAGE and cytosolic pp α F and translocated, signal-cleaved glycosylated 3gp α F detected by autoradiography. The experiment was performed 3 times.

Although the *sec61S2Y* mutation had been previously shown to have no effect on post-translational import of pp α F *in vivo*, *in vitro* the *sec61S2Y* mutation led to a reduction in the import of pp α F into yeast microsomes (Fig. 3.14) (KR, unpublished). As Sec61S2Yp is expressed at levels lower than wildtype Sec61p (see 3.3) and microsomes are generally present in excess when 0.5 eq are added to the *in vitro* translocation reaction, to investigate post-translational import into *sec61S2Y* microsomes in further detail, I decided to monitor the ability of *sec61S2Y* membranes to import pp α F *in vitro* adjusting for equal amounts of Sec61p and Sec61S2Yp and in the presence of limiting amounts of microsomes. To identify the amount of microsomes limiting for pp α F import *in vitro*, I tested pp α F import into 0, 0.0625, 0.125, 0.1875, 0.25, 0.3125, 0.375, 0.4375 and 0.5 eq of wildtype microsomes for 30 min (Fig. 3.15).

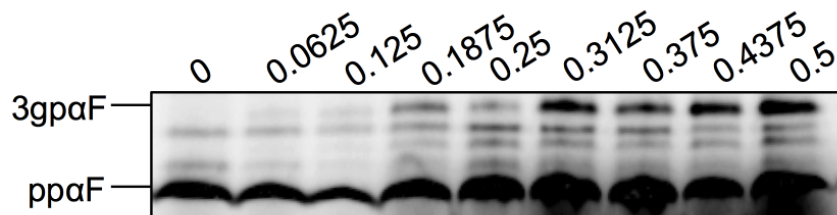


Figure 3.15. *In vitro* post-translational import of pp α F into increasing amounts (0-0.5 eq) of wildtype microsomes. The mRNA for pp α F was translated in the presence of 35 S-methionine *in vitro* and radiolabeled pp α F was translocated into the indicated amounts (eq) of wildtype microsomes at 20°C in the presence of ATP and an ATP-regenerating system. After 30 min, 2x SDS-buffer was added and samples were resolved by SDS-PAGE and cytosolic pp α F and translocated, signal-cleaved glycosylated 3gp α F detected by autoradiography.

As shown in Fig. 3.15, the levels of glycosylated 3gp α F substantially decreased when 0.25 eq of microsomes or less were present in the reaction. On the other hand, in the presence of 0.3125 eq of microsomes or higher the levels of 3gp α F were comparable to the ones of the sample containing 0.5 eq of membranes (Fig. 3.15). I therefore chose 0.25 eq as the amount of wildtype membranes to use for the experiment under limiting conditions. As determined by densitometric analysis of bands of wildtype and *sec61S2Y* microsomes resolved by SDS-PAGE and blotted with antibodies against Sec61p, equal amounts of Sec61p and Sec61S2Yp were contained in 0.25 and 0.7 eq of my preparations of wildtype and *sec61S2Y* microsomes, respectively (not shown). Thus, *sec61S2Y* microsomes were already present in limiting amounts in the experiment shown in Fig. 3.15. Results of the post-translational import experiment in the presence of limiting amounts of membranes and adjusting for equal amounts of Sec61p are shown in Fig. 3.16.

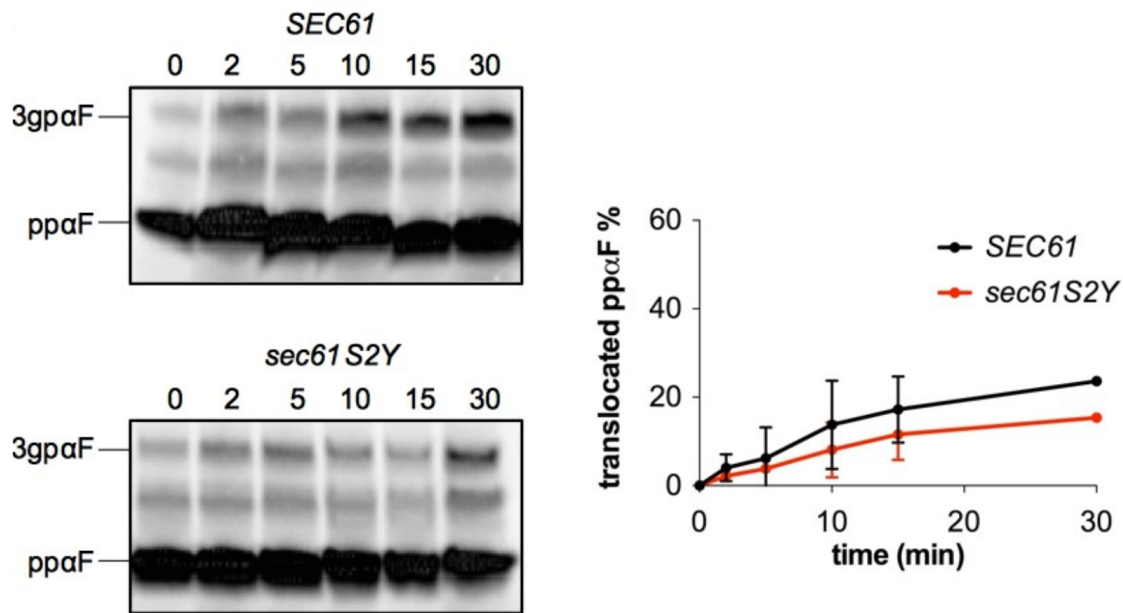


Figure 3.16. *In vitro* post-translational import of pp α F into limiting amounts of *sec61S2Y* microsomes. The mRNA for pp α F was translated in the presence of 35 S-methionine *in vitro* and radiolabeled pp α F was translocated into wildtype and mutant microsomes at 20°C in the presence of ATP and an ATP-regenerating system. At the indicated time points (min), 2x SDS-buffer was added and samples were resolved by SDS-PAGE and cytosolic pp α F and translocated, signal-cleaved glycosylated 3gp α F detected by autoradiography. Bands were quantified using the ImageQuant TL software. Experiments were performed 3 times. The graph in A represents the average of 2 representative independent experiments. Error bars represent standard deviation.

Data in Fig. 3.16 confirm that *in vitro* the *sec61S2Y* mutation causes a reduction in the import of pp α F into yeast microsomes, as already suggested by Fig. 3.14.

To further explore the role of the Sec61p N-terminus in post-translational soluble protein import into the ER, I also attempted to investigate pp α F import into 0.5 eq of *sec61ΔH1* and *sec61ΔN21* microsomes (Fig. 3.17).

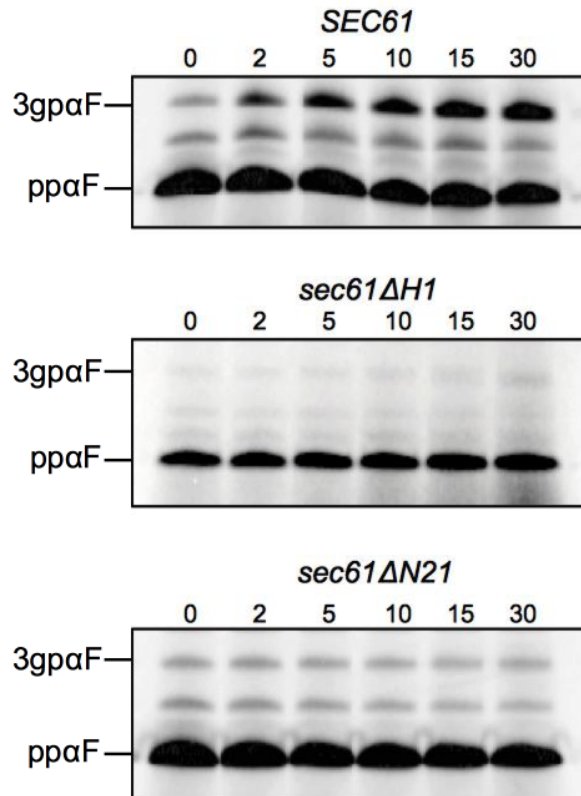


Figure 3.17. *In vitro* post-translational import of pp α F into *sec61* Δ H1 and *sec61* Δ N21 microsomes. The mRNA for pp α F was translated in the presence of 35 S-methionine *in vitro* and radiolabeled pp α F was translocated into wildtype and mutant microsomes at 20°C in the presence of ATP and an ATP-regenerating system. At the indicated time points (min), 2x SDS-buffer was added and samples were resolved by SDS-PAGE and cytosolic pp α F and translocated, signal-cleaved glycosylated 3gp α F detected by autoradiography. The experiment was performed 3 times.

Both *sec61* Δ H1 and *sec61* Δ N21 microsomes were highly defective in post-translational import of pp α F, and no glycosylated 3gp α F could be detected even after 30 min (Fig. 3.17). Given the dramatic effect of the *sec61* Δ H1 and *sec61* Δ N21 deletions on post-translational import *in vitro*, I repeated the experiment in Fig. 3.17 monitoring the levels of 3gp α F for 2 h (Fig. 3.18).

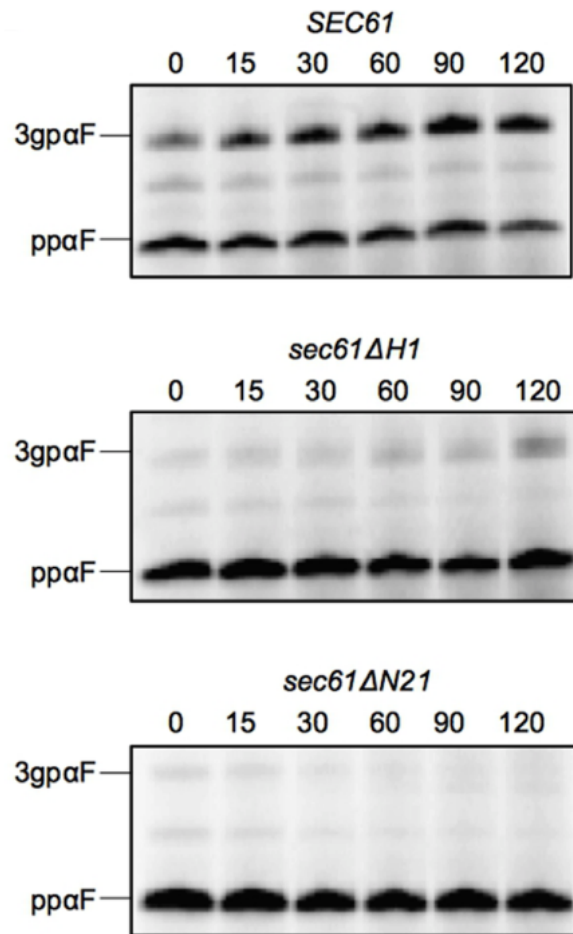


Figure 3.18. *In vitro* post-translational import of pp α F into *sec61* Δ H1 and *sec61* Δ N21 microsomes (2 h). The mRNA for pp α F was translated in the presence of 35 S-methionine *in vitro* and radiolabeled pp α F was translocated into wildtype and mutant microsomes at 20°C in the presence of ATP and an ATP-regenerating system. At the indicated time points (min), 2x SDS-buffer was added and samples were resolved by SDS-PAGE and cytosolic pp α F and translocated, signal-cleaved glycosylated 3gp α F detected by autoradiography. The experiment was performed 3 times.

Even after 2 h of incubation, however, I detected no glycosylated 3gp α F in the *sec61* Δ N21 samples, and only a very limited amount of 3gp α F in the presence of *sec61* Δ H1 membranes, whereas in the presence of wildtype membranes, as expected, 3gp α F was more abundant than pp α F (Fig. 3.18). These results confirm the critical role of the Sec61p N-terminus in post-translational soluble protein import into the ER.

Collectively, these data suggest a requirement for the Sec61p N-terminal amphipathic helix for post-translational protein import into the ER with a possible contribution by N-acetylation at the N-terminus of the helix.

3.9. Stability of heptameric Sec complexes in *sec61* N-terminal mutants

To test whether the severe defects in post-translational import found for *sec61ΔH1* and *sec61ΔN21* both *in vivo* and *in vitro* (Fig. 3.12, 3.13, 3.17, 3.18) were due to an impaired formation of heptameric Sec complexes, I solubilized wildtype, *sec61ΔH1*, and *sec61ΔN21* microsomes in digitonin, ultracentrifuged lysates to remove ribosome-bound Sec61 complexes, and precipitated Sec complexes from the supernatant using Concanavalin A (Con A) beads, which binds to the N-glycans of Sec71p, the only glycosylated Sec complex subunit (Pilon et al., 1998). Digitonin is a mild nonionic detergent that can effectively solubilize microsomes without affecting the integrity of Sec complexes (Tretter et al., 2013). Free Sec61 complexes were precipitated from supernatants after Con A precipitation. Equal amounts of each fraction were analyzed by gel electrophoresis and immunoblotting with antibodies against Sec63p and the C-terminus of Sec61p (Fig. 3.19).

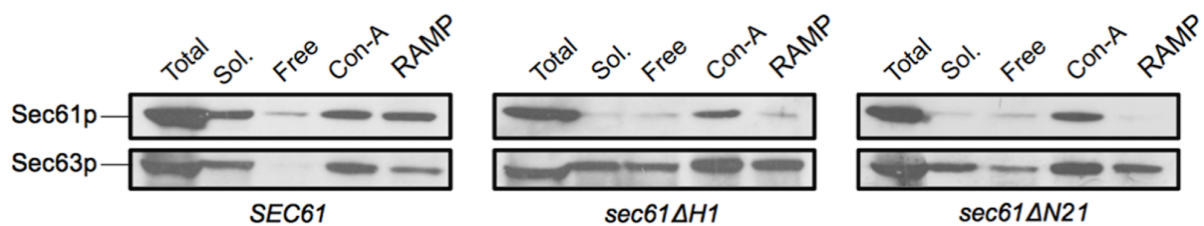


Figure 3.19. Stability of heptameric Sec complexes in *sec61ΔH1* and *sec61ΔN21* membranes. Wildtype, *sec61ΔH1*, and *sec61ΔN21* microsomes were solubilized in solubilization buffer containing 3% digitonin and lysates centrifuged at 110000 g to sediment ribosome-bound Sec61 complexes (ribosome-associated membrane proteins, RAMP). From the supernatants, heptameric Sec complexes were precipitated with Con A. Sec61p and Sec63p not bound to either Con A or ribosomes

were detected in the “Free” fraction. In all fractions, Sec61p and Sec63p were detected by immunoblotting with polyclonal antisera. The experiment was performed 3 times.

The solubility of Sec61 Δ H1p and Sec61 Δ N21p was dramatically reduced compared to wildtype, suggesting that Sec61p without its N-terminal helix is prone to aggregation (Fig. 3.19, Sol. fractions). Although I could only solubilize small amounts of Sec61 Δ H1p and Sec61 Δ N21p, I was able to detect amounts of both variants in the Con A fractions although the ratios of Sec61 Δ H1p and Sec61 Δ N21p to Sec63p in the Con A fractions were lower compared to wildtype (Fig. 3.19, Con-A fractions). In contrast, I observed a dramatic loss of both mutant *sec61* protein variants from the ribosome-associated membrane protein (RAMP) fractions (Fig. 3.19). I found Sec63p in comparable amounts in the Con A and RAMP fractions of wildtype, *sec61* Δ H1, and *sec61* Δ N21 membranes, but there was more Sec63p in the “Free” fraction in the mutants compared to wildtype (Fig. 3.19, bottom panels). These data suggest that despite the strong post-translational import defects shown by both the N-terminal helix deletion mutants, their heptameric Sec complexes are largely intact.

N-terminal acetylation has been proposed to enhance protein complex formation (Aksnes et al., 2016). Given also the post-translational import defect observed *in vitro* for *sec61S2Y* microsomes (Fig. 3.16), I next investigated by Con A precipitation of solubilized Sec complexes whether Sec61p N-acetylation at S2 was important for heptameric Sec complex formation (Fig. 3.20).

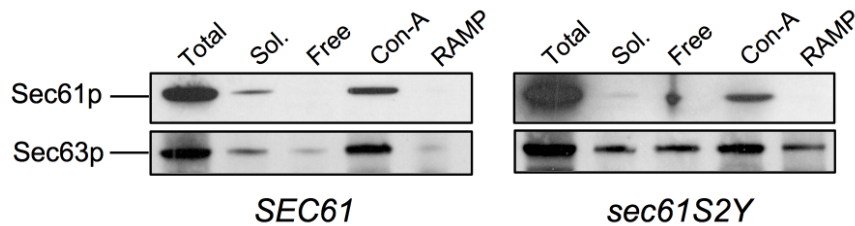


Figure 3.20. Stability of heptameric Sec complexes in *sec61S2Y* membranes. Wildtype and *sec61S2Y* microsomes were solubilized in solubilization buffer containing 3% digitonin and lysates centrifuged at 110000 g to sediment ribosome-bound Sec61 complexes (RAMP). From the supernatants, heptameric Sec complexes were precipitated with Con A. Sec61p and Sec63p not bound to either Con A or ribosomes were detected in the “Free” fraction. In all fractions, Sec61p and Sec63p were detected by immunoblotting with polyclonal antisera. The experiment was performed 2 times.

As for Sec61 Δ H1p and Sec61 Δ N21p, I could only solubilize small amounts of Sec61S2Yp in digitonin, although it has to be considered that in this experimental set the amount of detectable solubilized wildtype Sec61p was also substantially lower than expected (Fig. 3.20, Sol. fractions). Despite the difficulties in solubilizing Sec61S2Yp and wildtype Sec61p, comparable amounts of both wildtype and mutant protein could be detected in the Con A fractions obtained from the solubilized membrane fractions (Fig. 3.20, Con-A). No Sec61p and Sec61S2Yp were detected in the RAMP fractions (Fig. 3.20, RAMP). As already reported, the recovery of Sec61p in these fractions is variable from experiment to experiment due to difficulties in resuspension of the first high-speed pellet obtained in the experiment (Pilon et al., 1998). More Sec63p could be solubilized from *sec61S2Y* compared to wildtype membranes (Fig. 3.20). Sec63p was present in comparable amounts in the Con A fractions of wildtype and *sec61S2Y* membranes, but, as for *sec61 Δ H1* and *sec61 Δ N21* membranes, I detected more Sec63p in the “Free” fraction of *sec61S2Y* membranes compared to wildtype (Fig. 3.20, bottom panels). These data suggest that acetylation of Sec61p at S2 is not important for heptameric Sec complex formation.

In summary, none of the investigated mutations affected heptameric Sec complex formation strongly, suggesting that the post-translational import defects observed for the N-terminal mutants were not caused by a compromised interaction between Sec61p and the Sec63 complex.

3.10. Stability of trimeric Sec61 complexes in *sec61* N-terminal mutants

I next asked whether the post-translational import defects observed for the *sec61ΔH1* and *sec61ΔN21* mutants (see 3.7, 3.8) were caused by unstable Sec61 complexes in the absence of the N-terminal helix. I therefore investigated the stabilities of the *sec61ΔH1* and *sec61ΔN21* trimeric complexes directly. I solubilized wildtype, *sec61ΔH1*, and *sec61ΔN21* microsomes in 1% Triton X-100 and centrifuged solubilized Sec61 complexes through a shallow 0-15% sucrose gradient (Falcone et al., 2011). The stability of Sec61 complexes, but not of Sec complexes, is largely preserved in Triton X-100 (Falcone et al., 2011). Fractions were collected from top to bottom, proteins precipitated with TCA, resolved by SDS-PAGE, and Sec61 complex subunits detected in each fraction by blotting with antibodies against the C-termini of Sec61p, Sbh1p, and Sss1p.

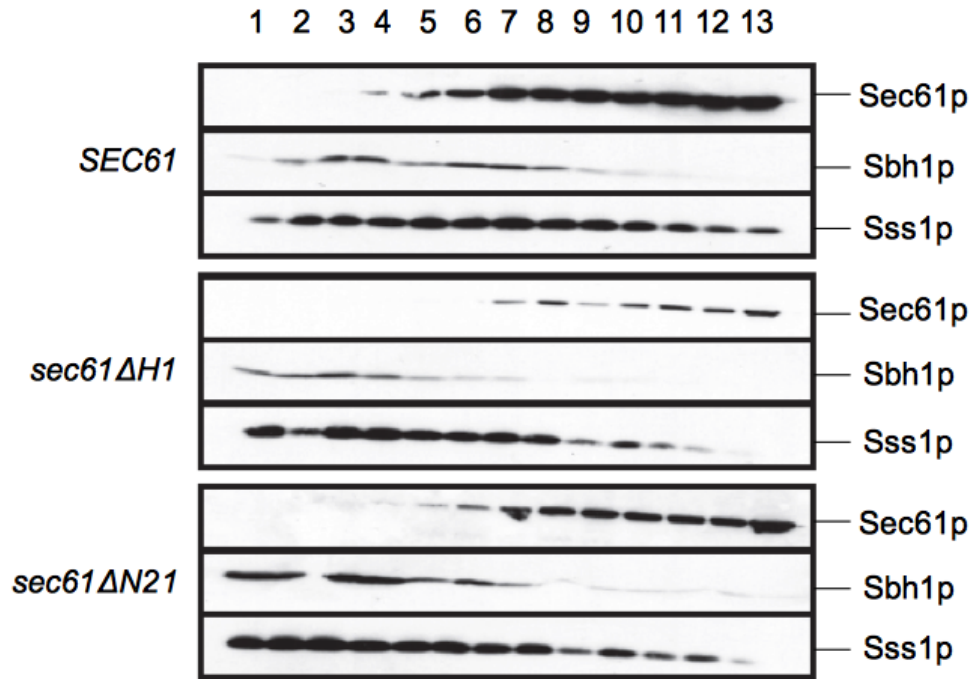


Figure 3.21. Stability of Sec61 complexes in *sec61ΔH1* and *sec61ΔN21* membranes. Microsomes were solubilized in 1% Triton X-100 and layered onto a 0-15% sucrose gradient. After centrifugation at 200000 g for 16 h, fractions were collected from top to bottom, and proteins resolved by SDS-PAGE. Sec61p, Sbh1p, and Sss1p were detected by immunoblotting. The experiment was performed 4 times.

A distinct loss of colocalization of Sec61p, Sbh1p, and Sss1p could be observed in gradient fractions from both *sec61ΔH1* and *sec61ΔN21* complexes (Fig. 3.21). A reduced number of fractions contained all three proteins for the two deletion mutants (wildtype: fractions 4-10; *sec61ΔH1*: fraction 7; *sec61ΔN21*: fractions 5-7). In addition, the destabilization of trimeric Sec61 complexes was more pronounced in *sec61ΔH1* microsomes compared to *sec61ΔN21* microsomes. Sbh1p colocalized with Sec61ΔH1p in only 1 and with Sec61ΔN21p in only 3 fractions, respectively (Fig. 3.21). These data suggest that the N-terminal amphipathic helix of Sec61p is required for stability of the Sec61 complex. These data also suggest that interaction of Sbh1p with Sec61p is more strongly dependent on the Sec61p N-terminal helix than that of Sss1p with Sec61p.

To test whether the *sec61S2Y* mutation had also an impact on trimeric Sec61 complex stability, I solubilized microsomes derived from *sec61S2Y* cells in 1% Triton X-100 and centrifuged solubilized Sec61 complexes through a shallow 0-15% sucrose gradient (Fig. 3.22).

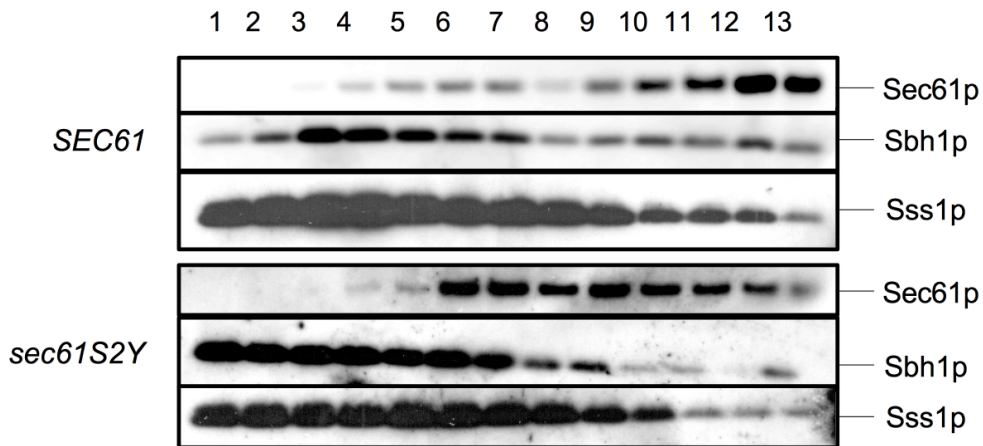


Figure 3.22. Stability of Sec61 complexes in *sec61S2Y* membranes. Microsomes were solubilized in 1% Triton X-100 and layered onto a 0-15% sucrose gradient. After centrifugation at 200000 g for 16 h, fractions were collected from top to bottom, and proteins resolved by SDS-PAGE. Sec61p, Sbh1p, and Sss1p were detected by immunoblotting. The experiment was performed 2 times.

As shown in Fig. 3.22, the interaction of Sec61S2Yp with Sbh1p and Sss1p was not significantly altered compared to wildtype, despite more Sbh1p localized in the upper fractions obtained from *sec61S2Y* membranes and Sec61p itself was more widely distributed across the *sec61S2Y* gradient (fractions 6-11) compared to wildtype (fractions 11-13).

Collectively, these data suggest that the N-terminal amphipathic helix of Sec61p, but not its acetylation at S2, is important for stability of the Sec61 complex.

3.11. Growth of *sec61* N-terminal mutants upon *Sbh1p* overexpression

Data in Fig. 3.21 show that interaction of *Sbh1p* with *Sec61p* is more strongly dependent on the *Sec61p* N-terminal helix than that of *Sss1p* with *Sec61p*. Given the proximity of the *Sbh1p* cytosolic domain to the cytosolic N-terminus of *Sec61p*, I asked whether the growth defects found for *sec61ΔH1* and *sec61ΔN21* cells at 24°C, 30°C, and 37°C (Fig. 3.3) could be rescued upon overexpression of *SBH1* from a multi-copy plasmid (Zhao and Jäntti, 2009). The *SEC61*, *sec61ΔH1*, and *sec61ΔN21* strains were transformed with the pRS424-*SBH1* plasmid and transformants selected on minimal medium without tryptophan. Cells (10^4 - 10^5) of *sec61ΔH1*, *sec61ΔN21*, and the corresponding wildtype (*SEC61*) were grown for 3.5 days on minimal medium plates without tryptophan in the presence of glucose or galactose, respectively (Fig. 3.23).

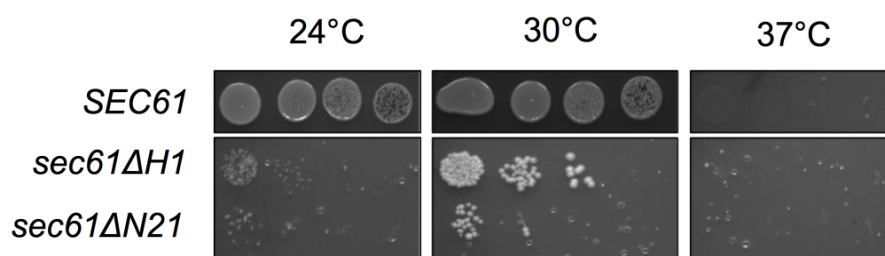


Figure 3.23. Temperature sensitivity of *sec61ΔH1* and *sec61ΔN21* cells overexpressing *SBH1*. *sec61ΔH1*, *sec61ΔN21*, or wildtype cells (10^4 - 10^5) overexpressing *SBH1* were grown for 3.5 days on minimal medium plates without tryptophan at the indicated temperatures.

Not only the growth defects of the *sec61ΔH1* and *sec61ΔN21* strains could not be rescued upon *SBH1* overexpression, but also all of the strains tested (including the wildtype control) became temperature-sensitive at 37°C (Fig. 3.23). Even at 24°C and 30°C, overexpression of *SBH1* was not sufficient to stabilize the *sec61ΔH1* and *sec61ΔN21* channels.

I also tested whether the temperature sensitivity of the *sec61S2Y* strain at 37°C could be rescued upon *SBH1* overexpression, but, since both the *sec61S2Y* strain and the wildtype control carrying the pRS424-*SBH1* plasmid were temperature-sensitive at 37°C, data are not shown.

3.12. Clogging of the Sec61 translocon in *sec61* N-terminal and $\Delta sbh1\Delta sbh2$ mutants

I next tested whether unclogging of Sec61 translocons was affected in the absence of the N-terminal helix of Sec61p or when the Sec61p N-acetyl acceptor serine had been mutated. SRP-independent translocation substrates can undergo premature cytosolic folding, precluding them from being linearly threaded through the translocon pore (Ast et al., 2014). Cytosolic chaperones disengage from these substrates once translocation has started, and it might occur that post-translational import substrates already bound by Kar2p in the lumen fold domains that are still in the cytosol (Plath and Rapoport, 2000; Ast et al., 2016). These proteins can therefore neither continue to translocate into the ER nor retrotranslocate to the cytosol, thus clogging the translocon. The metalloprotease Ste24p was recently found in *S. cerevisiae* to approach the SRP-independent translocon and mediate the degradation of clogged substrates after their extraction from the translocon mediated by Cdc48p (Ast et al., 2016). I attempted to integrate a folding-prone clogger construct under the control of a galactose inducible promoter into the HO locus of the *sec61ΔH1*, *sec61ΔN21*, and *sec61S2Y* strains. This construct is characterized by the fusion of the SRP-independent translocation substrate Pdi1p (bearing 5 glycosylation sites), the stably folding dihydrofolate reductase enzyme, three glycosylation sites, and a hemagglutinin (HA) tag (Ast et al., 2016). When clogged, this fusion protein can be easily recognized on a Western blot using anti-HA antibodies because it runs as an intermediate hemiglycosylated form (Fig. 3.24).

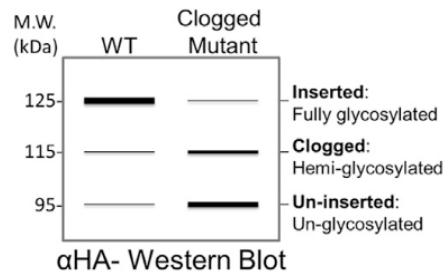


Figure 3.24. Measuring translocon clogging. The glycosylation status of the clogger fusion protein can be monitored by Western blotting. When clogged, the protein runs as an intermediate hemiglycosylated form at 115 kDa (Ast et al., 2016).

The integrative clogger construct (including the nourseothricin resistance marker) was amplified from the pMS529 plasmid and transformed into the *SEC61*, *sec61ΔH1*, *sec61ΔN21*, and *sec61S2Y* strains. Transformants were selected on YPD or YPG (*SEC61*) plates in the presence of nourseothricin. To our surprise, all *sec61* N-terminal mutants including *sec61S2Y* were synthetically lethal with the clogging construct, confirming that the Sec61p N-terminus enhances efficiency of post-translational protein import into the ER.

As part of a project focused on the role of Sbh1p in protein translocation across the ER membrane, I also monitored translocon clogging in a *Δsbh1Δsbh2* strain (KRY588). The clogger construct was integrated into the HO locus of the *Δsbh1Δsbh2* strain and transformants selected on YPD plates in the presence of nourseothricin. The *Δsbh1Δsbh2* strain carrying the integration of the clogger construct was transformed with a pRS414-*SBH1* plasmid (*SBH1*) or with an empty pRS414 plasmid as a control (*Δsbh1Δsbh2*). Cells were grown in minimal medium without tryptophan and in the presence of galactose and cell extracts prepared by bead-beating. Cell extracts were resolved by SDS-PAGE and the glycosylation status of the clogger construct in the *SBH1* and *Δsbh1Δsbh2* strains was analyzed by Western blotting using antibodies directed against HA (Fig. 3.25).

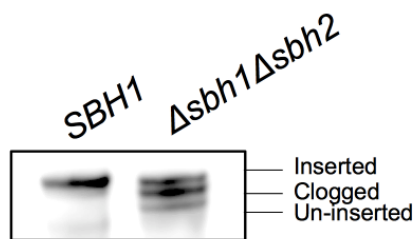


Figure 3.25. Translocon unclogging in the *Δsbh1Δsbh2* strain. Cells were grown at 30°C in minimal medium without tryptophan and in the presence of galactose to an $OD_{600} = 1$, extracts were prepared by bead-beating, and samples resolved by SDS-PAGE. Proteins were transferred to nitrocellulose and analyzed with an anti-HA antibody and enhanced chemiluminescence.

Results in Fig. 3.25 show that while in the *SBH1* strain most of the clogger is fully glycosylated, in the *Δsbh1Δsbh2* strain the hemiglycosylated clogged form of the construct is prevalent. As both Sbh1p and Sbh2p were previously reported to be dispensable for ERAD (and thus for extraction mediated by the Cdc48 complex), these data suggest that, in the absence of Sbh1p, Ste24p cannot properly be recruited to the SRP-independent translocon. Other factors involved in this quality control mechanism and in Ste24p recruitment, however, remain to be elucidated.

4. Discussion

In the present work, I have investigated the function of the N-terminus of Sec61p, the pore-forming subunit of the Sec61 complex (Johnson and van Waes, 1999). On its own the Sec61 complex mediates co-translational import of newly synthesized proteins, while it associates with the heterotetrameric Sec63 complex for post-translational protein import into the ER (Johnson and van Waes, 1999). The Sec61 complex is also a candidate channel for the dislocation of ERAD substrates to the cytosol (Schäfer and Wolf, 2009; Xie and Ng, 2010; Brodsky, 2012).

Prior to my work the role of the Sec61p N-terminus in yeast was largely unknown. The N-terminal region of yeast Sec61p was, however, likely to be functionally important, given that a 6-histidine tag at the Sec61p N-terminus was found to exacerbate the import defects of several *sec61* point mutants (Pilon et al., 1998). In addition, together with the Sbh1p N-terminus, the Sec61p N-terminus is exposed at one side of the transmembrane channel and might thus play a role in mediating Sec61p interactions with other proteins (van den Berg et al., 2003). Moreover, given its potential to form an amphipathic α -helical structure that is probably partially embedded in the plane of the membrane bilayer, the Sec61p N-terminus might stabilize the channel via interaction with the cytosolic side of the ER membrane (Wilkinson et al., 1996). Sec61p is N-terminally acetylated (Soromani et al., 2012). The biological role of Sec61p N-acetylation is still unclear, but a *sec61* mutant carrying a serine to tyrosine substitution in position 2 (*sec61S2Y*) was previously found in our laboratory to be temperature-sensitive at 37°C and defective in ERAD of a soluble substrate (Soromani et al., 2012; KR, unpublished). The S2Y substitution results in the initiator methionine being left uncleaved and the Sec61S2Yp N-terminus being acetylated by the minor NatC N-terminal acetylation complex (Hoffmann and Munro, 2006).

To gain insight into the function of the Sec61p N-terminus, I further characterized the *sec61S2Y* mutant and generated a *sec61* mutant carrying a deletion of the N-terminal helix but preserving the N-terminal acetylation site in its original sequence context, *sec61ΔH1*, and a *sec61* mutant lacking both the N-terminal acetylation site and the N-terminal helix, *sec61ΔN21*. My data show that the N-terminal acetylation site and the N-terminal helix of Sec61p are both functionally important and involved in different aspects of Sec61p function.

4.1. Role of Sec61p N-acetylation

The mutant strains investigated stably expressed Sec61p at wildtype level (*sec61ΔH1*) or approximately 60% of wildtype (*sec61S2Y* and *sec61ΔN21*) (Fig. 3.4, 3.5). In a GAL shut-off experiment, ER translocation defects only occurred when Sec61p levels fell below 20% of wildtype (KR, personal communication). As the *sec61S2Y* mutation had no effect on co-translational and post-translational import and the *sec61ΔN21* mutation only affected post-translational import into the ER *in vivo*, it can be concluded that Sec61p expression levels were not limiting in my *sec61* N-terminal mutants (KR, unpublished; Fig. 3.10, 3.11, 3.12, 3.13). For several proteins, N-acetylation at the initiator methionine constitutes a degradation signal termed Ac/N-degron and targeted by the Ac/N-end rule pathway (Shemorry et al., 2013). This pathway recognizes Ac/N-degrons, polyubiquitylates them, and thus causes their degradation by the proteasome if they do not become “shielded” by hetero-oligomeric interactions during synthesis or shortly after its completion (Varshavsky, 2011; Shemorry et al., 2013). As Sec61S2Yp was stable in a cycloheximide chase over 3 h, the mutant protein does not seem to be targeted by the Ac/N-end rule pathway (Fig. 3.5). Since mutation (*sec61S2Y*) or removal of the N-terminal acetylation site (*sec61ΔN21*) did not influence the stability of Sec61p, but resulted in lower expression levels, our data suggest that N-acetylation at S2 may play a role in biosynthesis of Sec61p.

Although *sec61S2Y* cells were temperature-sensitive at 37°C, incubation at higher temperature did not affect co- or post-translational import (KR, unpublished; Fig. 3.11). *In vitro* experiments with limiting amounts of microsomes and adjusting for equal amounts of Sec61p and Sec61S2Yp, however, showed a reduced post-translational import of ppαF into *sec61S2Y* microsomes (Fig. 3.16). This difference between the *sec61S2Y* effect in intact cells and in the cell-free assay might be due to an increase in mutation-associated instability of Sec61p as a consequence of the microsome preparation procedure. It is also possible that absence of the stabilizing molecular crowding effects of the cellular environment contributed to the defect observed *in vitro*. N-terminal acetylation has been shown to increase N-terminal helicity, an effect that likely results from the known ability of an N-acetyl group to act as a helix cap, which would stabilize the transient helical structure formed at the N-terminus (Maison et al., 2001; Fauvet et al., 2012; Kang et al., 2012). In addition, this helical character generated by N-acetylation at the very N-terminal region of proteins has been suggested to increase their affinity for physiological membranes (Eliezer et al., 2001; Bussell and Eliezer, 2003; Bartels et al., 2010). Although N-acetylation in the *sec61S2Y* mutant is preserved, the helix stabilizing effect is probably lost due to the increased bulk of the N-terminus generated by the presence of both the initiator methionine and the tyrosine aromatic ring at position 2 (Fig. 4.1) (Dikiy and Eliezer, 2014).

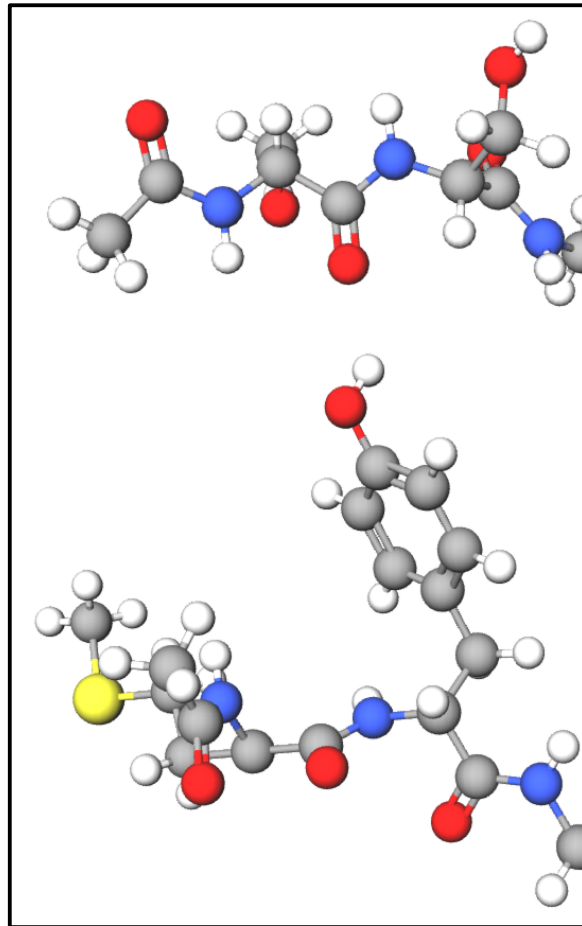


Figure 4.1. The acetylated Sec61p and Sec61S2Yp N-termini. Ball-and-stick models of the Sec61p (Ac-SS, top panel) and Sec61S2Yp (Ac-MY, bottom panel) N-termini. Carbon atoms are depicted in grey, hydrogen atoms in white, nitrogen atoms in blue, oxygen atoms in red, sulphur atoms in yellow. Models were generated with the MolView web-application.

Helicity of the N-terminus of Sec61p thus becomes more important for post-translational import *in vitro* and the S2Y mutation is likely associated with fraying of the N-terminal helix, which is essential for post-translational import into the ER (see 4.2).

I have confirmed that ERAD of the soluble substrate CPY* is delayed in *sec61S2Y* cells (Fig. 3.9) (KR, unpublished). Since the *sec61S2Y* mutant is not defective for ER protein import *in vivo*, this effect is likely direct (KR, unpublished; Fig. 3.11). Due to time constraints I have

not been able to monitor the decay of newly-synthesized CPY* in *sec61S2Y* cells with pulse-chase experiments conducted at 37°C, but CHX chase experiments showed that the ERAD defect of the *sec61S2Y* strain was probably not exacerbated at 37°C (Fig. 3.9), thus the temperature-sensitivity of the mutant remains unexplained.

N-terminal acetylation is a direct mediator for protein-protein interactions (Starheim et al., 2012). Since these interactions are often dependent on N-terminal acetylation in a specific sequence context, my data may indicate that Sec61p N-acetylation at S2 is required for interaction of the Sec61 channel with components of the ERAD machinery like the ubiquitin-ligase Hrd1p that polyubiquitylates ERAD substrates on the cytosolic side of the ER membrane (Stolz and Wolf, 2010; Starheim et al., 2012). Alternatively, Sec61p N-acetylation at its canonical site might be important for interaction with the Cdc48 complex, involved in the delivery of both misfolded ERAD substrates and partially translocated proteins to the proteasome (Braunstein et al., 2015). On the other hand, interaction with the Sec63 complex required for post-translational import was not impaired in *sec61S2Y* membranes, as shown by Con A precipitation of solubilized Sec complexes, although I could only solubilize limited amounts of Sec61p and Sec61S2Yp (Fig. 3.20). In addition, gradient fractionation experiments with *sec61S2Y* microsomes solubilized in Triton X-100, a detergent that largely preserves the stability of Sec61 complexes, showed that interaction of Sec61p with Sbh1p and Sss1p is not strongly dependent on Sec61p N-acetylation at its canonical site (Fig. 3.22).

Despite its temperature-sensitivity, in the *sec61S2Y* mutant the UPR was not induced (Fig. 3.6). The *sec61ΔN21* mutant, carrying the deletion of both the N-terminal acetylation site and the N-terminal helix, was also not UPR-induced (Fig. 3.6). Surprisingly, the only *sec61* N-terminal mutant that displayed significant UPR induction was *sec61ΔH1*, although it

preserves the N-acetylation site (Fig. 3.6). Since the mutant protein is stable (Fig. 3.4), this is unlikely to be a result of Sec61 Δ H1p eliciting the UPR itself as a misfolded protein. It is possible, however, that the N-acetylation of Sec61 Δ H1p might recruit an interacting partner to its N-terminus, but that in the absence of the helix the interaction is not functional and further interferes with transport through the Sec61 channel (Fig. 3.6).

4.2. Role of the Sec61p N-terminal amphipathic helix

Growth of the *sec61 Δ H1* and *sec61 Δ N21* mutants was compromised under all conditions tested, suggesting an important role for the N-terminal amphipathic helix in Sec61p function (Fig. 3.3). The growth defect was caused by a strong post-translational import defect (Fig. 3.12, 3.13) which - due to the overlap between import and export during CHX chase experiments - made it difficult to evaluate possible defects in ERAD of CPY* in both helix deletion mutants (Fig. 3.7). In addition, I found that all *sec61* N-terminal mutants including *sec61S2Y* were synthetically lethal with an inefficiently translocating inducible post-translational ER import substrate that clogs the Sec61 channel, confirming that the Sec61p N-terminus enhances efficiency of post-translational protein import into the ER (Ast et al., 2016). In contrast, pulse-labeling experiments showed that co-translational translocation into the ER was not affected in the *sec61 Δ H1* and *sec61 Δ N21* strains (3.10).

A possible explanation for the almost exclusive post-translational import defects exhibited by the *sec61 Δ H1* and *sec61 Δ N21* mutants was that the interaction of Sec61p with the Sec63 complex required for post-translational import is compromised in the absence of the N-terminal helix. I examined this by Con A precipitation of solubilized Sec complexes (Fig. 3.19), but surprisingly found no reduction in Sec complex formation in the mutants (Fig. 3.19). Instead, I identified a loss of Sec61p from the RAMP fractions of *sec61 Δ H1* and

sec61ΔN21 membranes compared to wildtype, suggesting reduced affinity of mutant Sec61 complexes for ribosomes or reduced Sec61 complex stability (Fig. 3.19). Loss of Sec61ΔH1p and Sec61ΔN21p from the RAMP fractions might also be due to the formation of SDS-resistant aggregates in digitonin, a scenario not uncommon for *sec61* large deletion mutants, and the resulting technical difficulties in resuspending high-speed pellets (Tretter et al., 2013).

Gradient fractionation experiments with solubilized Sec61 complexes corroborated the hypothesis that the N-terminal helix of Sec61p is important for Sec61 complex stability (Fig. 3.21). Membranes were solubilized with Triton X-100 because Sec61 complexes are only marginally stable in this detergent, thus even minor perturbations of complex stability result in dissociation of complex subunits (Falcone et al., 2011). The distribution of Sec61 complex subunits in the gradient fractions suggests that the Sec61p N-terminal helix is required for Sec61 complex stability, and that interaction of Sbh1p with Sec61p is more strongly dependent on the Sec61p N-terminal helix than that of Sss1p with Sec61p, as Sbh1p colocalized with Sec61ΔH1p in only 1 and with Sec61ΔN21p in only 3 fractions, respectively (Fig. 3.21). Sbh1p consists of a single transmembrane helix that is close to transmembrane domain 4 of Sec61p in the crystal structure, and its cytosolic domain is physically close to the cytosolic N-terminus of Sec61p (Zhao X and Jäntti J, 2009; Voorhees and Hegde, 2016). Upon membrane solubilization, the interaction between the cytosolic domains of Sec61p and Sbh1p might become more important, and the dissociation of Sbh1p from Sec61ΔH1p and Sec61ΔN21p after Triton X-100 solubilization suggests that the Sec61p N-terminal helix might be the cytosolic Sbh1p interacting partner. I tried to confirm this interaction by cross-linking experiments, but unfortunately the cross-linking reagent disuccinimidyl suberate masked the epitopes for our antibodies against Sbh1p (data not shown). I also attempted to

test whether *SBHI* overexpression could rescue the growth defects of the *sec61ΔHI* and *sec61ΔN21* strains and the temperature-sensitivity at 37°C of the *sec61S2Y* mutant (Fig. 3.23). Surprisingly, all of the strains overexpressing *SBHI* including the wildtype control were temperature-sensitive at 37°C (Fig. 3.23). In yeast, the intrinsic disorder content of a protein is an important determinant of dosage-sensitivity (Vavouri et al., 2009). In fact, disordered regions are prone to make promiscuous molecular interactions when their concentrations are increased, and this is a frequent cause of dosage-sensitivity (Vavouri et al., 2009). The N-terminus of Sbh1p is largely unstructured and at higher temperatures it is likely characterized by increased instability and structural fluctuations (van den Berg et al., 2003). Upon overexpression of the protein these structural fluctuations might have become responsible for promiscuous molecular interactions leading to the temperature-sensitivity of the strains investigated. Sss1p makes contact to Sec61p at multiple sites, including the transmembrane helices H6, H7, and H8 (Wilkinson et al., 1996). The reduced interaction of Sss1p with Sec61p lacking its N-terminal helix (see Fig. 3.21; wildtype: fractions 4-13; *sec61ΔHI*: fractions 7-12; *sec61ΔN21*: fractions 7-12) might therefore be caused by structural changes in the overall conformation of Sec61p that affect some of its interaction sites with Sss1p.

Opening of the Sec61 channel engaged by a signal sequence was recently described as a rigid-body rotation involving the N-terminal half of Sec61p as a compact bundle of helices (Voorhees and Hegde, 2016). The N-terminal half of Sec61p is characterized by greater mobility compared to the C-terminal one during translocation probably to permit nascent chain sampling of the lipid bilayer during translocation. Structure of the N-terminal half of Sec61p might be stabilized by the association of the amphipathic N-terminal helix with the cytosolic ER membrane surface and thus coordinated movement of the N-terminal half of

Sec61p during channel opening might be compromised if the helix is missing (Voorhees and Hegde, 2016). Given that I observed no DPAPB import defects in *sec61ΔH1* and *sec61ΔN21* cells (Fig. 3.10), the Sec61 complex lacking the N-terminal helix seems to be sufficiently stabilized by the ribosome (with a possible contribution from TM domain 7 in the lateral gate) to function during co-translational protein import into the ER. Alternatively, in the absence of a stabilizing effect, the energy provided by GTP hydrolysis during translation is sufficient to push the nascent chain through the pore of the Sec61 channel (Tsai et al., 2002). My data suggest that, in the absence of the N-terminal helix of Sec61p, the Sec61 complex is unstable, and that its interactions with the Sec63 complex are insufficient to stabilize the channel for post-translational import.

4.3. Concluding remarks

In this study, by characterizing a set of *sec61* N-terminal mutants, I have shown that the Sec61p N-terminus contains two structural elements that are functionally important: N-acetylation at serine in position 2 plays a role in ERAD, likely stabilizes the N-terminal helix, and may play a role in Sec61p biogenesis, whereas the Sec61p N-terminal amphipathic helix is essential for post-translational import into the ER and Sec61 complex stability. These data clarify the role of the N-terminus of the essential protein Sec61p, and, in a broader perspective, suggest that N-terminal acetylation may not only increase the affinity of soluble proteins for physiological membranes, but also favor transmembrane protein-membrane interactions (Dikiy and Eliezer, 2013).

In order to be conclusive, the experiments described in this work will have to be repeated with wildtype control cells expressing *SEC61* from its own promoter on a pRS315 plasmid and grown in YPD. Although I expressed *SEC61* from a *GAL* promoter, given that Sec61p on

its own is likely unstable and can therefore only form stable channels when Sss1p is present in equal amounts, yeast cells did control *SEC61* expression such that even from a *GAL* promoter the gene was not massively overexpressed. It is therefore highly likely that the results obtained with cells expressing *SEC61* from its own promoter in glucose will confirm my data.

5. References

Agarraberes FA, Dice JF. Protein translocation across membranes. *Biochim Biophys Acta*. 2001 Jul 2;1513(1):1-24.

Aksnes H, Drazic A, Marie M, Arnesen T. First Things First: Vital Protein Marks by N-Terminal Acetyltransferases. *Trends Biochem Sci*. 2016 Sep;41(9):746-60.

Araki K, Nagata K. Protein folding and quality control in the ER. *Cold Spring Harb Perspect Biol*. 2011 Nov 1;3(11):a007526.

Arnesen T, Van Damme P, Polevoda B, Helsens K, Evjenth R, Colaert N, Varhaug JE, Vandekerckhove J, Lillehaug JR, Sherman F, Gevaert K. Proteomics analyses reveal the evolutionary conservation and divergence of N-terminal acetyltransferases from yeast and humans. *Proc Natl Acad Sci USA*. 2009;106(20):8157-8162.

Ast T, Aviram N, Chuartzman SG, Schuldiner M. A cytosolic degradation pathway, prERAD, monitors pre-inserted secretory pathway proteins. *J Cell Sci*. 2014 Jul 15;127(Pt 14):3017-23.

Ast T, Cohen G, Schuldiner M. A network of cytosolic factors targets SRP-independent proteins to the endoplasmic reticulum. *Cell*. 2013 Feb 28;152(5):1134-45.

Ast T, Michaelis S, Schuldiner M. The Protease Ste24 Clears Clogged Translocons. *Cell*. 2016 Jan 14;164(1-2):103-14.

Aviram N, Ast T, Costa EA, Arakel EC, Chuartzman SG, Jan CH, Haßdenteufel S, Dudek J, Jung M, Schorr S, Zimmermann R, Schwappach B, Weissman JS, Schuldiner M. The SND proteins constitute an alternative targeting route to the endoplasmic reticulum. *Nature*. 2016 Nov 30;540(7631):134-138.

Barlowe CK, Miller EA. Secretory protein biogenesis and traffic in the early secretory pathway. *Genetics*. 2013 Feb;193(2):383-410.

Bartels T, Ahlstrom LS, Leftin A, Kamp F, Haass C, Brown MF, Beyer K. The N-Terminus of the Intrinsically Disordered Protein α -Synuclein Triggers Membrane Binding and Helix Folding. *Biophys J*. 2010;99(7):2116-2124.

Behnia R, Panic B, Whyte JR, Munro S. Targeting of the Arf-like GTPase Arl3p to the Golgi requires N-terminal acetylation and the membrane protein Sys1p. *Nat Cell Biol*. 2004 May;6(5):405-13.

Bhamidipati A, Denic V, Quan EM, Weissman JS. Exploration of the topological requirements of ERAD identifies Yos9p as a lectin sensor of misfolded glycoproteins in the ER lumen. *Mol Cell*. 2005 Sep 16;19(6):741-51.

Blobel G. Intracellular protein topogenesis. *Proc Natl Acad Sci USA*. 1980 Mar;77 (3):1496-1500.

Boeke JD, Trueheart J, Natsoulis G, Fink GR. 5-Fluoroorotic acid as a selective agent in yeast molecular genetics. *Methods Enzymol*. 1987;154:164-75.

Boyer HW, Roulland-Dussoix D. A complementation analysis of the restriction and modification of DNA in *Escherichia coli*. *J Mol Biol*. 1969 May 14;41(3):459-72.

Bradshaw N, Neher SB, Booth DS, Walter P. Signal Sequences Activate the Catalytic Switch of SRP RNA. *Science*. 2009 Jan 2;323(5910):127-30.

Braunstein I, Zach L, Allan S, Kalies KU, Stanhill A. Proteasomal degradation of preemptive quality control (pQC) substrates is mediated by an AIRAPL-p97 complex. *Mol Biol Cell*. 2015 Nov 1;26(21):3719-27.

Brodsky JL. Cleaning up: ER-associated degradation to the rescue. *Cell*. 2012 Dec 7;151(6):1163-7.

Brodsky JL, Goeckeler J, Schekman R. BiP and Sec63p are required for both co- and posttranslational protein translocation into the yeast endoplasmic reticulum. *Proc Natl Acad Sci USA*. 1995;92:9643-9646.

Burda P, Aebi M. The dolichol pathway of N-linked glycosylation. *Biochim Biophys Acta*. 1999 Jan 6;1426(2):239-57.

Bussell R Jr, Eliezer D. A structural and functional role for 11-mer repeats in α -synuclein and other exchangeable lipid binding proteins. *J Mol Biol*. 2003 Jun 13;329(4):763-78.

Cao X, Ballew N, Barlowe C. Initial docking of ER-derived vesicles requires Usa1p and Ypt1p but is independent of SNARE proteins. *EMBO J.* 1998;17:2156–2165.

Caplan S, Green R, Rocco J, Kurjan J. Glycosylation and structure of the yeast MF alpha 1 alpha-factor precursor is important for efficient transport through the secretory pathway. *J Bacteriol.* 1991;173(2):627-635.

Carvalho P, Goder V, Rapoport TA. Distinct ubiquitin-ligase complexes define convergent pathways for the degradation of ER proteins. *Cell.* 2006 Jul 28;126(2):361-73.

Carvalho P, Stanley AM, Rapoport TA. Retro-translocation of a misfolded luminal ER protein by the ubiquitin-ligase Hrd1p. *Cell.* 2010 Nov 12;143(4):579-91.

Chavan M, Yan A, Lennarz WJ. Subunits of the translocon interact with components of the oligosaccharyl transferase complex. *J Biol Chem.* 2005 Jun 17;280(24):22917-24.

Chen X, VanValkenburgh C, Liang H, Fang H, Green N. Signal peptidase and oligosaccharyltransferase interact in a sequential and dependent manner within the endoplasmic reticulum. *J Biol Chem.* 2001;276:2411–2416.

Cheng Z, Jiang Y, Mandon EC, Gilmore R. Identification of cytoplasmic residues of Sec61p involved in ribosome binding and cotranslational translocation. *J Cell Biol.* 2005 Jan 3;168(1):67-77.

Chirico WJ, Walters MG, Blobel G. 70K heat shock related proteins stimulate protein translocation into microsomes. *Nature*. 1988 Apr 28;332(6167):805-10.

Ciechanover A, Ben-Saadon R. N-terminal ubiquitination: more protein substrates join in. *Trends Cell Biol*. 2004 Mar;14(3):103-6.

Cox JS, Shamu C, Walter P. Transcriptional induction of genes encoding endoplasmic reticulum resident proteins requires a transmembrane protein kinase. *Cell*. 1993 Jun 18;73(6):1197-206.

Cox JS, Walter P. A novel mechanism for regulating activity of a transcription factor that controls the unfolded protein response. *Cell*. 1996 Nov 1;87(3):391-404.

Cross BC, Sinning I, Lührink J, High S. Delivering proteins for export from the cytosol. *Nat Rev Mol Cell Biol*. 2009 Apr;10(4):255-64.

Delic M, Valli M, Graf AB, Pfeffer M, Mattanovich D, Gasser B. The secretory pathway: exploring yeast diversity. *FEMS Microbiol Rev*. 2013 Nov;37(6):872-914.

Deshaies RJ, Schekman R. Structural and functional dissection of Sec62p, a membrane-bound component of the yeast endoplasmic reticulum protein import machinery. *Mol Cell Biol*. 1990;10(11):6024-6035.

Diekmann Y, Pereira-Leal JB. Evolution of intracellular compartmentalization. *Biochem J*. 2013 Jan 15;449(2):319-31.

Dikiy I, Eliezer D. N-terminal acetylation stabilizes N-terminal helicity in lipid- and micelle-bound α -synuclein and increases its affinity for physiological membranes. *J Biol Chem.* 2014 Feb 7;289(6):3652-65.

Drazic A, Myklebust LM, Ree R, Arnesen T. The world of protein acetylation. *Biochim Biophys Acta.* 2016 Oct;1864(10):1372-401.

Eliezer D, Kutluay E, Bussell R Jr, Browne G. Conformational properties of α -synuclein in its free and lipid-associated states *J Mol Biol.* 2001 Apr 6;307(4):1061-73.

Ellgaard L, Helenius A. Quality control in the endoplasmic reticulum. *Nat Rev Mol Cell Biol.* 2003 Mar;4(3):181-91.

Ellgaard L, Molinari M, Helenius A. Setting the standards: quality control in the secretory pathway. *Science.* 1999 Dec 3;286(5446):1882-8.

Erdmann, F., Schäuble, N., Lang, S., Jung, M., Honigmann, A., Ahmad, M., ... Zimmermann, R. Interaction of calmodulin with Sec61 α limits Ca²⁺leakage from the endoplasmic reticulum. *EMBO J.* 2011 Jan 5;30(1):17-31.

Evjenth R, Hole K, Karlsen OA, Ziegler M, Arnesen T, Lillehaug JR. Human Naa50p (Nat5/San) displays both protein N alpha- and N epsilon-acetyltransferase activity. *J Biol Chem.* 2009 Nov 6;284(45):31122-9.

Falcone D, Henderson MP, Nieuwland H, Coughlan CM, Brodsky JL, Andrews DW. Stability and function of the Sec61 translocation complex depends on the Sss1p tail-anchor sequence. *Biochem J*. 2011 Jun 1;436(2):291-303.

Fauvet B, Fares MB, Samuel F, Dikiy I, Tandon A, Eliezer D, Lashuel HA. Characterization of semisynthetic and naturally *N* α -acetylated α -synuclein *in vitro* and in intact cells. Implications for aggregation and cellular properties of α -synuclein. *J Biol Chem*. 2012 Aug 17;287(34):28243-62.

Feldheim D, Rothblatt J, Schekman R. Topology and functional domains of Sec63p, an ER membrane protein required for secretory protein translocation. *Mol Cell Biol*. 1992;12:3288–3296.

Feldheim D, Schekman R. Sec72p contributes to the selective recognition of signal peptides by the secretory polypeptide translocation complex. *J Cell Biol*. 1994 Aug;126(4):935–943.

Feldheim D, Yoshimura K, Admon A, Schekman R. Structural and functional characterization of Sec66p, a new subunit of the polypeptide translocation apparatus in the yeast endoplasmic reticulum. *Mol Biol Cell*. 1993;4(9):931-939.

Feng D, Zhao X, Soromani C, Toikkanen J, Römisch K, Vembar SS, et al. The transmembrane domain is sufficient for Sbh1p function, its association with the Sec61 complex, and interaction with Rtn1p. *J Biol Chem*. 2007 Oct 19;282(42):30618-28.

Feyder S, De Craene JO, Bär S, Bertazzi DL, Friant S. Membrane Trafficking in the Yeast *Saccharomyces cerevisiae* Model. *Int J Mol Sci*. 2015 Jan; 16(1): 1509–1525.

Finger A, Knop M, Wolf DH. Analysis of two mutated vacuolar proteins reveals a degradation pathway in the endoplasmic reticulum or a related compartment of yeast. *Eur J Biochem*. 1993;218:565–574

Finke K, Plath K, Panzner S, et al. A second trimeric complex containing homologs of the Sec61p complex functions in protein transport across the ER membrane of *S. cerevisiae*. *EMBO J*. 1996;15(7):1482-1494.

Finley D, Ulrich HD, Sommer T, Kaiser P. The ubiquitin-proteasome system of *Saccharomyces cerevisiae*. *Genetics*. 2012 Oct;192(2):319-60.

Forster C, Kane PM. Cytosolic Ca²⁺ Homeostasis Is a Constitutive Function of the V-ATPase in *Saccharomyces cerevisiae*. *J Biol Chem*. 2000 Dec 8;275(49):38245-53.

Forte GMA, Pool MR, Stirling CJ. N-Terminal Acetylation Inhibits Protein Targeting to the Endoplasmic Reticulum. *PLoS Biol*. 2011;9(5):e1001073.

Gardner BM, Pinkus D, Gotthardt K, Gallagher CM, Walter P. Endoplasmic Reticulum Stress Sensing in the Unfolded Protein Response. *Cold Spring Harb Perspect Biol*. 2013 Mar 1;5(3):a013169.

Gasper R, Meyer S, Gotthardt K, Sirajuddin M, Wittinghofer A. It takes two to tango: regulation of G proteins by dimerization. *Nat Rev Mol Cell Biol.* 2009 Jun;10(6):423-9.

Gauss R, Jarosch E, Sommer T, Hirsch C. A complex of Yos9p and the HRD ligase integrates endoplasmic reticulum quality control into the degradation machinery. *Nat Cell Biol.* 2006 Aug;8(8):849-54.

Gauss R, Kanehara K, Carvalho P, Ng DT, Aebi M. A complex of Pdi1p and the mannosidase Htm1p initiates clearance of unfolded glycoproteins from the endoplasmic reticulum. *Mol Cell.* 2011 Jun 24;42(6):782-93.

Gilmore R, Walter P, Blobel G. Protein translocation across the endoplasmic reticulum. II. Isolation and characterization of the signal recognition particle receptor. *J Cell Biol.* 1982;95(2):470-477.

Gomez-Navarro N and Miller E. Protein sorting at the ER-Golgi interface. *J Cell Biol.* 2016 Dec 19;215(6):769-778.

Hanahan D. Studies on transformation of *Escherichia Coli* with plasmids. *J Mol Biol.* 1983 Jun 5;166(4):557-80.

Hanna J, Leggett DS, Finley D. Ubiquitin Depletion as a Key Mediator of Toxicity by Translational Inhibitors. *Mol Cell Biol.* 2003;23(24):9251-9261.

Hansen W, Garcia PD, Walter P. In vitro protein translocation across the yeast endoplasmic reticulum: ATP-dependent posttranslational translocation of the prepro-alpha-factor. *Cell*. 1986 May 9;45(3):397-406.

Hansson MD, Rzeznicka K, Rosenbäck M, Hansson M, Sirijovski N. PCR-mediated deletion of plasmid DNA. *Anal Biochem*. 2008 Apr 15;375(2):373-5.

Harty C, Römisch K. Analysis of Sec61p and Ssh1p interactions in the ER membrane using the split-ubiquitin system. *BMC Cell Biol*. 2013 Mar 11;14:14.

Hebert DN, Molinari M. Flagging and docking: dual roles for N-glycans in protein quality control and cellular proteostasis. *Trends Biochem Sci*. 2012 Oct;37(10):404-10.

Helbig AO, Rosati S, Pijnappel PWWM, van Breukelen B, Timmers MHTH, et al. Perturbation of the yeast N-acetyltransferase NatB induces elevation of protein phosphorylation levels. *BMC Genomics* 2010;11:685.

Helsens K, Van Damme P, Degroeve S, Martens L, Arnesen T, Vandekerckhove J, Gevaert K. Bioinformatics analysis of a *Saccharomyces cerevisiae* N-terminal proteome provides evidence of alternative translation initiation and post-translational N-terminal acetylation. *J Proteome Res*. 2011 Aug 5;10(8):3578-89.

Hetz C. The unfolded protein response: controlling cell fate decisions under ER stress and beyond. *Nat Rev Mol Cell Biol*. 2012 Jan 18;13(2):89-102.

Hetz C, Martinon F, Rodriguez D, Glimcher LH. The unfolded protein response: integrating stress signals through the stress sensor IRE1 α . *Physiol Rev*. 2011 Oct;91(4):1219-43.

Higashio H, Kohno K. A genetic link between the unfolded protein response and vesicle formation from the endoplasmic reticulum. *Biochem Biophys Res Commun*. 2002;296:568–574.

Hiller MM, Finger A, Schweiger M, Wolf DH. ER degradation of a misfolded luminal protein by the cytosolic ubiquitin-proteasome pathway. 1996 Sep 20;273(5282):1725-8.

Hirsch C, Gauss R, Horn SC, Neuber O, Sommer T. The ubiquitylation machinery of the endoplasmic reticulum. *Nature*. 2009;458:453–460.

Hoffman I, Munro S. An N-terminally acetylated Arf-like GTPase is localised to lysosomes and affects their motility. *J Cell Sci*. 2006 Apr 15;119(Pt 8):1494-503.

Hollien J, Weissman JS. Decay of endoplasmic reticulum-localized mRNAs during the unfolded protein response. *Science*. 2006 Jul 7;313(5783):104-7.

Hwang CS, Shemorry A, Varshavsky A. N-Terminal Acetylation of Cellular Proteins Creates Specific Degradation Signals. *Science*. 2010;327(5968):973-977.

Isakov E, Stanhill A. Stalled proteasomes are directly relieved by P97 recruitment. *J Biol Chem*. 2011;286:30274–30283.

Jermy AJ, Willer M, Davis E, Wilkinson BM, Stirling CJ. The Brl domain in Sec63p is required for assembly of functional endoplasmic reticulum translocons. *J Biol Chem*. 2006 Mar 24;281(12):7899-906.

Jiang Y, Cheng Z, Mandon EC, Gilmore R. An interaction between the SRP receptor and the translocon is critical during cotranslational protein translocation. *J Cell Biol*. 2008 Mar 24;180(6):1149-61.

Johnson AE, van Waes MA. The translocon: a dynamic gateway at the ER membrane. *Annu Rev Cell Dev Biol*. 1999;15:799-842.

Johnson N, Haßdenteufel S, Theis M, Paton AW, Paton JC, Zimmermann R, High S. The signal sequence influences post-translational ER translocation at distinct stages. *PLoS One*. 2013 Oct 9;8(10):e75394.

Kaiser ML, Römisch K. Proteasome 19S RP binding to the Sec61 channel plays a key role in ERAD. *PLoS One*. 2015 Feb 6;10(2):e0117260.

Kalies KU, Allan S, Sergeyenko T, Kröger H, Römisch K. The protein translocation channel binds proteasomes to the endoplasmic reticulum membrane. *EMBO J*. 2005 Jul 6;24(13):2284-93.

Kalies KU, Rapoport TA, Hartmann E. The beta subunit of the Sec61 complex facilitates cotranslational protein transport and interacts with the signal peptidase during translocation. *J Cell Biol.* 1998 May 18;141(4):887-94.

Kanehara K, Xie W, Ng DT. Modularity of the Hrd1 ERAD complex underlies its diverse client range. *J Cell Biol.* 2010 Mar 8;188(5):707-16.

Kang L, Moriarty GM, Woods LA, Ashcroft AE, Radford SE, Baum J. N-terminal acetylation of α -synuclein induces increased transient helical propensity and decreased aggregation rates in the intrinsically disordered monomer. *Protein Sci.* 2012;21(7):911-917.

Kapp K, Schrempf S, Lemberg MK, Dobberstein B. Post-Targeting Functions of Signal Peptides. *Madame Curie Bioscience Database. Landes Bioscience*; 2000-2013.

Kimata Y, Kohno K. Endoplasmic reticulum stress-sensing mechanisms in yeast and mammalian cells. *Curr Opin Cell Biol.* 2011 Apr;23(2):135-42.

Knop M, Finger A, Braun T, Hellmuth K, Wolf DH. Der1, a novel protein specifically required for endoplasmic reticulum degradation in yeast. *EMBO J.* 1996 Feb 15;15(4):753-63.

Kostova Z, Wolf DH. For whom the bell tolls: protein quality control of the endoplasmic reticulum and the ubiquitin–proteasome connection. *EMBO J.* 2003;22(10):2309-2317.

Lakkaraju AKK, Thankappan R, Mary C, Garrison JL, Taunton J, Strub K. Efficient secretion of small proteins in mammalian cells relies on Sec62-dependent posttranslational translocation. *Mol Biol Cell*. 2012;23(14):2712-2722.

Lee MC, Miller EA. Molecular mechanisms of COPII vesicle formation. *Semin Cell Dev Biol*. 2007 Aug;18(4):424-34.

Lee RJ, Liu CW, Harty C, McCracken AA, Latterich M, Römisch K, DeMartino GN, Thomas PJ, Brodsky JL. Uncoupling retro-translocation and degradation in the ER-associated degradation of a soluble protein. *EMBO J*. 2004;23:2206–2215.

Letourneur F, Gaynor EC, Hennecke S, Démollière C, Duden R, Emr SD, Riezman H, Cosson P. Coatamer is essential for retrieval of dilysine-tagged proteins to the endoplasmic reticulum. *Cell*. 1994 Dec 30;79(7):1199-207.

Levy R, Wiedmann M, Kreibich G. In vitro binding of ribosomes to the β subunit of the Sec61p protein translocation complex. *J. Biol. Chem*. 2001 Jan 26;276(4):2340-6.

Li W, Schulman S, Boyd D, Erlandson K, Beckwith J, Rapoport TA. The plug domain of the SecY protein stabilizes the closed state of the translocation channel and maintains a membrane seal. *Mol Cell*. 2007 May 25;26(4):511-21.

Lin JH, Li H, Yamasura D, Cohen HR, Zhang C, Panning B, Shokat KM, Lavail MM, Walter P. IRE1 signaling affects cell fate during the unfolded protein response. *Science*. 2007 Nov 9;318(5852):944-9.

Lord C, Ferro-Novick S, Miller EA. The Highly Conserved COPII Coat Complex Sorts Cargo from the Endoplasmic Reticulum and Targets It to the Golgi. *Cold Spring Harb Perspect Biol.* 2013 Feb; 5(2): a013367.

Lyman SK, Schekman R. Interaction between BiP and Sec63p is required for the completion of protein translocation into the ER of *Saccharomyces cerevisiae*. *J Cell Biol.* 1995;131(5):1163-1171.

Mackinnon AL, Paavilainen VO, Sharma A, Hegde RS, Taunton J. An allosteric Sec61 inhibitor traps nascent transmembrane helices at the lateral gate. *Elife.* 2014;3:e01483.

Mades A, Gotthardt K, Awe K, Stieler J, Döring T, Füsler S, Prange R. Role of Human Sec63 in Modulating the Steady-State Levels of Multi-Spanning Membrane Proteins. *PLoS ONE.* 2012;7(11):e49243.

Maison W, Arce E, Renold P, Kennedy RJ, Kemp DS. Optimal N-caps for N-terminal helical templates. Effects of changes in H-bonding efficiency and charge. *J Am Chem Soc.* 2001 Oct 24;123(42):10245-54.

Mandon EC, Trueman SF, Gilmore R. Protein Translocation across the Rough Endoplasmic Reticulum. *Cold Spring Harb Perspect Biol.* 2013 Feb 1;5(2).

Matlack KE, Misselwitz B, Plath K, Rapoport TA. BiP acts as a molecular ratchet during posttranslational transport of prepro-alpha factor across the ER membrane. *Cell*. 1999 May 28;97(5):553-64.

McCracken AA, Brodsky JL. Assembly of ER-associated protein degradation in vitro: dependence on cytosol, calnexin, and ATP. *J Cell Biol*. 1996;132(3):291-298.

Mezzacasa A, Helenius A. The transitional ER defines a boundary for quality control in the secretion of tsO45 VSV glycoprotein. *Traffic*. 2002 Nov;3(11):833-49.

Miller JH. *Experiments in molecular genetics*. Cold Spring Harbor Laboratory. 1972.

Mori K, Ogawa N, Kawahara T, Yanagi H, Yura T. mRNA splicing-mediated C-terminal replacement of transcription factor Hac1p is required for efficient activation of the unfolded protein response. *Proc Natl Acad Sci USA*. 2000;97(9):4660-4665.

Morris LL, Hartman IZ, Jun DJ, Seemann J, DeBose-Boyd RA. Sequential actions of the AAA-ATPase valosin-containing protein (VCP)/p97 and the proteasome 19 S regulatory particle in sterol-accelerated, endoplasmic reticulum (ER)-associated degradation of 3-hydroxy-3-methylglutaryl-coenzyme a reductase. *J Biol Chem*. 2014;289:19053–19066.

Mothes W, Prehn S, Rapoport TA. Systematic probing of the environment of a translocating secretory protein during translocation through the ER membrane. *EMBO J*. 1994 Sep 1;13(17):3973-82.

Müller L, de Escauriaza MD, Lajoie P, Theis M, Jung M, Müller A, Burgard C, Greiner M, Snapp EL, Dudek J, Zimmermann R. Evolutionary Gain of Function for the ER Membrane Protein Sec62 from Yeast to Humans. *Mol Biol Cell*. 2010;21(5):691-703.

Mutka SC, Walter P. Multifaceted physiological response allows yeast to adapt to the loss of the signal recognition particle-dependent protein-targeting pathway. *Mol Biol Cell*. 2001 Mar;12(3):577-88.

Ng W, Sergeyenko T, Zeng N, Brown JD, Römisch K. Characterization of the proteasome interaction with the Sec61 channel in the endoplasmic reticulum. *J Cell Sci*. 2007 Feb 15;120(Pt 4):682-91.

Ngosuwan J, Wang NM, Fung KL, Chirico WJ. Roles of cytosolic Hsp70 and Hsp40 molecular chaperones in post-translational translocation of presecretory proteins into the endoplasmic reticulum. *J Biol Chem*. 2003 Feb 28;278(9):7034-42.

Nyathi Y, Wilkinson BM, Pool MR. Co-translational targeting and translocation of proteins to the endoplasmic reticulum. *Biochim Biophys Acta*. 2013 Nov;1833(11):2392-402.

Ogg SC, Barz WP, Walter P. A functional GTPase domain, but not its transmembrane domain, is required for function of the SRP receptor beta-subunit. *J Cell Biol*. 1998 Jul 27;142(2):341-54.

Orci L, Starnes M, Ravazzola M, Amherdt M, Perrelet A, Söllner TH, Rothman JE. Bidirectional transport by distinct populations of COPI-coated vesicles. *Cell*. 1997 Jul 25;90(2):335-49.

Osborne AR, Rapoport TA. Protein translocation is mediated by oligomers of the SecY complex with one SecY copy forming the channel. *Cell*. 2007 Apr 6;129(1):97-110.

Osowski CM, Urano F. Measuring ER stress and the unfolded protein response using mammalian tissue culture system. *Methods Enzymol*. 2011;490:71-92.

Paetzel M, Karla A, Strynadka NC, Dalbey RE. Signal peptidases. *Chem Rev*. 2002 Dec;102(12):4549-80.

Pagny S, Lerouge P, Faye L, Gomord V. Signals and mechanisms for protein retention in the endoplasmic reticulum. *J Exp Bot*. 1999;50:157–164.

Park E, Rapoport TA. Mechanisms of Sec61/SecY-mediated protein translocation across membranes. *Annu Rev Biophys*. 2012;41:21-40.

Parlati F, Dominguez M, Bergeron JJ, Thomas DY. *Saccharomyces cerevisiae* CNE1 encodes an endoplasmic reticulum (ER) membrane protein with sequence similarity to calnexin and calreticulin and functions as a constituent of the ER quality control apparatus. *J Biol Chem*. 1995 Jan 6;270(1):244-53.

Patil C, Walter P. Intracellular signaling from the endoplasmic reticulum to the nucleus: the unfolded protein response in yeast and mammals. *Curr Opin Cell Biol.* 2001 Jun;13(3):349-55.

Pelham HR, Hardwick KG, Lewis MJ. Sorting of soluble ER proteins in yeast. *EMBO J.* 1988 Jun;7(6):1757-62.

Pilon M, Römisch K, Quach D, Schekman R. Sec61p serves multiple roles in secretory precursor binding and translocation into the endoplasmic reticulum membrane. *Mol Biol Cell.* 1998 Dec;9(12):3455-73.

Pilon M, Schekman R, Römisch K. Sec61p mediates export of a misfolded secretory protein from the endoplasmic reticulum to the cytosol for degradation. *EMBO J.* 1997 Aug 1;16(15):4540-8.

Plath K, Rapoport TA. Spontaneous release of cytosolic proteins from posttranslational substrates before their transport into the endoplasmic reticulum. *J. Cell Biol.* 2000;151:167-178.

Plempner RK, Wolf DH. Retrograde protein translocation: ERADication of secretory proteins in health and disease. *Trends Biochem Sci.* 1999 Jul;24(7):266-70.

Polevoda B., Norbeck J., Takakura H., Blomberg A., Sherman F. Identification and specificities of N-terminal acetyltransferases from *Saccharomyces cerevisiae*. *EMBO J.* 1999 Nov 1;18(21):6155-68.

Quan EM, Kamiya Y, Kamiya D, et al. Defining the Glycan Destruction Signal for Endoplasmic Reticulum-Associated Degradation. *Mol Cell*. 2008;32(6):870-877.

Rapoport TA. Protein translocation across the eukaryotic endoplasmic reticulum and bacterial plasma membranes. *Nature*. 2007 Nov 29;450(7170):663-9.

Roberts CJ, Pohl G, Rothman JH, Stevens TH. Structure, biosynthesis, and localization of dipeptidyl aminopeptidase B, an integral membrane glycoprotein of the yeast vacuole. *J Cell Biol*. 1989;108(4):1363-1373.

Römisch K. Surfing the Sec61 channel: bidirectional protein translocation across the ER membrane. *J Cell Sci*. 1999 Dec;112 (Pt 23):4185-91.

Römisch K. Endoplasmic reticulum-associated degradation. *Annu Rev Cell Dev Biol*. 2005;21:435-56.

Ruggiano A, Foresti O, Carvalho P. Quality control: ER-associated degradation: protein quality control and beyond. *J Cell Biol*. 2014 Mar 17;204(6):869-79.

Sanderfoot AA, Raikhel NV. The specificity of vesicle trafficking: coat proteins and SNAREs. *Plant Cell*. 1999 Apr;11(4):629-42.

Saraogi I, Shan SO. Molecular mechanism of co-translational protein targeting by the signal recognition particle. *Traffic*. 2011 May;12(5):535-42.

Schäfer A, Wolf DH. Sec61p is part of the endoplasmic reticulum-associated degradation machinery. *EMBO J.* 2009 Oct 7;28(19):2874-84.

Schäuble N, Cavalié A, Zimmermann R, Jung M. Interaction of *Pseudomonas aeruginosa* Exotoxin A with the human Sec61 complex suppresses passive calcium efflux from the endoplasmic reticulum. *Channels.* 2014;8(1):76-83.

Scheper W, Thaminy S, Kais S, Stagljar I, Römisch K. Coordination of N-glycosylation and protein translocation across the endoplasmic reticulum membrane by Sss1 protein. *J Biol Chem.* 2003 Sep 26;278(39):37998-8003.

Scott DC, Monda JK, Bennett EJ, Harper JW, Schulman BA. N-Terminal Acetylation Acts as an Avidity Enhancer Within an Interconnected Multiprotein Complex. *Science.* 2011;334(6056):674-678.

Scott DC, Schekman R. Role of Sec61p in the ER-associated degradation of short-lived transmembrane proteins. *J Cell Biol.* 2008 Jun 30;181(7):1095-105.

Servas C, Römisch K. The Sec63p J-Domain Is Required for ERAD of Soluble Proteins in Yeast. *PLoS One.* 2013; 8(12): e82058.

Shan S, Chandrasekar S, Walter P. Conformational changes in the GTPase modules of the signal reception particle and its receptor drive initiation of protein translocation. *J Cell Biol.* 2007 Aug 13; 178(4): 611–620.

Shan S, Stroud RM, Walter P. Mechanism of Association and Reciprocal Activation of Two GTPases. *PLoS Biol.* 2004 Oct; 2(10): e320.

Shemorry A, Hwang CS, Varshavsky A. Control of protein quality and stoichiometries by N-terminal acetylation and the N-end rule pathway. *Mol Cell.* 2013 May 23;50(4):540-51.

Shen SH, Chretien P, Bastien L, Slilaty SN. Primary sequence of the glucanase gene from *Oerskovia xanthineolytica*. Expression and purification of the enzyme from *Escherichia coli*. *J Biol Chem.* 1991;266:1058–1063.

Simons JF, Ferro-Novick S, Rose MD, Helenius A. BiP/Kar2p serves as a molecular chaperone during carboxypeptidase Y folding in yeast. *J Cell Biol.* 1995;130:41–49.

Sitia R, Braakman I. Quality control in the endoplasmic reticulum protein factory. *Nature.* 2003 Dec 18;426(6968):891-4.

Song OK, Wang X, Waterborg JH, Sternglanz R. An Nalpha-acetyltransferase responsible for acetylation of the N-terminal residues of histones H4 and H2A. *J Biol Chem.* 2003 Oct 3;278(40):38109-12.

Soromani C, Zeng N, Hollemeyer K, Heinzle E, Klein M-C, Tretter T, et al. N-acetylation and phosphorylation of Sec complex subunits in the ER membrane. *BMC Cell Biol.* 2012 Dec 13;13:34.

Spang A. Traffic COPs: rules of detection. *EMBO J.* 2013 Apr 3;32(7):915-6.

Spiller MP, Stirling CJ. Preferential Targeting of a Signal Recognition Particle-dependent Precursor to the Ssh1p Translocon in Yeast. *J Biol Chem.* 2011;286(25):21953-21960.

Starheim KK, Gevaert K, Arnesen T. Protein N-terminal acetyltransferases: when the start matters. *Trends Biochem Sci.* 2012 Apr;37(4):152-61.

Starheim KK, Gromyko D, Evjenth R, Rynningen A, JE Varhaug, JR Lillehaug, Arnesen T. Knockdown of Human N^α-Terminal Acetyltransferase Complex C Leads to p53-Dependent Apoptosis and Aberrant Human Arl8b Localization. *Mol Cell Biol.* 2009;29(13):3569-3581.

Stevens T, Esmon B, Schekman R. Early stages in the yeast secretory pathway are required for transport of carboxypeptidase Y to the vacuole. *Cell.* 1982 Sep;30(2):439-48.

Stolz A, Wolf DH. Endoplasmic reticulum associated protein degradation: a chaperone assisted journey to hell. *Biochim Biophys Acta.* 2010 Jun;1803(6):694-705.

Szathmary R, Biemann R, Nita-Lazar M, Burda P, Jakob CA. Yos9 Protein Is Essential for Degradation of Misfolded Glycoproteins and May Function as Lectin in ERAD. *Mol Cell.* 2005 Sep 16;19(6):765-75.

Thibault G, Ng DT. The endoplasmic reticulum-associated degradation pathways of budding yeast. *Cold Spring Harb Perspect Biol.* 2012 Dec 1;4(12).

Toikkanen J, Gatti E, Takei K, Saloheimo M, Olkkonen VM, Söderlund H, De Camilli P, Keränen S. Yeast protein translocation complex: isolation of two genes SEB1 and SEB2 encoding proteins homologous to the Sec61 beta subunit. *Yeast*. 1996 Apr;12(5):425-38.

Travers KJ, Patil CK, Wodicka L, Lockhardt DJ, Weissman JS, Walter P. Functional and genomic analyses reveal an essential coordination between the unfolded protein response and ER-associated degradation. *Cell*. 2000 Apr 28;101(3):249-58.

Tretter T, Pereira FP, Ulucan O, Helms V, Allan S, Kalies KU, et al. ERAD and protein import defects in a sec61 mutant lacking ER-luminal loop 7. *BMC Cell Biol*. 2013 Dec 6;14:56.

Trueman SF, Mandon EC, Gilmore R. A gating motif in the translocation channel sets the hydrophobicity threshold for signal sequence function. *J Cell Biol*. 2012 Dec 10; 199(6): 907–918.

Tsai B, Ye Y, Rapoport TA. Retro-translocation of proteins from the endoplasmic reticulum into the cytosol. *Nat Rev Mol Cell Biol*. 2002 Apr;3(4):246-55.

Tu BP, Weissman JS. Oxidative protein folding in eukaryotes: mechanisms and consequences. *J Cell Biol*. 2004 Feb 2;164(3):341-6.

van Anken E, Braakman I. Versatility of the endoplasmic reticulum protein folding factory. *Crit Rev Biochem Mol Biol*. 2005 Jul-Aug;40(4):191-228.

Van Damme P, Arnesen T, Gevaert K. Protein alpha-N-acetylation studied by N-terminomics. *FEBS J.* 2011 Oct;278(20):3822-34.

van den Berg B, Clemons WM Jr, Collinson I, Modis Y, Hartmann E, Harrison SC, Rapoport TA. X-ray structure of a protein-conducting channel. *Nature.* 2004 Jan 1;427(6969):36-44.

Varshavsky A. The N-end rule pathway and regulation by proteolysis. *Protein Sci.* 2011 Aug;20(8):1298-345.

Vashist S, Ng DT. Misfolded proteins are sorted by a sequential checkpoint mechanism of ER quality control. *J Cell Biol.* 2004 Apr;165(1):41-52.

Vavouri T, Semple JI, Garcia-Verdugo R, Lehner B. Intrinsic protein disorder and interaction promiscuity are widely associated with dosage sensitivity. *Cell.* 2009;138:198–208.

Vembar SS, Brodsky JL. One step at a time: endoplasmic reticulum-associated degradation. *Nat Rev Mol Cell Biol.* 2008 Dec;9(12):944-57.

Vitale A, Denecke J. The endoplasmic reticulum-gateway of the secretory pathway. *Plant Cell.* 1999 Apr;11(4):615-28.

von Heijne G. Patterns of amino acids near signal-sequence cleavage sites. *Eur J Biochem.* 1983 Jun 1;133(1):17-21.

von Heijne G. Signal sequences. The limits of variation. *J Mol Biol.* 1985 Jul 5;184(1):99-105.

von Heijne G. A new method for predicting signal sequence cleavage sites. *Nucleic Acids Res.* 1986 Jun 11;14(11):4683-90.

Voorhees RM, Fernández IS, Scheres SHW, Hegde RS. Structure of the Mammalian Ribosome-Sec61 Complex to 3.4 Å Resolution. *Cell.* 2014;157(7):1632-1643.

Voorhees RM, Hegde RS. Structure of the Sec61 channel opened by a signal sequence. *Science.* 2016 Jan 1;351(6268):88-91.

Wahlman J, DeMartino GN, Skach WR, Bulleid NJ, Brodsky JL, Johnson AE. Real-time fluorescence detection of ERAD substrate retrotranslocation in a mammalian in vitro system. *Cell.* 2007 Jun 1;129(5):943-55.

Walter P, Blobel G. Translocation of proteins across the endoplasmic reticulum III. Signal recognition protein (SRP) causes signal sequence-dependent and site-specific arrest of chain elongation that is released by microsomal membranes. *J Cell Biol.* 1981 Nov;91(2 Pt 1):557-61.

Wiertz EJ, Tortorella D, Bogyo M, Yu J, Mothes W, Jones TR, Rapoport TA, Ploegh HL. Sec61-mediated transfer of a membrane protein from the endoplasmic reticulum to the proteasome for destruction. *Nature.* 1996 Dec 5;384(6608):432-8.

Wilkinson BM, Critchley AJ, Stirling CJ. Determination of the transmembrane topology of yeast Sec61p, an essential component of the endoplasmic reticulum translocation complex. *J Biol Chem.* 1996 Oct 11;271(41):25590-7.

Wilkinson BM, Esnault Y, Craven RA, Skiba F, Fieschi J, Kepes F, et al. Molecular architecture of the ER translocase probed by chemical crosslinking of Sss1p to complementary fragments of Sec61p. *EMBO J.* 1997 Aug 1;16(15):4549-59.

Wilkinson BM, Tyson JR, Stirling CJ. Ssh1p determines the translocation and dislocation capacities of the yeast endoplasmic reticulum. *Dev Cell.* 2001 Sep;1(3):401-9.

Winther JR, Stevens TH, Kielland-Brandt MC. Yeast carboxypeptidase Y requires glycosylation for efficient intracellular transport, but not for vacuolar sorting, in vivo stability, or activity. *Eur J Biochem.* 1991;197:681-689.

Wiseman RL, Koulov A, Powers E, Kelly JW, Balch WE. Protein energetics in maturation of the early secretory pathway. *Curr Opin Cell Biol.* 2007 Aug;19(4):359-67.

Wittke S, Dünnwald M, Johnsson N. Sec62p, A Component of the Endoplasmic Reticulum Protein Translocation Machinery, Contains Multiple Binding Sites for the Sec-Complex. *Mol Biol Cell.* 2000;11(11):3859-3871.

Wu H, Ng BSH, Thibault G. Endoplasmic reticulum stress response in yeast and humans. *Bioscience Reports.* 2014;34(4):e00118.

Xiao H, Smeeckens JM, Wu R. Quantification of tunicamycin-induced protein expression and N-glycosylation changes in yeast. *Analyst*. 2016 Jun 21;141(12):3737-45.

Xie W, Kanehara K, Sayeed A, Ng DT. Intrinsic Conformational Determinants Signal Protein Misfolding to the Hrd1/Htm1 Endoplasmic Reticulum-associated Degradation System. *Mol Biol Cell*. 2009 Jul 15; 20(14): 3317–3329.

Xie W, Ng DT. ERAD substrate recognition in budding yeast. *Semin Cell Dev Biol*. 2010 Jul;21(5):533-9.

Xu C, Ng DT. Glycosylation-directed quality control of protein folding. *Nat Rev Mol Cell Biol*. 2015 Dec;16(12):742-52.

Ye Y, Shibata Y, Yun C, Ron D, Rapoport TA. A membrane protein complex mediates retrotranslocation from the ER lumen into the cytosol. *Nature*. 2004 Jun 24;429(6994):841-7.

Yoshida H, Matsui T, Yamamoto A, Okada T, Mori K. XBP1 mRNA is induced by ATF6 and spliced by IRE1 in response to ER stress to produce a highly active transcription factor. *Cell*. 2001 Dec 28;107(7):881-91.

Young BP, Craven RA, Reid PJ, Willer M, Stirling CJ. Sec63p and Kar2p are required for the translocation of SRP-dependent precursors into the yeast endoplasmic reticulum in vivo. *EMBO J*. 2001 Jan 15;20(1-2):262-71.

Zattas D, Hochstrasser M. Ubiquitin-dependent protein degradation at the yeast endoplasmic reticulum and nuclear envelope. *Crit Rev Biochem Mol Biol*. 2015 Jan-Feb;50(1):1-17.

Zhang X, Rashid R, Wang K, Shan SO. Sequential checkpoints govern substrate selection during cotranslational protein targeting. *Science*. 2010 May 7;328(5979):757-60.

Zhang X, Schaffitzel C, Ban N, Shan S. Multiple conformational switches in a GTPase complex control co-translational protein targeting. *Proc Natl Acad Sci USA*. 2009 Feb 10;106(6):1754-9.

Zhao X, Jääntti J. Functional characterization of the trans-membrane domain interactions of the Sec61 protein translocation complex beta-subunit. *BMC Cell Biol*. 2009 Oct 26;10:76.

Zimmermann R, Eyrich S, Ahmad M, Helms V. Protein translocation across the ER membrane. *Biochim Biophys Acta*. 2011 Mar;1808(3):912-24.

Publications

Elia F, Römisch K. The N-terminus of Sec61p Is Essential for Post-translational Protein Import into and Misfolded Soluble Protein Export from the ER (poster). EMBO Meeting 2016, Mannheim, Germany.

Elia F, Römisch K. Function of the Sec61p N-terminus in Protein Translocation across the ER membrane (poster). FEBS EMBO 2014 Conference, Paris, France.

Acknowledgements

First of all, I would like to thank my PhD supervisor Prof. Dr. Karin Römisch for giving me the chance to explore the interesting field of protein translocation, and for allowing me to conduct my research independently and grow as a research scientist. Her advice on research, career, and especially Scientific Writing has been of great value for me. I would also like to thank her for the patience shown during the last months of my PhD, when my data turned out to be not as satisfactory as we both expected.

I would also like to thank my second PhD supervisor Prof. Dr. Manfred J. Schmitt for his interest in my work and the valuable suggestions he gave me during our meetings.

Many thanks to Prof. Dr. Gert-Wieland Kohring for his words of encouragement, advice on experiments, help with the Sephadex G-25 column, comments on the final version of my thesis, all the fun conversations, and the list could keep going.

Special thanks to my predecessors in the lab Dr. Christina Servas and Dr. Thomas Tretter for the invaluable help they provided particularly during the first year of my PhD and to my fellow labmates Angela Molinaro and Fábio Pereira for all the highs and lows, fun and bad times we shared. Thank you Dr. Thomas Tretter and Fábio Pereira for being, besides great colleagues to work with, good friends.

Many thanks go also to Carmen Clemens and Birgit Hasper for the technical support they provided throughout these years, and in particular during the BSc Microbiology Praktika we organized. Carmen Clemens, besides always being a positive influence, went above and beyond her duties of lab technician, patiently helping me out countless times with issues

related to my poor knowledge of the German language, and for this I will be always grateful to her.

I also want to express my gratitude to Juncal Z. González for her patience and help provided with various administrative matters, which more often than not were beyond her job responsibilities.

I am also grateful to Dr. Mirjam Selzer for kindly proofreading the German version of the abstract of this thesis.